

## Durham Research Online

---

### Deposited in DRO:

28 November 2019

### Version of attached file:

Accepted Version

### Peer-review status of attached file:

Peer-reviewed

### Citation for published item:

Evans, David J.A. and Atkinson, Nigel and Phillips, Emrys (2020) 'Glacial geomorphology of the Neutral Hills Uplands, southeast Alberta, Canada : the process-form imprints of dynamic ice streams and surging ice lobes.', *Geomorphology*, 350 .

### Further information on publisher's website:

<https://doi.org/10.1016/j.geomorph.2019.106910>

### Publisher's copyright statement:

© 2019 This manuscript version is made available under the CC-BY-NC-ND 4.0 license  
<http://creativecommons.org/licenses/by-nc-nd/4.0/>

### Additional information:

## Use policy

---

The full-text may be used and/or reproduced, and given to third parties in any format or medium, without prior permission or charge, for personal research or study, educational, or not-for-profit purposes provided that:

- a full bibliographic reference is made to the original source
- a [link](#) is made to the metadata record in DRO
- the full-text is not changed in any way

The full-text must not be sold in any format or medium without the formal permission of the copyright holders.

Please consult the [full DRO policy](#) for further details.

# **Glacial geomorphology of the Neutral Hills Uplands, southeast Alberta, Canada: the process-form imprints of dynamic ice streams and surging ice lobes**

David J. A. Evans<sup>1</sup>, Nigel Atkinson<sup>2</sup> and Emrys Phillips<sup>3</sup>

1. Department of Geography, Durham University, South Road, Durham DH1 3LE, UK

2. Alberta Geological Survey, Twin Atria Building Suite 402, 4999-98 Avenue, Edmonton, Alberta, T6B 2X3, Canada

3. British Geological Survey, The Lyell Centre, Research Avenue South, Edinburgh, EH14 4AP, UK

## **Abstract**

The Neutral Hills Uplands of southern Alberta, Canada is an area of complex and varied glacial landforms dominated by glacitectonic compressional structures but also containing expansive areas of hummocky terrain and kame and kettle topography. It lies between the strongly streamlined trunks of the former Central Alberta (CAIS) and Maskwa palaeo-ice streams of the SW Laurentide Ice Sheet (LIS) and hence comprises an inter-ice stream regional moraine zone, constructed at around 15.5 cal ka BP. This study aimed to compile a regional map of the glacial geomorphology of the central southeast Alberta in order to decipher the landform-sediment signatures of overprinted ice stream margins in terrestrial continental environments, and to refine the palaeoglaciological reconstructions for the southwest LIS. Detailed mapping from LiDAR and aerial imagery identifies distinctive glacial landsystems diagnostic of the partial overprinting of cross-cutting ice stream trunks and fast flow lobes. Widespread evidence of surge-diagnostic features indicates that the ice streams experienced repeated flow instabilities, consistent with the broader scenario of a highly dynamic and unstable SW LIS, characterised by markedly transitory and cross-cutting palaeo-ice streams. The inter-ice stream moraine zone is characterised by spectacular glacitectonic compression of bedrock, cupola hill construction and mega raft displacement but also displays evidence of multi-phase stagnant ice melt-out, where partially overprinted surge lobes advanced into large areas of buried glacier ice. Contemporaneous ice melting led to the widespread development of glacier karst and the production of eskers at a range of scales, the largest of which record deranged drainage patterns indicative of ice-walled channel sedimentation controlled by the regional bedrock slope towards the northeast. These process-form regimes have created a significant local relief that is a product of not only glacitectonic compression of bedrock but also the creation and melting of a melange of ice and bedrock/sediment blocks of variable ice volume, which

are representative of former buried snout ice with a glacier karst system that was repeatedly proglacially thrust due to surging. Widespread evidence for subglacial channel cutting is likely strongly linked to the transitory, surging and cross-cutting nature of the palaeo-ice streams in the region, whereby ice streams switched on and surged in response to the build-up, migration and marginal outbursts of subglacial water reservoirs. In addition to the reduced basal friction caused by the low permeability of the Cretaceous bedrock, pressurized groundwater and potentially also shallow biogenic gas deposits were likely important to the process-form regimes of surging lobes of soft-bedded ice streams in a region where ice flow was against an adverse bed slope; a scenario that gave rise to a variety of enigmatic landforms such as doughnuts, doughnut chains, apparent blow-out features and possible till eskers, as well as glacitectonic mega-rafts.

**Key words:** Palaeo-ice stream; inter-ice stream moraine; glacitectonics; hummocky terrain.

## 1. Introduction

The glacial geomorphology of the Canadian prairies of Alberta and Saskatchewan has been critical to palaeoglaciological reconstructions of the southwestern Late Wisconsinan Laurentide Ice Sheet (LIS). These reconstructions demonstrate that during full glacial and deglacial conditions, this sector of the ice sheet was subject to ice streaming and the intermittent operation of surging lobes, which promoted dramatic switches in ice flow directions (Clayton et al., 1985; Evans et al., 1999, 2008; Ó Cofaigh et al., 2010; Margold et al., 2015; Atkinson et al., 2016; Fig. 1). The evidence for this complex and dynamic behaviour is manifest in glacial landform-sediment assemblages and landsystems arranged in large, arcuate ice-marginal subaerial depo-centres and moraines, lying downflow of subglacially streamlined bedform corridors (Evans et al., 1999, 2008, 2012, 2014). This palaeoglaciological signature has been likened to the terrestrial equivalent of ice stream/trough-mouth fan systems of submarine settings (Evans et al., 2012), and on the prairies is representative of marginal lobation and partial overprinting along the termini of fast ice flow corridors (Patterson, 1997, 1998; Colgan et al., 2003; Jennings, 2006; Evans et al., 2008; Ó Cofaigh et al., 2010; Margold et al., 2015; Norris et al., 2018). The role of surging and changing basal thermal regimes in driving spatial and temporal variability in landsystems associated with lobate ice stream margins are being increasingly emphasised as higher resolution geomorphological mapping is undertaken (e.g., Mooers, 1990; Colgan et al., 2003; Evans et al., 2014, 2016a; Sookhan et al. 2018; Mulligan et al. 2019). Additionally, thinning and recession of these ice margins occurred down the adverse slope of the regional drainage gradient, which promoted the development of large proglacial lakes, gave rise to complex meltwater drainage patterns and ice-contact glacialfluvial features (Christiansen, 1979; Kehew and Lord, 1986; Evans, 2000; Clayton et al., 2008; Utting et al., 2016). Also important are the geomorphological implications of pressurised groundwater and possibly shallow gas in glacierized Cretaceous bedrock terrains such as those of the Canadian prairies, where groundwater recharge and over-pressurization of aquifers induced by ice sheet advance is thought to initiate substantial blow-out features (cf. Mandl and Harkness, 1987; Bluemle, 1993; Boulton and Caban, 1995; Grasby et al., 2000; Grasby and Chen, 2005; Lemieux et al., 2008).

Despite these improved reconstructions, a number of outstanding problems persist in the interpretation of glacial landforms on the Canadian prairies, some of which have significant longevity. For example, hummocky terrain and associated features like prairie mounds and doughnuts (Gravenor and Kupsch, 1959) have been explained variously as the products of subglacial pressing by passive deformation (Stalker, 1960; Eyles et al., 1999; Boone and Eyles, 2001), pingo

development (Bik, 1969), lake floor gas escape vents or lake ice features (Mollard, 2000), and groundwater expulsion (Bluemle, 1993; Boulton and Caban, 1995; Evans, 2003; Evans et al., 2014). Also, since the seminal work of Moran et al., (1980), glacitectonic processes have been widely employed to explain a range of prairie landforms including hummocky terrain (e.g., Bluemle and Clayton, 1984; Tsui et al., 1989; Evans, 2000; Evans et al., 2014). The role of glacitectonics is evident at some classic sites (e.g., Mud Buttes; cf. Slater, 1927), which have been revisited to provide further details into the nature of glacier-substrate interactions (Phillips et al., 2017). The range of alternative explanations for glacial landforms on the Canadian prairies drives the need to critically examine the wider and more diverse landform-sediment assemblages of the southwest LIS. Indeed, all these explanations may play significant complementary roles in the development of the glacial landsystems of the Canadian prairies, especially if the palaeoglaciological setting was, as widely proposed, one of fast ice flow, changing basal thermal regimes, intermittently surging lobate ice stream margins, and rapidly changing proglacial lake configurations.

One area that has been proposed as a former location of lobate and partly overprinted termini of fast ice flow corridors is the Neutral Hills Uplands (Evans et al., 2008; Ó Cofaigh et al., 2010; Phillips et al., 2017; Fig. 2), where complex glacial landform assemblages offer an opportunity to decipher the patterns of deglacial ice sheet dynamics and their inter-relationships with regional topography, climate and bedrock characteristics. The widespread juxtaposition in this area of enigmatic forms such as prairie mounds, doughnuts, geometric ridge networks and hummocky terrain (Gravenor and Kupsch, 1959; Mollard, 2000), in association with some of the most spectacular glacitectonic features in North America (Hopkins, 1923; Slater, 1927; Aber et al., 1989; Fenton et al., 1993; Aber and Ber 2007; Phillips et al., 2017), indicate that they likely emerge from a common, although complex process-form regime and thereby constitute a specific glacial landsystem signature. The aim of this study is therefore to compile a regional map of the glacial geomorphology of the central portion of southeast Alberta, primarily the Neutral Hills Uplands, with the objective of deciphering the landform-sediment signatures of overprinted lobate ice stream margins in terrestrial continental environments, and to refine the palaeoglaciological reconstructions for the southwest LIS.

## **2. Study area and methods**

The Neutral Hills Uplands comprises an area of glacitectonic constructional terrain which includes the substantial composite ridges of the Neutral Hills (120 m high), Misty Hills (85 m high) and Nose Hill (100 m high), as well as the more widely known cupola hill at Mud Buttes (50 m high) with its

well-exposed internal structures of intensely folded and thrust Late Cretaceous sandstones, siltstones and mudstones (Figs. 2, 3, 4). These prominent landforms have long been recognized as glacitectonised bedrock (Hopkins, 1923; Slater, 1927; Kupsch, 1962; Bayrock, 1967; Moran et al., 1980; Shetsen, 1987, 1990; Evans et al., 2008; Phillips et al., 2017) and together form a suite of landforms large enough to constitute a regional physiographic zone (Bostock, 1970a, b; Pettapiece, 1986). Geologically, the region is located in the south-central part of the Western Canada Sedimentary Basin, which is characterised by fluvial and marine deposits associated with the transgression of the Western Interior Seaway during the Late Cretaceous (Mossop and Shetsen, 1994). Previous work on the glacial landforms of the Neutral Hills Uplands includes surficial geology mapping (Gravenor and Bayrock, 1955; Bayrock, 1958a, b, 1967; Shetsen, 1987, 1990; Kjearsgaard, 1988) as well as local studies on the Mud Buttes and the large composite ridges of the Neutral and Misty hills (Hopkins, 1923; Slater, 1927; Fenton et al., 1993; Phillips et al., 2017). The location of the glacially thrust masses of the Neutral Hills Uplands has been related to LIS readvances against the northernmost extension of the NW-SE orientated Missouri Coteau escarpment (Bretz, 1943; Evans et al., 2008).

The geomorphology of the study area was mapped from a 15 m light detection and ranging (LiDAR) bare-earth digital elevation model (DEM) specifically for more localised and larger scale detail and the 30 m Shuttle Radar Topography Mission (SRTM) DEM for more regional trends. Features were identified using their non-genetic, morphometric characteristics and then later assigned genetic classifications. Reference was made to aerial photograph mosaics flown and compiled by the Alberta Department of Lands and Forest in the 1950s, as well as Google Earth imagery. Also important were archival maps of the glacial geology of the region, compiled by Gravenor and Bayrock (1955) and Bayrock (1958a, b, 1967). This approach facilitated the identification and classification of ten types of landform signature, each characterised by the occurrence and nature of linear or curvilinear features or lineaments (sub-divided further according to parallel or non-parallel alignments), conspicuous mounds with either rectilinear or rounded margins, hummocky terrain (including distinctly patterned forms such as ridge-rimmed depressions or doughnuts and discontinuous ridges), sinuous ridges and major channels and erosional cliffs or terraces.

The stratigraphy and sedimentology of the landforms was investigated wherever exposures were available. As such exposures are relatively rare and/or ephemeral, archival material was utilised wherever possible. Field exposures were recorded in scaled section sketches which included information on primary sedimentary structures, bed contacts, sediment body geometry, sorting and

texture, as well as any pertinent data on clast macrofabric. These data were then used to characterize lithofacies types and to allocate facies codes following the procedures of Evans and Benn (2004). Clast macrofabrics were measured on samples of 30 or 50 clasts from diamictons using A-axis orientation and dip, and plotted on Schmidt equal-area lower hemisphere diagrams using Rockworks™. Contouring of the stereoplots represents standard deviations from the mean.

### 3. Glacial geomorphology

The glacial geomorphology map of southeast central Alberta, featuring the Neutral Hills Uplands, is presented in Fig. 3 (see also Supplementary Information for high-resolution version). The ten types of landform-sediment signature identified on this map are systematically described and interpreted using typical example areas.

#### 3.1 Major glacitectonic thrust masses

Both major glacitectonic thrust masses and lower amplitude lineaments and ridges (see section 3.2) are recognised on the imagery as a series of closely spaced, parallel or sub-parallel, often sinuous ridges and troughs. The ridges are the surface expressions of the crests of large-scale folds and/or thrust-blocks and are clearly related to thrusting/glacitectonism of the underlying Cretaceous bedrock and, to a lesser extent, pre-existing sediments (Fig. 4) (e.g., Kupsch, 1962; Christiansen and Whitaker, 1976; Sauer, 1978; Moran et al., 1980; Bluemle and Clayton, 1984; Tsui et al., 1989; Fenton et al., 1993). The intervening troughs demarcate the bounding thrust faults and synclinal folds. A protocol for differentiating between glacitectonic ridges and similar looking recessional push-moraines on the prairies was proposed by Evans et al. (2014). The large glacitectonic thrust masses (composite ridges and hill-hole pairs, *sensu* Aber et al., 1989) of the region are well-documented (e.g., Neutral Hills, Nose Hill, Misty Hills, Mud Buttes, Sharp Hills; cf. Shetsen, 1987, 1990; Fenton et al., 1993; Atkinson et al., 2014a, 2018; Fig. 2), consequently their surface expression is easily recognised and mapped. Many prominent arcuate assemblages, for example in the Prospect Valley area, document bedrock folding, detachment and displacement associated with readvances and subsequent stagnation of Laurentide Ice Sheet lobes across existing Quaternary deposits (see section 4). The orientation of these ridges is predominantly uni-directional and generally transverse to the direction of applied stress (ice-push/glacier ice flow) and thereby can be used to delineate the boundaries of individual thrust masses. However, multiple ridge orientations are also preserved in some areas and record the presence of juxtaposed thrust masses or those with apparently superimposed or overprinted glacitectonic signatures. In some areas, the overprinting is so extensive

that individual thrust masses cannot be delineated, but instead the landform patterns are mapped as zones of lineaments and ridges (see section 3.2).

The juxtaposition of separate thrust masses and the overprinting of tectonic fabrics clearly records repeated phases of glacitectonism which led to the construction of composite ridges and hill-hole pairs. An excellent example occurs around the south shore of Killarney Lake, where a thrust mass has been displaced to form the depression now occupied by this, and several other large lakes (Fig. 5a). Mapped as thrust bedrock by Bayrock (1967), the surface crenulations of the main thrust mass are orientated in two directions of NNW-SSE and WNW-ESE, both indicating displacement from the source depression immediately to the north. Although the sequence of overprinting is difficult to determine, it appears that the thrusting was initially from the NNE (phase 1) and probably coincided with the detachment and transport of a ~18 km<sup>2</sup> bedrock raft 25 km further to the southwest, which now forms a low hill between Fleeinghorse and Laurence lakes (Fig. 5a) and likely relates to flow at the westernmost edge of Maskwa Ice Stream (cf. Norris et al., 2018). A subsequent phase of compression from the ENE (phase 2) resulted in the development of ridges which crosscut the earlier phase 1 thrust mass (Fig. 5a) as well as a series of densely-spaced crenulations aligned NNW-SSE on the east shore of Killarney Lake (Fig. 5a) which continue northwards for some 13 km towards the town of Chauvin, where they form part of the hill-hole pair now occupied by Reflex Lakes (Fig. 3). The final phase of glacitectonism in the Killarney Lake area led to the formation of an arcuate set of crenulations on the proximal side of the main thrust mass which cross-cut the earlier phase 2 landforms and are consistent with a direction of ice-push from the north and NNE (phase 3).

Outcrops through the Killarney Lake thrust mass are located on the summit and proximal slopes (KL1 and KL2; Fig. 5a) and expose a core of Quaternary sediment rather than bedrock (Fig. 5b). Section KL1 reveals >1 m of laminated sands and fines with massive gravel lenses unconformably capped by a 1.2 m thick matrix-supported diamicton that exhibits a lower pseudo-laminated and upper massive appearance. This diamicton is in turn overlain by a massive, matrix supported diamicton with a more clay-rich matrix. The contact of the two diamictons is sharp and is also marked by an attenuated lens of mudstone derived from the local bedrock and which thickens to 1.1 m in mid-section and pinches out to the right and left sides of the exposure. The diamictons are typical of the tills in the region. Where pseudo-laminated, they have been derived by glacitectonic cannibalisation of underlying glacialacustrine deposits, here represented by the lower laminated deposits; vertical gradation to a massive appearance reflects homogenisation in the deforming layer (Evans et al., 2006, 2012; Evans, 2018). A clast macrofabric from the lower Dml indicates an early glacier stress direction from 322°,



which corresponds with subtle fluting orientations to the north and east of the site (Fig. 3). The emplacement and attenuation of the mudstone lens relates to a later phase of ice flow but a macrofabric on the upper diamicton does not provide a clear sense of the shearing direction; it instead displays high dip angles (average of 47°) typical of crevasse squeeze deposits (cf. Evans and Rea, 2003; Evans, 2018). Section KL2 displays up to 4 m of pseudo-laminated diamicton within which there is a <0.5 m layer of sheared and attenuated sand and silt laminae, glacitectonically interleaved with the overlying and underlying diamicton (Fig. 5b). Repetition of the lower Dml and overlying sheared sands, silts and diamict within the lower part of the section provide evidence of larger-scale thrust-repetition and imbrication of the sequence. Importantly this lower imbricated sequence is truncated by the base of the upper Dml (see Fig. 5b). The stress direction for this event is recorded in a clast macrofabric from the lower part of the upper diamicton, which displays a weak easterly to northeasterly dipping signature. The consistency of the lower fabrics from both Killarney Lake sections is a record of early ice flow over glacialacustrine deposits in the area, after which thrusting displaced and attenuated glacialacustrine deposits and bedrock. Of the thrust directions apparent in the surface crenulations of the thrust mass, only the northeasterly imposed stress (phase 3) is recorded in the upper till fabric.

A further example of overprinted tectonic fabrics is the assemblage of thrust masses comprising the western Neutral Hills and the Nose Hill/Ribstone Creek area (Figs. 3, 5c). Here the predominant ice flow direction and displacement is from north to south, but individual thrust masses recording this displacement are superimposed on an older set of more subtle ridges recording glacitectonic stress from the WNW or NW, which is consistent with the relative age and orientation of large-scale flutings in the region (Ó Cofaigh et al., 2010; Atkinson et al., 2014b). Additionally, the most recent thrust masses display arcuate ridge patterns and evidence of periclinal to dome-like folding of the bedrock strata, created as they were displaced from up-ice depressions to form hill-hole pairs (especially well illustrated by the thrust masses south of Sounding Lake and by Nose Hill; Fig. 5c). Although the cores of these thrust masses are clearly bedrock, the relatively smaller ridges located on their distal slopes are composed of deformed (folded and thrust) penecontemporaneous Quaternary glacialigenic deposits. Collectively, these glacitectonic landforms form an east-west aligned assemblage which can be traced across the centre of the map area, which because it has not been glacially overrun, must demarcate the limit of an ice sheet readvance. In contrast, the older, more subtle ridges comprise elongate chains of hummocks, locally heavily incised and overprinted with glacialfluvial landforms (see sections 3.6-3.8) and appear to have been developed mostly in Quaternary deposits.

247

248 To the south of the Neutral Hills, complex overprinting of thrust masses is evident in the multiple  
249 ridge orientations of the Misty Hills, Sharp Hills, Mud Buttes and Esther uplands (Figs. 2, 3). Here the  
250 outermost (southern) thrust masses form an arcuate assemblage indicative of an ice lobe that  
251 advanced towards the south and displacement of bedrock derived from the large topographic  
252 depression now partially occupied by Grassy Island Lake and its subsidiaries (Fenton et al., 1993; Fig.  
253 6). The subsequent displacement and partial rotation of thrust masses in the horizontal plane inside  
254 the arcuate assemblage records further thrusting events, manifest in the construction and overriding  
255 of the Mud Buttes cupola hill (Phillips et al., 2017; see section 3.3). Towards the east of the Misty  
256 Hills complex lies a terrain with similar partially overprinted lineations but recognising the  
257 boundaries of the individual thrust masses is difficult due to a discontinuous blanket of glacialfluvial  
258 landforms and sediments (Grassy Island Moraine of Phillips et al., 2017) deposited during the final  
259 downwasting of the ice lobe within the Grassy Island Lake depression (see section 4). The western  
260 edge of the complex comprises a block with strongly N-S aligned ridges and furrows, which are  
261 muted on their westernmost flank due to an overlying layer of till (Fig. 6). This till relates to a subtle  
262 fluting alignment (see section 3.4) recording ice flow from the west and the construction of the  
263 western thrust block at the margin of this flow event. The eastward displacement of the western  
264 block was significant enough to superimpose N-S-trending glacitectonic ridge pattern upon an  
265 arcuate but predominantly E-W structural grain observed within the centre of the Misty Hills  
266 complex.

267

268 Although these major thrust masses are mantled by discontinuous till veneers that predate a series  
269 of later ice lobe readvances, they are clearly composed of Cretaceous bedrock. Nevertheless, ridges  
270 and furrows on their summits locally contain features normally associated with sediment-cored  
271 glacialigenic landform-sediment associations. These include ridge-rimmed depressions or doughnuts  
272 and isolated ponds reminiscent of kettle holes, as well as areas that have been subject to mass  
273 movement and the production of apparent retrogressive flow scars (Fig. 7).

274

275 Like the doughnuts observed between recessional push moraines in other areas of the prairies  
276 (Evans, 2003; Evans et al., 2014), those on the summits of the major thrust masses are often aligned  
277 to form discontinuous chains within the tectonically controlled furrows (Fig. 7a). Previous  
278 observations of such features on the proximal slopes of thrust masses (e.g. Dirt Hills, Saskatchewan)  
279 have been attributed to the escape of over-pressurized groundwater or artesian escape vents, which  
280 played a critical role in the large-scale displacement of bedrock and was then released through the

fractured thrust mass once glacier stress dropped (“extrusion moraines” of Boulton and Caban, 1995). Similar features have been reported from the immediate distal slopes of prairie-based glacitectonic thrust masses, where they are termed hydrodynamic blowouts (Bluemle, 1993) and in some cases eskers can emerge from source depressions, indicating that pressurised water created tunnels beneath the glacier snout where it overrode the thrust mass (Bluemle and Clayton, 1984).

Modern analogues for this process have been reported from the distal slopes of composite ridges created by glacier surging in Iceland, where pipes emerge from the moraine front and have clearly discharged meltwater into channels on the foreland (Kjær et al., 2006). Not unrelated is Bik’s (1969) theory that doughnuts might represent pingo scars, whereby groundwater emerging from upwellings in the immediate proglacial zone has the potential to freeze in winter and construct icings or aufeis, such as occurs on glacier forelands in Svalbard (Gokhman, 1987; Hodgkins et al., 2004). This process may be accentuated by supercooling due to rapid de-pressurization as groundwater migrates from the subglacial system into the proglacial zone (cf. Cook and Knight, 2009). Sedimentologically, all of these blowout or injection features would be recorded as clastic dykes or hydrofracture infills (Mandl and Harkness, 1987; Le Heron and Etienne, 2005; van der Meer et al., 2009; Phillips et al., 2013). Although groundwater is more widely cited as the cause of blowout features, another potential driver in the Cretaceous strata of the prairies could be methane release during the last deglaciation. Changing pressure and temperature regimes associated with the retreat of the Scandinavian Ice sheet are proposed to have triggered dissociation of shallow gas hydrates and the release of methane, resulting in widespread pockmarks on the floors of the North, Barents and Norwegian seas (Cremiere et al., 2016; Mazzini et al., 2017). On the prairies, the influx of meltwater from the LIS is proposed to have displaced brines that previously inhibited microbial action within organic rich units of the Western Canada Sedimentary Basin, thereby triggering methanogenesis and re-establishing conditions suitable for the formation of shallow biogenic gas deposits (Grasby, 2013). Degassing of these deposits in terrestrial settings potentially produced doughnut-shaped ring forms similar to those of blowouts associated with escape of pressurised groundwater, since the preservation potential of constructional features would be higher than in subaqueous environments.

Larger burst-out structures are evident on the crests and distal slopes of some large thrust masses, the best example being on the eastern end of the eastern Neutral Hills (Fig. 7a). This feature comprises a fan shaped assemblage of doughnut forms, which blanket and mostly mask the structural lineaments, with an apex located at a discontinuous but deep channel through the thrust

mass summit occupied by a chain of ponds. An esker starts at the eastern side of the channel and extends towards the ENE through the glaciectonic ridges and furrows as an ice-margin parallel feature directed by the topography emerging from the thinning snout (cf. Storrar et al. in press). The esker likely represents a later stage of water release after near surface pressurised water was initially driven through the thrust mass to emerge through artesian pipes and then via the surface as a fan.

Isolated pits, often containing small ponds, are enclosed by cliffed or steep margins that cut across the structural grain represented by the ridges and furrows (Fig. 7b). Larger pits, often occurring in chains and bounded by fault scarps, also cut across structural ridges but appear to represent the collapse of larger volumes of the thrust masses, especially around their lower margins (Fig. 7c). These depressions most likely represent voids created by the melt-out of glacier ice and hence are kettle holes but their occurrence on the summits of thrust bedrock masses is difficult to reconcile with such an origin unless debris-covered stagnating ice was lying on the land surface prior to proglacial thrusting. More extensive buried glacier ice is evidenced by the larger pits and associated fault scarp boundaries. Where these occur on proximal slopes of thrust masses they are associated with greater fragmentation of structural lineaments and more hummocky terrain and hence represent melt-out of the glacier snout that overrode the back of the moraine. Where they lie on distal slopes their boundaries/cliffed shorelines often tend to be rectilinear or arcuate and they parallel the structural grain of the surrounding lineaments (Fig. 7c). This indicates that large bodies of glacier ice were incorporated in the thrust mass and that they constituted thrust slices that later melted out to form elongate depressions. The corollary is that, prior to thrusting by the readvancing ice lobes, large areas of stagnating glacier ice occupied the prairie surface and these buried ice masses likely contained glaciﬂuvial sediment assemblages such as eskers and kamiform features.

More enigmatic are conspicuous mass movement features that resemble large retrogressive flow scars. They are often associated with melt-out pits and lie in and around the major thrust masses where they appear to relate to mass failure in the oversteepened topography. One enormous example, up to 40 m deep and hosting a large (1.4 km long) lake, lies on the distal slope of the west end of the eastern Neutral Hills, immediately south of Sounding Lake (Fig. 7d). Here the displacement of mass was towards the northeast to form an arcuate cliff and source depression and a ridged, lobate failure mass with a leveed failure toe. As the volume of the failed mass appears to equate to the size of the source depression, an ice melt-out origin is unlikely and hence failure may have been triggered by pressurised groundwater driven from the thrust mass immediately to the

northwest of the site. Further similar features, more likely to relate to ice melt-out, occur throughout the major thrust masses in the arc of composite moraine ridges that demarcate the readvance margin of the Prospect Valley lobe to the north (see section 4).

### *3.2 Short lineaments and ridges*

A range of short lineaments and ridge types are evident in the map area and conform generally to the classifications of major transverse ridges (MTR) types 1 and 2 of Evans et al. (2014). In many areas, differentiating MTR type 1 and 2 from the imagery is difficult, especially in the absence of outcrops, and therefore the map unit is defined as “lineaments and ridges (including definite and possible glacetectonic structures and areas of recessional push moraines)” (Fig. 3). The potential occurrence of esker fragments in these assemblages is also acknowledged.

The MTR type 1 constitute corrugation patterns indicative of glacetectonic thrusting but, unlike those reported by Evans et al. (2014), are not always fluted and hence many do not have the appearance of unequivocally being glacially overrun (Figs. 8a, b). They are interpreted as the product of shallow, thin-skinned folding and thrusting of bedrock or sediment and resemble, albeit with lower amplitudes, the ridged and furrowed surfaces of the relatively deeper-seated major thrust masses described above. Cross-cutting lineaments, similar to those identified in major thrust masses, record superimposed or overprinted glacetectonic signatures, although individual thrust masses cannot be delineated in areas of extensive overprinting. Instead, the landform patterns are mapped as zones of lineaments and ridges (Fig. 8c). Large areas such as this are also characterised by ridge fragmentation due to dense pitting and the occurrence of kettle holes whose margins dissect all lineament sets. Although there is a hummocky appearance to these areas, the preservation of cross-cutting lineaments indicates that pitting was due to melt-out after the tectonic grain was developed. Hence it appears that large bodies of glacier ice were incorporated in the thrust masses as thrust slices that later melted out to form elongate depressions. Similar to the kettle holes and melt-out pits developed on the major thrust masses, these landform associations indicate that large areas of stagnating glacier ice occupied the prairie surface prior to thrusting by readvancing ice lobes, and glacialfluvial sediment assemblages such as eskers and hummocky kamiform features (cf. Eyles et al., 1982) developed prior to and after thrusting.

The MTR type 2 are recessional push moraines similar to those developing at modern active temperate glacier snouts (Fig. 8d) and only locally occur in the southern part of the map area. In areas where ridge patterns are extensively overprinted and are not mapped as major thrust masses,

some of the ridges could represent recessional push moraines superimposed over glacitectonic fabrics, especially if melt-out pits and kettle holes do not cross-cut all lineament sets. Alternatively, the multiple ridge orientations record superimposed tectonic fabrics typical of complexly folded and faulted strata (cf. Price and Cosgrove 1990; Hatcher 1995). A glacitectonic origin is favoured for these linear, sub-parallel ridges rather than a minor recessional push moraine origin (*sensu* Benn and Evans 2010), which tends to result in sinuous, crenulate or sawtooth and/or locally bifurcating planforms that preserve the shape of the former receding ice margin (MTR type 2 of Evans et al., 2014; cf. Boulton, 1986; Krüger, 1995; Evans and Twigg, 2002; Evans et al., 2016b, 2017; Chandler et al., 2016).

### *3.3 Conspicuous mounds and relatively higher topography (cupola hills and rubble terrain)*

Areas of smoothed, often fluted terrain that rise relatively abruptly above the surrounding prairie surface are characterised by the presence of muted ridges or corrugations on their surface similar to the sub-parallel lineations of thrust mass surfaces (Fig. 9). Such features have been reported previously from prairie settings by Evans et al. (2014), who classify them as MTR type 1 and interpret them as glacially overridden thrust masses or cupola hills (*sensu* Aber et al., 1989). Their arcuate or lobate plan forms often indicate an ice-marginal origin, as demonstrated by the terrain immediately north of the town of Coronation (Fig. 9a). A more elongate ridge lies immediately NE of Sounding Lake and is adorned with flutings and geometric ridge networks created during the last phase of subglacial streamlining of the area (Fig. 9b); its surface also contains pits indicative of ice melt-out, similar to the ice-cored drumlins reported by Schomacker et al. (2006). A classic example of a cupola hill is the Mud Buttes complex, where extensive exposures clearly demonstrate its multi-phase glacitectonic origins (Phillips et al., 2017; Fig. 4c). More difficult to identify are overridden thrust masses whose structural lineaments parallel the direction of the later overriding ice flow. One such example occurs in the south of the map area and was initially displaced southwards from the Sounding Creek depression. This was later overrun by ice flowing eastwards, as manifest in flutings that cross the cupola hill summit as well as the adjacent prairie surface. On the cupola hill summit, the underlying bedrock structures are apparent as sharp relief, narrow ridges that lie sub-parallel to the more linear flutings (Fig. 9c).

Smaller upstanding masses of displaced bedrock are common throughout Alberta and have been classified as “rubble terrain” by Fenton et al. (1993) or “aligned rubble” by Atkinson et al. (2018). They comprise assemblages of small hills, often with rectilinear edges, that have been displaced from a nearby source depression, but in contrast to hill-hole pairs the thrust mass has been

disaggregated down flow within narrow dispersal trains that typically parallel other ice flow features such as flutings (Atkinson et al., 2018). The blocks are essentially mega-rafts (*sensu* Stalker 1973, 1976; Aber et al., 1989) and may be located only a short distance from fault-bounded or fracture-bound source depressions, which are often visible as straight-edged lakes (Aber et al., 1989; Fenton et al., 1993). A range of examples exist in the map area and include elongate assemblages that have been widely dispersed from their likely source (e.g. southeast of Kirriemuir; Fig. 10a), isolated rafts that lie within other landform suites but are identifiable by their surface morphology (Fig. 10b), and incipient rafts that have been moved only a short distance from their fracture-bounded depressions (Fig. 10c). At smaller scales certain flutings appear to be composed of chains of closely spaced mega-rafts, here termed “rubble stripes” (Fig. 10d), where disaggregated bedrock has been differentially displaced downflow and increasingly broken down into smaller fragments, and consequently involved in grooving the glacier bed. Such fluting-like landforms are instructive in that they demonstrate the juxtaposition of subglacial grooving as well as stoss-and-lee streamlining processes in fluting production (see section 3.4).

Although the constituent blocks within rubble terrain are normally assumed to be bedrock, exposures can reveal that the displaced and disaggregated materials comprise Quaternary deposits. For example, at the Kirriemuir assemblage (Fig. 10a) a quarry exposure through one of the blocks reveals a core composed of normally faulted, rhythmically bedded sands, silts and clays with gravel lenses, coarsening upwards to horizontally bedded gravels and sandy gravels, which are in turn deformed and truncated by a massive, matrix-supported diamicton with attenuated sand lenses and stringers diagnostic of subglacial traction till (Evans et al., 2006; Evans, 2018; Fig. 10e). These sediments are compatible with initial sedimentation in an ice-walled lake plain (Clayton and Cherry 1967; Clayton et al., 2008; see Section 3.7) which was later glacitectonically displaced and overrun by ice flowing towards the SSE, as indicated by the subtle flutings running through the rubble assemblage (Fig. 10a) and asymmetrical folds and low-angle extensional faults in the deformed sediments (Fig. 10e); a clast macrofabric from the till on the southern edge of the block displays a WSW dipping signature indicative of till plastering over the distal slope of the feature.

### *3.4 Multiple parallel lineations (flutings and ice flow-aligned stripes)*

Areas of straight, parallel lineations represent subglacially streamlined terrain and comprise flutings and elongate drumlins up to 14 km long. They occur in assemblages that represent flow sets aligned at various orientations and thereby relate to sequential changes in ice flow directions. Flow sets have been employed over the wider region of the Canadian prairies to demarcate the imprints of

palaeo-ice streams and their cross-cutting relationships (Ross et al., 2009; Evans et al., 1999, 2008, 2014; Ó Cofaigh et al., 2010; Atkinson et al., 2014a, b; Paulen and McClenaghan, 2015; Norris et al., 2018) and in the map area represent the footprints of a number of lobate ice streams. The appearance of variously orientated flutings in association with other ice-stream marginal landforms enables establishing a relative chronology of events in the map area (see Section 4).

In the west, the bed of the Central Alberta Ice Stream (CAIS; cf. Evans et al., 2008) is recorded by NNW-SSE aligned flutings (Fig. 11a) south of Coronation. These features comprise corridors of grooved terrain, interspersed within bar-channel complexes of the “Coronation-Spondin scabland” (Sjogren and Rains, 1995). Importantly, the grooves narrow downflow, coincident with an increase in the number of progressively narrower positive relief flutings. Also significant in the area is the development of hill-hole pairs, which exhibit subtle superimposed flutings (Fig. 11a). The sequence of landform production in this area is evident from flutings cross-cutting the bar-channel complexes, indicating that the water flow responsible for this scabland pre-dated the subglacial streamlining and the production of the grooved corridors; indeed the more subtle flutings would not have survived the fluvial erosion. The configuration of many of the bar-channel complexes also appear to have been guided by the position of overridden thrust mass lineations. This detail, now evident in LiDAR imagery, contradicts an earlier reconstruction that the CAIS ice stream footprint was cross-cut by the flood features (cf. Evans et al., 2008), although the proposed subglacial origin of the fluvial erosion remains valid. This sequence of events is compatible with the proposal by Evans et al. (2008) that basal sliding rather than till deformation was driving fast ice flow in this area of thin till cover. Specifically, ice-bed decoupling may have been initiated by the subglacial meltwater activity, which itself was triggered by the sub-marginal decanting of ice-dammed lake waters from the receding LIS margin further to the west. The fluting production during ice streaming appears to have been developed at the up-ice end of the corridors by groove ploughing, with the southeastward narrowing of the grooves indicating progressive down-ice comminution of the displaced block. As the grooves begin at the overridden thrust moraine belt near Coronation (Fig. 9a), we propose that ploughing was initiated by displaced bedrock mega-rafts, a process that is evident in the study area in the widespread assemblages of rubble terrain and fluting-like rubble stripes. The creation of narrow upstanding flutings in a down-ice direction within the groove corridors is attributed to the combined effects of the stoss-and-lee deformation process (cf. Boulton, 1976; Rose, 1989; Benn, 1994) and longitudinal erosion of grooves by the remaining fragments of the mega-rafts, together with the accompanying lateral deformation/displacement of material to form the paraxial ridges (Atkinson et



al. 2018). Raft liberation within the groove corridors is evident also in the occurrence of streamlined hill-hole pairs.

Further evidence demonstrating the importance of bedrock mega-rafts to fluting construction are rubble stripes (Fig. 10d), where flow-parallel lineaments appear to be composed of chains of closely spaced mega-rafts. Excellent examples occur along the footprint of a palaeo-ice stream in the north of the map area (Fig. 11b), herein named the Fabyan-Amisk ice stream after the towns located in the north and south of the footprint respectively; this former ice stream bed extends some 22 km north of the map in Fig. 3. Large areas of the fluted ice stream bed contain disaggregated bedrock, with blocks in various stages of down-ice transport and comminution. The hypothesized role of rubble stripes and mega-rafts on the initiation of stoss-and-lee flutings as well as subglacial bed grooving can be tested by identifying raft origins and linking the starting points of both positive and negative relief flutings to those rafts. On the Fabyan-Amisk ice stream bed, the initiator clusters or partially disaggregated thrust masses occur at the south margin of a large preglacial valley thalweg (Stalker 1961; Farvolden 1963; Andriashek, 2018), where glacetectonic dislocation is widely known to liberate bedrock blocks (Tsui et al., 1989). Groove and mega-raft pairs also clearly illustrate the role of grooving in subglacial landform evolution (Fig. 11c).

### *3.5 Rectilinear ridges (geometric ridge networks)*

Geometric ridge networks (Bennett et al., 1996) are conspicuous landforms on the prairies and have been widely reported (Flint, 1928; Sproule, 1939; Deane, 1950; Colton, 1955; Gravenor and Kupsch 1959; Atkinson et al., 2018). They have been described as straight or slightly arcuate till-cored ridges that intersect at acute or right angles to form waffle, diamond, or box-shaped patterns and with some intersections resembling hairpins or wishbones. These characteristics were initially attributed to crevasse infills (Gravenor and Kupsch, 1959), with more recent studies on modern glacier forelands classifying such features as crevasse squeeze ridges (CSRs) related to surge-type behaviour (Sharp, 1985a, b; Bennett et al., 1996; Evans and Rea, 1999, 2003; Evans et al., 2007). These modern analogues have been used to infer palaeo-ice stream surging on the Canadian prairies by Evans et al. (1999, 2008, 2016a), where the arcuate, ice flow-transverse and subparallel sets of conjugate paired ridges are created by subglacial sediment injection into full depth, mode 1 tensional crevasses following the switch from surge to quiescence phases (cf. van der Veen, 1998a, 1998b; Rea and Evans, 2011).

The geometric ridge networks of the map area have all the characteristics of CSRs (Fig. 12). They occur across the full width of the various ice stream trunks or lobate footprints and predominantly display arcuate, downflow-convex limbs similar to those reported by Evans et al. (1999, 2008), rather than within discrete, relatively narrow corridors such as described by Evans et al. (2016a) within the trunk of the Maskwa Ice Stream to the east of the map area (cf. Ross et al., 2009; Ó Cofaigh et al., 2010; Norris et al., 2018; Fig. 1). They are everywhere intimately associated with long flutings indicative of fast flow trunk zones (Fig. 3), such as on the bed of the CAIS to the west, in the footprint of the Prospect Valley lobe (see section 4), and in the trunk zones of the Fabyan-Amisk (Fig. 11b) and Eyehill Creek-Sounding Lake ice streams (see section 4). They also occur immediately inside arcuate assemblages of thrust masses similar to their occurrence in modern surging glacier foreland records (Sharp, 1985a, b; Evans and Rea, 1999, 2003; Evans et al., 2007), for example, north of Provost and west of Wainwright (Fig. 3). The CSR field on the bed of the CAIS around the town of Brownfield displays further features considered diagnostic of glacier surging such as zig-zag eskers (Fig. 12a; Knudsen, 1995; Evans and Rea 1999, 2003; Evans et al., 2007).

Exposures through the CSRs in the region are rare but a road cut to the north of the map area, in the CSR field around Lloydminster (the northern extension of CSRs of the Prospect Valley lobe) (Fig. 12b), provides some insight into their sedimentology. This exposure is cut through a single CSR and displays a two tiered diamicton (till) sequence from which clast macrofabrics are generally weakly aligned NNW-SSE, especially at the core of the ridge, but weaken significantly at the ridge flanks and include some very high clast dip angles. Overall the clast dip angles are relatively high (averages ranging 25-44°; Fig. 12c) and indicate a significant squeeze component in landform construction (26-44° for modern Icelandic CSRs; cf. Evans and Rea, 2003; Evans, 2018). A clast fabric shape plot for the Albertan and modern Icelandic CSR tills also reveals a range of fabric strengths (Fig. 12b) but predominantly indicative of materials that have been subject to relatively low strains (Evans, 2018 and references therein).

### *3.6 Sinuous ridges (eskers)*

Sinuous ridges in formerly glaciated terrains are indicative of glaciifluvial sedimentation in ice-walled channels or tunnels and many have been previously mapped in the study area (Gravenor and Bayrock, 1955; Bayrock, 1958a, b, 1967; Shetsen, 1987, 1990; Kjarsgaard, 1988; Atkinson et al., 2018). Most eskers generally have narrow and often discontinuous, sharp-crested sinuous ridges but the map area also contains some very large, flat-topped examples that pass laterally into flat-topped hills (prairie mounds or plains plateaux of Gravenor and Kupsch, 1959; see section 3.7). These

unusually large landforms were previously partially identified in the area by Bayrock (1967). The most impressive example spans the Sounding Lake depression and extends for over 90 km, with parts of its flat summit reaching widths of 2 km (Fig. 13a). The main ridge of the Sounding Lake esker displays a tortuous alignment with predominant NW-SE and N-S trends and a conspicuous circular deflection that forms part of a 180° change in direction at the eastern end, immediately north of the lake. Additionally, the largely single crested main ridge is joined by tributaries and distributaries composed of smaller multiple ridges. In the south, the most intricate feeder system emerges from Neutral Valley and trends north-northeastwards, where it joins up the western elbows of the main ridge before continuing northwards beyond the town of Metiskow. Additional braided esker networks join the southern part of the main ridge from the Neutral Hills, on the west side of Sounding Lake. These widen and converge to form large flat-topped ridges where they meet the main ridge. A further branch of ridges trends northeastwards from the northern part of Sounding Lake esker past the town of Cadogan. The two northern ends of the esker extend towards the composite thrust moraine arc of the Prospect Valley lobe where readvance of the ice margin appears to have compressed the esker into the moraine (see Section 4). Although they do not occupy deeply incised valleys, these flat-topped esker ridges resemble Type 3, ice-walled canyon eskers (cf. Perkins et al., 2016) which exhibit flat-crested segments resulting from lake sedimentation. This depositional environment is compatible with our observations, particularly the close association between eskers and ice-walled lake plains in the map area (Fig. 13c). The multiple sharp-crested tributary and distributary eskers presumably represent the Type 1 subglacial eskers of Perkins et al. (2016), which fed into and linked the ice-walled canyon eskers.

Because of its complex network of tributaries and distributaries and its overall deranged alignment, palaeoflow directions in the Sounding Lake esker are difficult to assess. However, based upon the assumption that esker networks will widen and coalesce and their crests will flatten to open out into ice-walled lakes in a downstream direction, meltwater flow appears to have been from the Neutral Hills and into the Sounding Lake-Eyehill Creek depression, flowing first towards the east and then northwest and north after turning back on itself (Figs. 3, 13a). This somewhat counter-intuitive flow direction was originally proposed by Shetsen (1987) after the mapping of Bayrock (1967). Meltwater then likely developed a more direct route north-northeastwards from Neutral Valley towards Metiskow, cutting off the more deranged and lengthy routeway towards the east. Hence meltwater flowed back through the Neutral Hills after its summit had been exposed by downwasting ice, with the earliest drainage direction being recorded by a W-E aligned esker network running along the base of the proximal slope of the eastern block of the thrust moraine complex. The majority of the

drainage and glaciﬂuvial sedimentation was then concentrated along the large esker ridge. The origins of the water must have been from the large expanse of stagnant ice lying immediately distal to the Neutral Hills (see Section 3.9) as well as the numerous outsized and abandoned channels that converged on the gaps through the thrust moraine complex from the south and discharged regional meltwater decanting from proglacial lakes located to the west (see Section 3.10). In order to create such large eskers in the Sounding Lake-Eyehill Creek depression, meltwater must have descended into an extensive glacier body that still occupied this lowland terrain. Faint WNW-ESE ﬂutings in the depression, can be traced eastwards into a palaeo-ice stream footprint. This indicates that the area was occupied by a late stage easterly-ﬂowing ice mass which blocked northeasterly draining regional meltwater, thereby giving rise to the creation of the large eskers and their tributaries.

A further extensive network of large ﬂat-topped eskers with tributary and distributary branches occurs 10 km south of Wainwright, and in the terrain adjacent to Ribstone Lake (Fig. 13b). The largest features form a west-east orientated system in which a single, ﬂat-topped ridge is fed by tributaries converging from the southwest from the area north of Amisk, indicating that meltwater initially drained northward along the Fabyan-Amisk ice stream bed, and subsequently ﬂowed eastward to join the main esker ridge after the ice stream had shut down. The main esker ridge then fans out into a series of ﬂat-topped distributaries that terminate at an expansive, ﬂat and variably pitted outwash on the distal edge of the Prospect Valley composite thrust moraine belt (Fig. 13b; see Sections 3.8 and 4). This area appears to represent a former stagnant ice zone through which englacial and subglacial drainage created tunnel ﬁlls/eskers beneath a contemporaneous supraglacial to ice-contact outwash fan; the fan later locally collapsed to form isolated ﬂat-topped hills and to reveal the underlying eskers. Comparable depositional settings have been identiﬁed at modern temperate glacier snouts (e.g., Price, 1969, 1982; Howarth, 1971; Evans and Twigg, 2002; Storrar et al., 2015) but the size, low sinuosity and rapid lateral change from small sharp-crested esker tributaries to a single, ﬂat-topped esker terminating in a large area of buried glacier ice are characteristics very similar to those of downstream ice tunnel unroofing and re-entrant creation typical of jökulhlaup-fed systems (Russell et al., 2001a). Hence the Wainwright-Ribstone Lake esker is interpreted as a jökulhlaup-generated esker. Indeed, kettle-like depressions in both the Wainwright-Ribstone and the Sounding Lake-Eyehill Creek ﬂat-topped eskers indicate that both systems could have evolved by ice tunnel roof collapse during catastrophic discharges (Mokhtari Fard, 2002).

Numerous examples of minor eskers occur within areas of pitted or hummocky terrain, where they are associated with ﬂat-topped hills (Figs. 13c, d; see Sections 3.7-3.9). They appear as both

relatively continuous and discontinuous sinuous ridges and often link up with flat-topped hills. Linear flat-topped hills are also observed forming continuations of esker ridges, indicating that englacial and/or subglacial tunnels locally developed into supraglacial ice-walled channels. Together with the associated hummocky and pitted topography, this constitutes a landform assemblage diagnostic of glacier karst (cf. Clayton and Cherry, 1967; Clayton et al., 2008; Livingstone et al., 2010). The sinuous features identified here as likely eskers have been previously classified as types of “disintegration ridges” (e.g., Johnson and Clayton, 2003), although this term was also used by Gravenor and Kupsch (1959) to include crevasse fills (geometric ridge networks). Sinuous chains of elongate doughnut forms or rim ridges (cf. Gravenor and Kupsch, 1959; Parizek, 1969; Mollard, 2000) also occur in association with these inferred eskers, in places running parallel with the sinuous ridges (Figs. 13c, d and 14). Such features may relate to the process-form regime recognised on some modern glacier forelands in Svalbard and Iceland in which freshly abandoned subglacial tunnels become the foci of till squeezing from a deforming bed to form “till eskers” (Christoffersen et al., 2005; Larsen et al., 2006; Evans et al., 2010, 2016b). In the case of an insufficient pressure differential and/or low till supply, the squeezed material would not completely fill the tunnel, instead creating ridges along its walls. The squeezing of till into tunnels and esker cores has been recognised previously by, for example, Banerjee and McDonald (1975) and for the Canadian prairies by Burke et al. (2015). A similar scenario was envisaged by Parizek (1969) to explain “bead-like ice-contact rings”, but rather than a subglacial origin, he invoked the superimposition of ice-walled (supraglacial) channel fills on the glacier bed. However, none of these interpretations account satisfactorily for chains of circular forms or doughnuts, which we attribute on major thrust masses as piping orifices. A piping origin for sinuous chains of doughnuts associated with eskers would imply the escape of pressurised groundwater into low pressure abandoned subglacial tunnels or collapsed englacial tunnels, with long chains being created by the up-ice migration of production zones similar to those envisaged for normal eskers by Andersen (1931), Hebrand and Amark (1989), Hooke and Fastook (2007) and Storrar et al. (2014a, b). Hence, we propose a hypothesis whereby doughnut chains evolved due to the progressive activity of piping orifices along abandoned and/or collapsed tunnels. This is an alternative but not incompatible model to the subglacial pressing envisaged by Stalker (1960), Eyles et al. (1999) and Boon and Eyles (2001). Such a process could operate much like that of till esker formation where the settling and concomitant floor-melting of a widening englacial tunnel or moulin chain/ice-walled channel would create till ridges or doughnut chains by passive squeezing or pressing.

In many locations, eskers are associated with channels, either lying within and/or forming linear chains along them (Figs. 13c and d). In these settings, the channels are interpreted as subglacial tunnel channels (see Section 3.10) that evolved due to the lateral migration of tunnels through weak confining sediment and/or bedrock which was subsequently deposited in multiple esker ridges. This is illustrated by complex and often meandering esker ridges contained within channels of variable width and displaying arcuate cliff segments (Fig. 13d). Some tunnel channels contain segments that constitute flat-topped ridges that rise above the walls of the channels, such as in the area around Kinsella, just outside the western edge of the map area (Gravenor and Bayrock, 1956; Gravenor and Kupsch, 1959; Fig. 13c). These features are presumably eskers that locally infilled channels as a result of hydraulic jumps and hence prograded delta-like deposits that also aggraded upwards into the ice base, similar to the tunnel channel and ice-walled channel infill reported by Russell et al. (2001a, 2007) and Burke et al. (2008) following the 1996 jökuhlaup at Skeidararjökull, Iceland. The continuation of sinuous ridges (eskera) and doughnut chains across some tunnel channels at oblique angles clearly indicates that either the channel was ice filled and/or the ridges/chains were developed englacially or supraglacially (cf. Parizek, 1969).

### *3.7 Flat-topped hills (mounds)*

Clusters of flat-topped hills or mounds occur in association with glacialfluvial landforms, especially eskers and pitted terrain (Fig. 13c and d). Their close relationship with eskers, especially where eskers grade into elongate or linear assemblages of flat-topped mounds, indicate that they originated as the infillings of ice-walled channels or lakes, thereby constituting supraglacial eskers and ice-walled lake plains (*sensu* Clayton and Cherry, 1967; Clayton et al., 2008) respectively. Also visible in the map area are examples of rim ridges encircling flat-topped hills, features previously described as rim-ringed moraine plateaux (Hoppe, 1952; Stalker, 1960) and given a genetic classification of rim-ringed moraine-lake plateaux (Parizek, 1969). These ridge-rimmed mounds likely represent “unstable ice-walled lake plains” (Clayton and Cherry, 1967), where insufficient debris was available to fill the depression in the ice. In some cases, the lake infill was so thin that subglacial forms can be viewed through the lake plain (Fig. 14). Some very large flat-topped hills occur in the Sounding Lake-Eyehill Creek depression where they appear to be mostly disconnected from the eastern part of the large esker (Fig. 3). Closer inspection reveals that there are a number of minor eskers running between and alongside the hills and altogether these forms represent a drainage system that flowed towards the northeast and east, likely bleeding off from the large esker via a complex glacier karst network.

Smaller moulin infills have been envisaged by some researchers to account for doughnut forms (*sensu* Clayton, 1967), also known as prairie mounds (Gravenor, 1955), rimmed kettles (Christiansen, 1956) and closed disintegration ridges (Gravenor and Kupsch, 1959). In such a depositional scenario the doughnuts would effectively be small scale ice-walled lake plains created by the sloughing of supraglacial material into small ice-walled depressions or sinkholes. Elsewhere, doughnut forms appear to be linked to the construction of major thrust moraines (see Section 3.1), esker formation (see Section 3.6) or hummocky terrain development (see Section 3.9), indicating that they likely have polygenetic origins (cf. Mollard, 2000), the interpretive details of which need to be compatible with their geomorphic context.

### *3.8 Areas of pitted glacifluvial deposits*

Only areas of predominantly flat terrain with largely isolated surface depressions can be confidently classified as pitted glacifluvial deposits based upon morphology alone. Elsewhere, almost total collapse of buried ice cores renders the terrain similar to hummocky terrain. However, previous mapping by Bayrock (1967) identified some hummocky areas where surficial materials were of glacifluvial origin and hence these locations can be classified as areas of pitted glacifluvial deposits.

As discussed in Section 3.6, the most prominent area of pitted glacifluvial deposits forms an expansive, flat and variably pitted surface on the distal edge of the Prospect Valley composite thrust moraine belt southeast of Wainwright (Fig. 13b). At its northern edge, significant collapse due to ice melting is evidenced by the numerous water-filled depressions surrounding Ribstone Lake. The occurrence of discontinuous sinuous ridges (eskers) in this area are interpreted as the products of englacial and subglacial tunnel fills beneath a contemporaneous supraglacial to ice-contact outwash fan. Similar extensive collapses and channel incisions appear at the southern edge of this fan, which is fringed by arcuate lineaments that parallel the Prospect Valley moraine belt, which itself displays extensive pitting indicative of glacitectonic thrusting of the ice-cored outwash. Drainage westwards, contemporaneous with thrust moraine construction and over the top of pre-existing ice-cored outwash associated with the Wainwright-Ribstone Lake esker (see Section 3.6), is evident in a series of east-west aligned surface channels that deepen westward. A conspicuous sinuous chain of elongate depressions trending south-north on the outwash surface (Fig. 13b) likely represent the collapse of the material into a buried tunnel channel.

Some areas that appear to constitute pitted glacifluvial materials represent types of glacitectonic thrust masses, indicative of large areas of stagnating glacier ice juxtaposed with glacifluvial

sediment-landform assemblages and highly disturbed bedrock, all of which were thrust by readvancing ice lobes. Such process-form regimes are typical of modern surging glacier snouts (Raymond et al., 1987; Evans and Rea, 1999, 2003; Schomacker et al., 2006; Evans et al., 2007, 2009; Roberts et al., 2009; Evans, 2011). These are evidenced by two types of landform assemblage. Firstly, substantial lakes with cliffed, often rectilinear or arcuate boundaries are representative of the melt-out of extensive buried glacier ice and its overburden of glacialfluvial deposits juxtaposed with bedrock rafts; these have all been proglacially thrust to form linear or arcuate ridges and depressions that broadly parallel those of the more coherent thrust masses (i.e. bedrock) that were pushed into them (Figs. 7c and 15a). Limited exposures through hummocks in this terrain reveal significant deformation, thrust faulting and diapirism that has resulted in complex melanges of the component materials (Fig. 15a). Secondly, areas of largely chaotically pitted Quaternary materials but also displaying discontinuous lineaments (Fig. 15b) are likely representative of more fragmented thrust masses developed in former supraglacial outwash that was initially overlying more extensive buried glacier ice of variable thickness. A particularly prominent area of pitted thrust mass lies directly south of the East Neutral Hills, at the eastern extremity of the Altario Moraine of Phillips et al. (2017; see Section 3.9). This is a large, complex depression composed of multiple lakes and ponds of various size and depth and draped by a veneer of glaciallacustrine sediment (Bayrock, 1967). The southern rim of the complex, hereby named the “North Altario depression”, is composed of an arcuate thrust mass that is fragmented by sinuous chains of large water-filled depressions. Linear ridges also occur in the middle of the complex where they are surrounded by more chaotic mounds and ponds (Fig. 15c). The extensive collapse of both the complex depression and the southern bounding thrust mass, as evidenced by the many constituent depressions, indicates the melt-out of a large ice body or glacier snout, which initially constructed the arcuate thrust mass from pre-existing ice-cored deposits.

### *3.9 Areas of hummocky terrain*

In contrast to hummocky topography resulting from the superimposition of glacialtectonic signatures and ice melt-out (Fig. 8c) and chaotically pitted terrain displaying discontinuous lineaments (Fig. 15b), hummocky terrain lacks any clear linearity and contains the Types 1, 2 and 3 hummocks of Evans et al. (2014). An excellent example of the juxtaposition of these terrains occurs within the Veteran Moraine (Phillips et al., 2017) between Veteran and Nose Hill and the western Neutral Hills (Figs. 8b and 16a). Although the southernmost part of the Veteran Moraine contains large and densely spaced flat-topped hills interpreted as ice-walled lake plains (Fig. 16a), these are not attributed to pitted glacialfluvial deposits, because the surrounding hummocks appear to lack sand



and gravel cores, being composed instead of clay-rich diamicton with sheared sand lenses (Bayrock, 1967; Fig. 16b). However, numerous discontinuous sinuous ridges (probable eskers) and large esker networks do occur within the hummocks and link up with tunnel channels (Fig. 16a). At its southern edge, the Veteran Moraine hummocks end abruptly at the margin of the faintly streamlined bed of the CAIS (Fig. 16a). Modern drainage from this lower relief surface is clearly blocked by the hummocky terrain, as indicated by lakes that have been impounded against the higher topography. Eskers run into tunnel channels at the edge of the hummocky terrain, indicating that meltwater was evacuated from under the margin of the CAIS. The juxtaposition of these two contrasting landform assemblages indicates that large volumes of sediment accumulated within ice that lay outside of the CAIS but south of the Neutral Hills thrust moraine complex. Although glaci-fluvial landforms have clearly developed within this hummocky terrain, large areas of chaotic hummocks and doughnuts as well as highly fragmented sinuous ridges were constructed in sheared diamictons, a characteristic widely identified in comparable landforms elsewhere on the prairies (e.g., Gravenor and Kupsch, 1959; Stalker, 1960; Parizek, 1969; Johnson and Clayton, 2003). Hence the Veteran Moraine must have evolved from an extensive area of glacier karst that developed over and within till-cored hummocks immediately east of the CAIS.

Another large expanse of hummocky terrain occurs within the Altario Moraine (Phillips et al., 2017), directly south of the East Neutral Hills thrust complex. This moraine comprises an assemblage of chaotic hummocks, short sinuous hummocky ridges, contiguous doughnut mounds (*sensu* Mollard, 2000), ice-walled lake plains, eskers and associated doughnut chains (see Section 3.6), tunnel channels and scattered mega-rafts (Fig. 16c). Here, the hummocks are diamicton-cored (Bayrock, 1967) and locally vary from entirely chaotic to crudely aligned in sinuous chains; the chains are often linked to form sinuous, dual crested ridges that grade laterally into eskers and ice-walled lake plains. As with the hypothesized till eskers in Section 3.6, these associations favour a subglacial squeeze or pressing origin (Stalker, 1960; Eyles et al., 1999; Boone and Eyles, 2001), as well as glaci-fluvial tunnel fills, especially where locally draped by supraglacial lake plain sediments.

The largest expanse of hummocky terrain occurs around Kinsella in the extreme northwest corner of the map area, within the southern part of the regionally extensive Viking Moraine (Johnston and Wickenden 1931; Bretz 1943). This area is characterised by an inset series of major channels (see section 3.10 for further implications of this assemblage) and the prominent development of eskers and ice-walled lake plains, the latter draping tunnel channels and hummocks (Fig. 16d). These record the former existence of an expansive glacier karst within a lobate ice margin that abutted the

eastern edge of the CAIS (Figs. 13d and 14). Railway and road cuttings through the Viking Moraine immediately east and west of the town of Kinsella, provide valuable insights into the cores and possible origins of some of the hummocks (Fig. 16d). The exposures display stacked diamictons with prominent SE-directed shear zones defined by attenuated sand lenses and sand-filled thrust planes. In the west of the hummocky terrain (KW2, Fig. 16d) the thrusts dip towards the northwest. A southeast directed sense of shear is also recorded by similar shear zones observed in the centre of the hummocky terrain (KW, Fig. 16d). In this area the stacked diamictons also contain thrust-bound rafts of mudstone. The upper Dmm within the section possesses a NW-SE aligned clast macrofabric; consistent with the SE-directed sense of displacement on the thrust and shear zones. In contrast, the macrofabric present within the lower Dmm of KW displays a steeply dipping, weakly easterly-aligned signature more typical of crevasse squeeze processes (see Section 3.5). In the eastern part of the hummocky terrain, an exposure displays an upper massive to laminated diamicton containing attenuated sand lenses and sand-lined thrust faults dipping towards the northeast. The lenses represent pre-existing sands which were deformed and emplaced into the diamicton during thrusting. In contrast the sand-lined thrusts are thought to provide evidence that these glacitectonic structures subsequently acted as fluid pathways allowing water-escape and deposition of the sand lining. This is compatible with northerly and northeasterly aligned clast macrofabrics in both the upper and lower diamictons at this site. The characteristics of the diamictons are indicative of a subglacial origin for at least some of the hummock cores in this terrain (Evans, 2018 and references therein). The opposing stress directions from the northwest and north-northeast in the west and east parts of the hummocky terrain respectively are entirely compatible with its construction at the coalescence zone of the CAIS and eastern ice lobes.

An important distinction should be made between the hummocks and ridges in the hummocky terrain of the map area and those identified around the southern margin of the CAIS in southern Alberta by Evans et al. (2014). The MTR Type 3 moraine ridges and Type 1-3 hummocks of southern Alberta are arranged in arcuate zones located between MTR Type 2 moraines, collectively indicative of changing sub-marginal thermal regimes during ice sheet marginal recession. In the Neutral Hills Uplands, the hummocky terrain areas occur in large non-linear assemblages, more indicative of the in situ stagnation of ice lobes, and contain greater numbers of glacial features. The latter include eskers and possible eskers/till eskers (doughnut chains and short sinuous ridges) and ice-walled plains that are aligned with tunnel channels, collectively indicating meltwater drainage flowing oblique to former ice margins.

An unusual area of chaotic hummocky terrain lies within the Grassy Island Moraine (Phillips et al., 2017) between Grassy Island Lake and the Misty Hills. This area comprises a complex range of landforms including large kettle lakes, pitted glacialfluvial deposits, esker networks and ice-walled lake plains juxtaposed with and partially draping glacitectonically thrust bedrock in the west and hummocks containing heavily deformed stratified sediments and diamictos in the east (Fig. 6). Overall, the Grassy Island Moraine appears to represent an extensive former stagnant ice zone developed on the proximal slopes of the Misty Hills and Esther uplands thrust bedrock complex.

### *3.10 Erosional channels, large terraces and cliffs*

The map area contains numerous prominent channels with many displaying cliffed margins punctuated by modern landslides. These features have been termed “stream trenches” (Bayrock, 1958b; Gravenor and Ellwood, 1957) or “ice-walled channels” (Gravenor and Kupsch, 1959), and are reported as being partly covered by till and hummocky terrain. They therefore either predate glaciation, in the case of the thalwegs of bedrock valleys (cf. Stalker, 1961; Farvolden, 1963; Andriashek, 2018), or more commonly, relate to subglacial and/or proglacial meltwater/spillway incision. The Battle River occupies the largest of these trenches and its cliffed margins are largely postglacial, although the upper slope along some stretches comprises an outer set of sediment mantled preglacial cliffs which indicate that the modern river has re-occupied this earlier preglacial river course (Fig. 17a). A number of large, steep-sided and flat bottomed, mostly relict channels occur in the Hardisty area on the west side of the Battle River. These features are conspicuous by rectilinear segments with sharp, obtuse corners and their tendency in places to join one another so that they isolate polygonal-shaped areas of prairie surface. They constitute the southernmost extent of a 150 km long series of largely N-S aligned and inset channels that stretch outside the northwest corner of the map area. This regional channel system forms a wide arcuate assemblage fringing the Viking Moraine (see section 3.9). Most of these channels appear mantled by glacialigenic sediment, especially where they have not been re-occupied by deglacial and postglacial drainage. Evidence for this includes muted cliff lines and drapes of hummocky terrain and eskers as well as enclosed, elongate valley floor depressions, in places containing lakes. The latter characteristics in particular indicate a subglacial origin for the valleys (cf. Brennand and Shaw, 1994; Ó Cofaigh, 1996; Kehew and Kozlowski, 2007; Russell et al., 2007). Regionally, the channels widen southwards and also become less parallel and more reticulate in the Hardisty area, where the isolated, polygonal-shaped prairie surfaces display clear lineaments indicative of an overridden thrust moraine arc, initially constructed by an ice lobe flowing from the NNW. Subsequent flow from the WNW is recorded by minor flutings with clear stoss boulders, as well as N-S orientated lineaments on the northernmost polygonal-

shaped prairie surface (Fig. 17a). We hypothesize that the reticulate pattern of the channels in the Hardisty area is controlled by the fracture patterns produced by early glacitectonic thrust mass displacement, which were later exploited by both subglacial and deglacial meltwater drainage. This remarkable channel network demarcates the drainage pathways developed along the coalescence zone between the eastern margin of the CAIS and ice lobes flowing into the region from the east (see section 4).

More subtle channels, identifiable as sinuous chains of elongate lakes that are partially obscured by glacial depositional landforms are interpreted as subglacial tunnel channels (Patterson, 1994; Clayton et al., 1999; Evans, 2000; Kehew and Kozlowski, 2007). Numerous examples occur within every landform assemblage and are typically associated with eskers (see Section 3.6), whereby they either lie in sinuous chains (Figs. 12a and 17b), run alongside one another (Fig. 17b) or the eskers lie wholly within or overfill the channels (Figs 13c, d and 16a). The most spectacular subglacial drainage network in the map area is that of the Coronation-Spondin scablands (Fig. 11a), which Sjogren and Rains (1995) describe in significant detail as comprising anabranching channels with undulatory long profiles and separating eroded residuals.

Typical of the Canadian prairies, numerous large relict channels cross-cut all glacial landforms and hence are interpreted as spillways fed by water decanting from proglacial, ice-dammed lakes that developed at the margins of the retreating LIS (cf. Elson, 1957; St Onge, 1972; Christiansen, 1979; Kehew and Clayton, 1983; Kehew and Lord, 1986, 1987; Evans, 2000; Evans et al., 2006). The most prominent of such features occupy the drainage basins of Loyalist, Monitor and Sounding creeks, where multiple relict channels, in addition to those of the modern river courses, record the incision of the upstanding glacitectonic thrust masses and the progradation of material removed from the incisions to form channelled fans, especially in the Monitor Creek basin (Fig. 17c). The upper courses of these spillway systems link to the Coronation-Spondin scabland to the west, indicating that floodwater occupied the channels during and after the recession of the CAIS. The Monitor Creek spillway feeds into the Eyehill Creek/Sounding Lake depression where its floodwaters appear to have drained into stagnant ice in this area, contributing substantial amounts of sediment to the construction of the large esker and ice-walled lake plains and other smaller eskers which record drainage north and eastwards. Similarly, the Sounding Creek spillway appears to have drained into a substantial area of stagnant ice occupying the Grassy Island Lake area, forming a chaotic hummocky terrain of large kettle lakes, pitted glacial deposits, esker networks and ice-walled lake plains juxtaposed with glacitectonic thrust masses and hummocks containing heavily deformed stratified

sediments and diamictos (the Grassy Island Moraine of Phillips et al., 2017; Figs. 6 and 17c). To the north of this extensive former stagnant ice zone it appears that the water delivered by the Sounding Creek spillway drained into the Monitor Creek system.

#### **4. Glacial landsystems and palaeoglaciological reconstructions**

Based upon the distribution of the landform-sediment assemblages described above (Fig. 3), the Neutral Hills Upland and surrounding terrain can be classified according to a variety of landsystem signatures (Fig. 18a), some of which have been previously identified by Phillips et al. (2017), employing the mapping of Gravenor and Bayrock (1955), Bayrock (1958a, b, 1967), Shetsen (1987, 1990), Kjarsgaard (1988) and Fenton et al. (1993). Additionally, the area lies between the strongly streamlined trunks of the Central Alberta and Maskwa palaeo-ice streams previously mapped by Evans et al. (2008, 2014, 2016a), Ross et al. (2009), Ó Cofaigh et al. (2010) and Norris et al. (2018). The extent of these ice streams, together with the later cross-cutting “Ice Stream 2” flow sets as refined by Norris et al. (2018) are depicted in Figure 1, but this does not fully communicate the remarkably complex ice dynamics of the Neutral Hills Upland and hence some modifications to this palaeoglaciology based upon the new mapping presented here are now necessary (Fig. 18b). A series of six ice flow events were proposed for the area by Phillips et al. (2017), which are now refined using the cross-cutting relationships of various landsystem signatures.

The earliest landform imprints (pre-Event 1) appear to be the various examples of fluted or streamlined lineaments or small areas of MTR Type 1 ridges which have been strongly overprinted by subsequent vigorous ice stream or ice lobe advance (Fig. 18b). On the bed of the CAIS and on the prairie surface between the reticulate channels of the Hardisty area, arcuate sets of lineaments represent overridden thrust moraines constructed at the lobate margin of the advancing CAIS as it flowed south and southeastwards. The thrust masses were later exploited by multiple phases of thin-skinned glacitectonic raft displacement (Fig. 11c lower) and subglacial and deglacial meltwater erosion (Fig. 17) at the migrating coalescence zone of the CAIS and eastern ice flow units. They also appear to have been overprinted by more recent (Event 5) lobe advances. Further evidence for an early southeasterly flow is represented by the overprinted tectonic fabrics in the western Neutral Hills and the Nose Hill/Ribstone Creek area (Fig. 5b). A small area of NW-SE aligned flutings located north of Chauvin has survived overprinting firstly by the Maskwa Ice Stream (Event 1) and then by the Prospect Valley lobe (Event 5). This ice flow direction is recorded in the lowermost till in the area (Fig. 5a).

Event 1 is the first ice flow trajectory for which a regional landform signature can be recognised and is largely equated with the operation of the Maskwa palaeo-ice stream, directly east of the map area. Overprinted N-S orientated flutings at the eastern edge of the CAIS footprint indicate that it was also likely to have been operating at this time, after which the CAIS contracted to a narrower but persistent fast flow zone throughout Events 2-4.

Events 2 and 3 involved the construction and modification respectively of the major thrust complexes of the Neutral Hills Uplands. Contrary to the sequence of events proposed in previous reconstructions (Evans et al., 2008; Phillips et al., 2017), it appears that these features pre-date the operation of Ice Stream 2B of Ó Cofaigh et al. (2010; see below) and hence are not related to a late stage deglacial surge activity but instead record surging by ice lobes flowing into the region from the northeast. The implications of this are that the thrust masses were created within an inter-ice stream, locally ice-cored, moraine zone (inter-corridor terrain of Evans, 2000; Evans et al., 2008), where subsequent glacier overriding was restricted. Evidence of the latter is the narrow fast flow corridor associated with later deformation events at the Mud Buttes (Phillips et al., 2017) and hence designated here as Event 3 (Fig. 18b). There are three possible sub-phases to Event 2 (designated A-C) as recorded in the thrust mass complexes. The extent of ice during Event 2A is demarcated by the broad arc of bedrock-cored composite ridges comprising the Misty Hills, Sharp Hills and Esther Uplands and inset by the Grassy Island Moraine. Typical of surge lobes, this landsystem comprises outer thrust moraines and an inner zone of ice-cored hummocky terrain and extensively kettled glacifluvial deposits (Evans and Rea, 1999, 2003; Schomacker et al., 2006; Evans et al., 2007, 2009). Event 2B relates to the production of the Veteran and Altario moraines, which both constitute large areas of formerly ice-cored terrain. The ice cores likely constituted buried glacier ice that persisted across the landscape after earlier surges into the inter-ice stream zone. These assemblages of extensive ice karst and glacifluvial deposits interspersed with bedrock and glacial sediment thrust masses were then deformed by subsequent readvances/surges to form the rectilinear melt-out depressions and heavily pitted thrust masses that are especially well-developed in the Veteran Moraine around the Gooseberry Lake and Neutral Valley and the Altario depression of the Altario Moraine. Event 2C is represented by a substantial readvance that resulted in the construction of the prominent Neutral Hills and Nose Hill thrust-block moraines. The driving stress required to construct these impressive glacetectonic landforms could also have been responsible for thrusting of buried glacier ice within the proglacial areas of the Veteran and Altario moraines. Finally, a potentially further Event 2 fast flow corridor occurs further north, in the Wainwright area and records the operation of a narrow ice stream flowing south-southeastwards with a flow set parallel to Event 2A.

958

959 Event 4 is recorded by the overprinting of the Maskwa palaeo-ice stream footprint by a NW-SE  
960 flowing ice stream, previously designated Ice Stream 2B by Ó Cofaigh et al. (2010). They envisaged  
961 this as an offshoot of Ice Stream 2A located further north and fed by the Battleford Valley fast flow  
962 zone (Fig. 1). We have revised this reconstruction based upon our evidence for the Prospect Valley  
963 lobe landsystem (see below). The flowset and end-moraine imprint of the Prospect Valley lobe is  
964 clearly separate from, and overprints, that of Ice Stream 2B and hence we see no evidence for the  
965 elbow shaped bifurcation that separates Ice Stream 2 into two flow units (Fig. 1). Instead, Ice Stream  
966 2B is now considered to be a southeasterly flowing tributary of the ice streams that were operating  
967 in the region to the east of the Maskwa ice stream after it had effectively shutdown (Buffalo Ice  
968 Stream and James Lobe system; Ross et al. 2009; Margold et al. 2015). Indeed, not only the  
969 shutdown of the Maskwa but also the narrowing and/or weakening of the CAIS could have facilitated  
970 the westward propagation of the tributaries of the Buffalo/James Lobe ice stream system, as  
971 proposed by Ross et al. (2009).

972

973 Ice Stream 2B also paralleled the Battleford River fast flow trunk (Ice Stream 2A of Ó Cofaigh et al.  
974 2010) as well as the more southerly Ice Stream 2C of Norris et al. (2018; Fig. 18b). Our mapping  
975 indicates that a contemporaneous southeasterly flowing ice stream also operated in the area  
976 immediately south of Ice Stream 2B. The margin of this ice stream formed the southern limit of the  
977 Veteran Moraine and modified the western edge of the Misty Hills thrust moraine complex. It also  
978 streamlined the terrain to the south of the map area, where it eventually turned east-  
979 northeastwards to join Ice Stream 2B and overprinted the Maskwa Ice Stream footprint. After Ice  
980 Stream 2B had shutdown, it stagnated to develop a complex glacier karst and meltwater drainage  
981 system that was augmented by drainage through the Neutral Hills thrust complex from the buried  
982 ice in the Veteran and Altario moraines. It was also reworked into ice-cored thrust masses at its  
983 western end and northern edge by the advance of subsequent lobate ice stream margins during  
984 Event 5.

985

986 Event 5 is the most recent glacial geomorphic imprint identifiable in the study area. It comprises the  
987 footprint and associated terminal moraines of two lobate ice streams, one of which, the Prospect  
988 Valley lobe, created the most unequivocal surging glacier landsystem in the region (Fig. 19a). The  
989 trunk zone of this surging lobe has been mapped previously by Evans et al. (1999) and Evans and Rea  
990 (1999, 2003) and is remarkable for its extensive networks of crevasse squeeze ridges, which indicate  
991 surges propagated up-ice for more than 100 km. Mapping presented here identifies the multi-lobate

terminal moraine complex constructed by the surge, an offshoot of which has been reported by Evans et al. (2016a) to have excavated a hill-hole pair that cross-cuts the Maskwa palaeo-ice stream footprint (Fig. 18b). The multi-lobate terminal moraine comprises composite ridges with extensive evidence of ice melt-out (kettle holes and melt-out depressions), as well as numerous examples of large failure scars and associated failed blocks resembling retrogressive flow complexes. At its southern limit, the composite moraines appear to have been constructed from ice-cored glacial materials rather than bedrock (cf. Bayrock, 1967), likely due to the impingement of the Prospect Valley lobe on the stagnant ice and ice-cored glacial outwash of Ice Stream 2B. A modern analogue for this ice-cored surge moraine is that of the Skeiðarárjökull foreland in Iceland, created by a surge over dead ice in the late 19<sup>th</sup> century (Fig. 19b; Galon, 1973; Russell et al., 2001b). Because it is the best preserved lobate ice stream landform imprint in the study area, it provides the clearest evidence for the surging style of ice-marginal oscillations in the inter-ice stream moraine zones, most of which have otherwise been extensively overprinted.

The other clear Event 5 lobate ice stream imprint is located in the northwest corner of the map area (Fig. 18b) and was considered by Phillips et al. (2017) to relate to a much older event. However, based upon the higher resolution LiDAR imagery used in this study, the flutings within this imprint are clearly related to the later stages of south-southwesterly flow in the inter-ice stream zone and terminate at the broad arc of hummocky and ice-cored thrust terrain of the Viking Moraine (Fig. 15b). A smaller flow set extending southeastwards from the eastern edge of the CAIS footprint into the western Viking Moraine records a further Event 5 fast flow imprint. Together, these Event 5 flow sets verify the macrofabric evidence from the hummocks of the Viking Moraine, confirming that this landform represents interlobate deposition of subglacial tills and bedrock rafts overprinted by complex glacial sediment-landform assemblages indicative of an extensive glacier karst.

Taken in its broader context of the southwest LIS, the distinctive landform-sediment assemblage of the Neutral Hills Uplands (Fig. 20) is diagnostic of the partial overprinting of fast flow lobes that operated in the area at the margins of, and between, the major regional Central Alberta and Maskwa palaeo-ice streams. Widespread evidence of surge-diagnostic features, especially crevasse squeeze ridges, proglacial thrust masses, extensive ice stagnation topography and occasional zig-zag eskers, indicate that these ice streams experienced repeated flow instabilities. This is particularly evident in the inter-ice stream moraine zone of the Neutral Hills Uplands where substantial belts of thrust masses, hummocky terrain and ice stagnation topography make up the long recognised regional moraine belts constructed at around 15.5 cal ka BP (Fig. 20; Wickenden, 1931; Bretz, 1943;



Evans et al., 2008, 2014; cf. Margold et al., 2018 for dating control). The surge imprints of the Neutral Hills Uplands are typical of the broader scenario of a highly dynamic and unstable southwest LIS, characterised by markedly transitory and cross-cutting palaeo-ice streams. In the regional context of the juxtaposition of palaeo-ice stream beds with widespread tunnel channels and sub- to supraglacial drainage networks (cf. Patterson, 1997; Margold et al., 2015; Livingstone et al., 2016), such transitory and mobile ice stream behaviour is to be expected, especially given the role subglacial hydrology plays in the spatial and temporal variability of contemporary ice stream operation (e.g., Gray et al., 2005; Peters et al., 2007; Vaughan et al., 2008; Carter et al., 2013; Elsworth and Suckale, 2016; Siegfried et al., 2016). Moreover, modelling experiments by Lelandais et al. (2018) have indicated that ice streams can switch off when the drainage capacities of tunnel valleys are capable of suppressing subglacial water pressures. More importantly, in considering apparent ice stream surging, these modelling results demonstrate that ice streams switch on and accelerate in response to the build-up, migration and subsequent marginal outbursts of subglacial water reservoirs. This phase of basal decoupling is followed by deceleration when the subglacial drainage reorganizes into channels and creates tunnel channels and partial basal recoupling.

## Conclusions

A regional palaeoglaciology is now emerging from the study of the glacial geomorphology of the Canadian prairies. This features a highly dynamic southwest LIS, characterised by markedly transitory and cross-cutting palaeo-ice streams whose lobate margins are demarcated by large, arcuate ice-marginal moraine complexes (Fig. 20). Numerous overridden moraine arcs document the lobate margins during phases of more restricted ice cover, likely during ice sheet advance but in some instances related to recession. In the Neutral Hills Uplands, a distinctive landform-sediment assemblage is diagnostic of the partial overprinting of fast flow lobes that appear to have repeatedly surged into an inter-ice stream zone characterized by major moraine belts, the last surging dating to  $\leq 15.5$  cal ka BP.

The geomorphology of the inter-ice stream moraine zone is characterised by spectacular glacitectonic compression of bedrock, cupola hill construction and mega raft displacement but also displays evidence of multi-phase stagnant ice melt-out where partially overprinted surge lobes advanced into large areas of buried glacier ice (Fig. 20). Contemporaneous ice melting within these ice bodies gave rise to the widespread development of glacier karst and the production of eskers at a range of scales, the largest of which record deranged drainage patterns indicative of ice-walled

channel sedimentation controlled by the regional bedrock slope towards the northeast. The significant local relief created by the glacial geomorphology is likely a function of not only the glaciectonic compression of bedrock but also the production and melting of a melange of ice and bedrock/sediment blocks of variable ice volume, representative of buried snout ice often with well-developed or inherent glacier karst that is repeatedly proglacially thrust due to surging (Fig. 20).

Widespread evidence for subglacial channel cutting is likely strongly linked to the transitory, surging and cross-cutting nature of the palaeo-ice streams in the region. This is compatible with modelling of ice stream operation whereby they switch on and accelerate in response to the build-up, migration and marginal outburst of subglacial water reservoirs. Also significant with respect to the role of subglacial meltwater networks is the impact of pressurized groundwater in a region where ice flow is against an adverse bed slope and hence a variety of enigmatic glacial landforms such as doughnuts, doughnut chains, apparent blow-out features and possible till eskers, as well as glaciectonic mega-rafts, might be best explained through a better understanding of the interaction between such pressurised sub-surface systems and the surging lobes of soft-bedded ice streams.

## Acknowledgements

Thanks to Chris Orton, Durham University, for cartographic work, especially the compilation of the geomorphology map in Figure 3. Constructive comments by reviewers Martin Ross and Roger Paulen greatly helped us to clarify the contents of this paper.

## References

- Aber, J.S., Ber, A., 2007. Glaciotectonism. Development in Quaternary Science. Elsevier, Amsterdam.
- Aber, J.S., Croot, D.G., Fenton, M.M., 1989. Glaciotectonic Landforms and Structures. Kluwer, Dordrecht.
- Andersen, S.A., 1931. The waning of the last continental glacier in Denmark as illustrated by varved clays and eskers. *Journal of Geology* 39, 609-624.
- Andriashek, L.D., 2018. Thalwegs of bedrock valleys. Alberta Geological Survey. AER/AGS Digital Data 2018-0001.
- Atkinson, N., Utting, D.J., Pawley, S.M., 2014a. Glacial landforms of Alberta, Canada. Alberta Geological Survey. AER/AGS Map 604.
- Atkinson, N., Utting, D.J., Pawley, S.M., 2014b. Landform signature of the Laurentide and Cordilleran ice sheets across Alberta during the last glaciation. *Canadian Journal of Earth Sciences* 51, 1067-1083.
- Atkinson, N., Pawley, S.M., Utting, D.J., 2016. Flow-pattern evolution of the Laurentide and Cordilleran ice sheets across west-central Alberta, Canada: implications for ice sheet growth, retreat and dynamics during the last glacial cycle. *Journal of Quaternary Science* 31, 753-768.
- Atkinson, N., Utting, D.J., Pawley, S.M., 2018. An update to the glacial landforms map of Alberta. Alberta Geological Survey. AER/AGS Open File Report 2018-08.
- Banerjee, I., McDonald, B.C., 1975. Nature of esker sedimentation. In: Jopling, A.V., McDonald, B.C.

1095 (eds.), Glaciofluvial and Glacilacustrine Sedimentation. SEPM: Oklahoma; 304–320.  
 1096 Bayrock, L.A., 1958a. Glacial Geology, Alliance-Brownfield District, Alberta. Preliminary Report 57-2.  
 1097 Research Council of Alberta.  
 1098 Bayrock, L.A., 1958b. Glacial Geology, Galahad-Hardisty District, Alberta. Preliminary Report 57-3.  
 1099 Research Council of Alberta.  
 1100 Bayrock, L.A., 1967. Surficial Geology of the Wainwright Area (East Half), Alberta. Report 67-4.  
 1101 Research Council of Alberta.  
 1102 Benn, D.I., 1994. Fluted moraine formation and till genesis below a temperate glacier:  
 1103 Slettmarkbreen, Jotunheimen, Norway. *Sedimentology* 41, 279–292.  
 1104 Benn, D.I., Evans, D.J.A. 2010. *Glaciers and Glaciation*. Hodder Education, London.  
 1105 Bennett, M.R., Hambrey, M.J., Huddart, D., Ghienne, J.F., 1996. The formation of a geometrical ridge  
 1106 network by the surge-type glacier Kongsvegen, Svalbard. *Journal of Quaternary Science* 11,  
 1107 437–449.  
 1108 Bik, M.J.J., 1969. The origin and age of the prairie mounds of southern Alberta, Canada. *Biuletyn*  
 1109 *Peryglacjalny* 19, 85–130.  
 1110 Bluemle, J.P., 1993. Hydrodynamic blowouts in North Dakota. In: Aber, J.S. (Ed.), *Glaciotectonics and*  
 1111 *Mapping Glacial Deposits*. Canadian Plains Research Centre, University of Regina, pp. 259–  
 1112 266.  
 1113 Bluemle, J.P., Clayton, L., 1984. Large-scale glacial thrusting and related processes in North Dakota.  
 1114 *Boreas* 13, 279–299.  
 1115 Boone, S.J., Eyles, N., 2001. Geotechnical model for great plains hummocky moraine formed by till  
 1116 deformation below stagnant ice. *Geomorphology* 38, 109–124.  
 1117 Bostock, H.J., 1970a. Physiographic Regions of Canada. Geological Survey of Canada. Map 1254A,  
 1118 scale 1:5 000 000.  
 1119 Bostock, H.J., 1970b. Physiographic subdivisions of Canada. In: Douglas, R.J.W. (ed.), *Geology and*  
 1120 *Economic Minerals of Canada*. Geological Survey of Canada, Economic Geology Report 1, pp.  
 1121 11–30.  
 1122 Boulton, G.S., 1976. The origin of glacially fluted surfaces: observations and theory. *Journal of*  
 1123 *Glaciology* 17, 287–309.  
 1124 Boulton, G.S., 1986. Push moraines and glacier contact fans in marine and terrestrial environments.  
 1125 *Sedimentology* 33, 677–698.  
 1126 Boulton, G.S., Caban, P., 1995. Groundwater flow beneath ice sheets, part II: Its impact on glacier  
 1127 tectonic structures and moraine formation. *Quaternary Science Reviews* 14, 563–587.  
 1128 Brennand, T.A., Shaw, J., 1994. Tunnel channels and associated landforms, southcentral Ontario:  
 1129 their implication for ice-sheet hydrology. *Canadian Journal of Earth Sciences* 31, 505–522.  
 1130 Bretz, J.H., 1943. Keewatin end moraines in Alberta, Canada. *Geological Society of America Bulletin*  
 1131 54, 31–52.  
 1132 Burke, M.J., Brennand, T.A., Sjogren, D.B., 2015. The role of sediment supply in esker formation and  
 1133 ice tunnel evolution. *Quaternary Science Reviews* 115, 50–77.  
 1134 Carter, S.P., Fricker, H.A., Siegfried, M.R., 2013. Evidence of rapid subglacial water piracy under  
 1135 Whillans Ice Stream, West Antarctica. *Journal of Glaciology* 59, 1147–1162.  
 1136 Chandler, B.M.P., Evans, D.J.A., Roberts, D.H., 2016. Characteristics of recessional moraines at a  
 1137 temperate glacier in SE Iceland: Insights into patterns, rates and drivers of glacier retreat.  
 1138 *Quaternary Science Reviews* 135, 171–205.  
 1139 Christiansen, E.A., 1956. Glacial geology of the Moose Mountain area, Saskatchewan. Saskatchewan  
 1140 Department of Mineral Resources, Report 21, 35p.  
 1141 Christiansen, E.A., 1979. The Wisconsinan deglaciation of southern Saskatchewan and adjacent

1142 areas. *Canadian Journal of Earth Sciences* 16, 913-938.

1143 Christiansen, E.A., Whitaker, S.H., 1976. Glacial thrusting of drift and bedrock. In: Leggett, R.F.  
 1144 (ed.), *Glacial Till*. Royal Society of Canada, Special Publication 12, pp. 121-130.

1145 Christoffersen, P., Piotrowski, J.A., Larsen, N.K., 2005. Basal processes beneath an arctic glacier and  
 1146 their geomorphic imprint after a surge, Elisebreen, Svalbard. *Quaternary Research* 64, 125–  
 1147 137.

1148 Clayton, L., Cherry, J.A., 1967. Pleistocene Superglacial and Ice Walled Lakes of West central North  
 1149 America. *Miscellaneous Series* 30. North Dakota Geological Survey, pp. 47-52.

1150 Clayton, L., Attig, J.W., Ham, N.R., Johnson, M.D., Jennings, C.E., Syverson, K.M., 2008. Ice-walled-  
 1151 lake plains: implications for the origin of hummocky glacial topography in middle North  
 1152 America. *Geomorphology* 97, 237-248.

1153 Clayton, L., Teller, J.T., Attig, J.W., 1985. Surging of the south- western part of the Laurentide ice  
 1154 sheet. *Boreas* 14, 235-241.

1155 Clayton, L., Attig, J.W., Mickelson, D.M., 1999. Tunnel Channels Formed in Wisconsin during the Last  
 1156 Glaciation. *Geological Society of America (Special Paper)* 337, pp. 69-82.

1157 Colgan, P.M., Mickelson, D.M., Cutler, P.M., 2003. Ice marginal terrestrial landsystems: southern  
 1158 Laurentide Ice Sheet margin. In: Evans, D.J.A. (Ed.), *Glacial Landsystems*. Arnold, London, pp.  
 1159 111–142.

1160 Colton, R.B., 1955. *Geology of the Wolf Point quadrangle, Montana*. USGS, Geology Quadrangle  
 1161 Map.

1162 Cook, S.J., Knight, P.G., 2009. Glaciohydraulic supercooling. *Progress in Physical Geography* 33,  
 1163 705-710.

1164 Crémière, A., Lepland, A., Chand, S., Sahy, D., Condon, D.J., Noble, S.R., Martma, T., Thorsnes, T.,  
 1165 Sauer, S., Brunstad, H., 2016. Timescales of methane seepage on the Norwegian margin  
 1166 following collapse of the Scandinavian Ice Sheet. *Nature Communications* 7:11509.

1167 Deane, R.E., 1950. Pleistocene geology of the Lake Simcoe District, Ontario. *Memoir* 256. Geological  
 1168 Survey of Canada, Ottawa.

1169 Elson, J.A., 1957. Souris basin glacial lakes, southwestern Manitoba. *Abstract, Geological Society of*  
 1170 *America* 68, 1722.

1171 Elsworth, C. W., Suckale, J., 2016. Rapid ice flow rearrangement induced by subglacial drainage in  
 1172 West Antarctica. *Geophysical Research Letters* 43, 697–707.

1173 Evans, D.J.A., 2000. Quaternary geology and geomorphology of the Dinosaur Provincial Park area  
 1174 and surrounding plains, Alberta, Canada: the identification of former glacial lobes, drainage  
 1175 diversions and meltwater flood tracks. *Quaternary Science Reviews* 19, 931–958.

1176 Evans, D.J.A., 2003. Ice-marginal terrestrial landsystems: active temperate glacier margins. In:  
 1177 Evans, D.J.A. (Ed.), *Glacial Landsystems*. Arnold, London, pp.12–43.

1178 Evans, D.J.A., 2011. Glacial landsystems of Satujökull, Iceland: a modern analogue for glacial  
 1179 landsystem overprinting by mountain icecaps. *Geomorphology* 129: 225-237.

1180 Evans, D.J.A., 2018. *Till: A Glacial Process Sedimentology*. Wiley-Blackwell, Chichester: 390p.

1181 Evans, D.J.A., Benn, D.I., 2004. Facies description and the logging of sedimentary exposures. In:  
 1182 Evans, D.J.A., Benn, D.I. (Eds.), *A Practical Guide to the Study of Glacial Sediments*. Arnold,  
 1183 London, pp. 11–51.

1184 Evans, D.J.A., Rea, B.R., 1999. The geomorphology and sedimentology of surging glaciers: A land-  
 1185 systems approach. *Annals of Glaciology* 28, 75-82.

1186 Evans, D.J.A., Rea, B.R., 2003. Surging glacier landsystem. In: Evans, D.J.A. (Ed.), *Glacial Landsystems*.  
 1187 Arnold, London, pp. 259–288.

1188 Evans, D.J.A., Twigg, D.R. 2002. The active temperate glacial landsystem: a model based on

1189 Breiðamerkurjökull and Fjallsjökull, Iceland. *Quaternary Science Reviews* 21, 2143-2177.  
 1190 Evans, D.J.A., Clark, C.D., Rea, B.R., 2008. Landform and sediment imprints of fast glacier flow in the  
 1191 southwest Laurentide Ice Sheet. *Journal of Quaternary Science* 23, 249–272.  
 1192 Evans, D.J.A., Ewertowski M., Orton, C., 2016b. Fláajökull (north lobe), Iceland: active temperate  
 1193 piedmont lobe glacial landsystem. *Journal of Maps* 12, 777-789.  
 1194 Evans, D.J.A., Ewertowski, M., Orton, C., 2017. Skaftafellsjökull, Iceland: glacial geomorphology  
 1195 recording glacier recession since the Little Ice Age. *Journal of Maps* 13, 358-368.  
 1196 Evans, D.J.A., Hiemstra, J.F., Boston, C.M., Leighton, I., Ó Cofaigh, C., Rea, B.R., 2012. Till stratigraphy  
 1197 and sedimentology at the margins of terrestrially terminating ice streams: case study of the  
 1198 western Canadian prairies and high plains. *Quaternary Science Reviews* 46, 80–125.  
 1199 Evans, D.J.A., Lemmen, D.S., Rea, B.R., 1999. Glacial landsystems of the southwest Laurentide Ice  
 1200 Sheet: modern Icelandic analogues. *Journal of Quaternary Science* 14, 673–691.  
 1201 Evans, D.J.A., Nelson, C.D., Webb, C., 2010. An assessment of fluting and till esker formation on the  
 1202 foreland of Sandfellsjökull, Iceland. *Geomorphology* 114, 453–465.  
 1203 Evans, D.J.A., Phillips, E.R., Hiemstra, J.F., Auton, C.A., 2006. Subglacial till: formation,  
 1204 sedimentary characteristics and classification, *Earth Science Reviews* 78, 115-132.  
 1205 Evans, D.J.A., Storrar, R.D., Rea B.R. 2016a. Crevasse-squeeze ridge corridors: diagnostic features of  
 1206 late-stage palaeo-ice stream activity. *Geomorphology* 258, 40-50.  
 1207 Evans, D.J.A., Twigg, D.R., Rea B.R., Orton, C. 2009. Surging glacier landsystem of Tungnaárjökull,  
 1208 Iceland. *Journal of Maps* 2009: 134-151.  
 1209 Evans, D. J. A., Twigg, D.R., Rea, B.R., Shand, M., 2007. Surficial geology and geomorphology of the  
 1210 Brúarjökull surging glacier landsystem. *Journal of Maps* 3:1, 349-367.  
 1211 Evans, D.J.A., Young, N.J.P., Ó Cofaigh, C. 2014. Glacial geomorphology of terrestrial-  
 1212 terminating fast flow lobes/ice stream margins in the southwest Laurentide Ice Sheet.  
 1213 *Geomorphology* 204: 86-113.  
 1214 Eyles, N., Boyce, J.I., Barendregt, R.W., 1999. Hummocky moraine: sedimentary record of stagnant  
 1215 Laurentide Ice Sheet lobes resting on soft beds. *Sedimentary Geology* 123, 163–174.  
 1216 Eyles, N., Sladen, J.A., Gilroy, S., 1982. A depositional model for stratigraphic complexes and facies  
 1217 superimposition in lodgement tills. *Boreas* 11, 317-333.  
 1218 Farvolden, R.N., 1963. Bedrock channels of southern Alberta. *Research Council of Alberta Bulletin*  
 1219 12, 63–75.  
 1220 Fenton, M.M., Langenberg, W., Pawlowicz, J., 1993. Glacial deformation phenomena of east-central  
 1221 Alberta in the Stettler-Coronation region. Field trip B-1, Guidebook. Geological Association of  
 1222 Canada/Mineralogical Association of Canada, 46 pp.  
 1223 Fenton, M.M., Waters, E.J., Pawley, S.M., Atkinson, N., Utting, D.J., McKay, K., 2013. Surficial Geology  
 1224 of Alberta. Alberta Geological Survey AER/AGS Map 601.  
 1225 Flint, R.F., 1928. Eskers and crevasse fillings. *American Journal of Science* 15, 410-16.  
 1226 Galon, R., 1973b. Geomorphological and geological analysis of the proglacial area of Skeiðarárjökull.  
 1227 *Geographica Polonica* 26, 15-56.  
 1228 Gokhman, V. V. 1987. Two types of intraglacial meltwater regime for the Bertil Glacier, Svalbard.  
 1229 *Polar Geography and Geology* 11, 241-248.  
 1230 Grasby, S.E., Osadetz, K., Betcher, R., Render, F. 2000. Reversal of the regional-scale flow system  
 1231 of the Williston basin in response to Pleistocene glaciation. *Geology* 28, 635–638.  
 1232 Grasby, S.E., Chen, Z., 2005. Subglacial recharge into the Western Canada Sedimentary Basin -  
 1233 impact of Pleistocene glaciation of basin hydrodynamics. *Geological Society of America*  
 1234 *Bulletin* 117, 500-514.  
 1235 Grasby, S.E., 2013. Pickled shale gas play – How continental glaciation drives biogenic gas formation.

1236 GeoConvention. Canadian Society of Petroleum Geologists, Calgary.

1237 Gravenor C.P., Bayrock L.A. 1955. Glacial Geology, Coronation District, Alberta. Preliminary Report

1238 55-1. Research Council of Alberta, 38pp.

1239 Gravenor, C.P., Kupsch, W.O., 1959. Ice disintegration features in western Canada. *Journal of*

1240 *Geology* 67, 48-64.

1241 Gravenor, C.P., Ellwood, R.B., 1957. Glacial geology, Sedgewick District, Alberta. Alberta Research

1242 Council, Preliminary Report 57-1.

1243 Gray, L., Joughin, I., Tulaczyk, S., Spikes, V. B., Bindshadler, R., Jezek, K., 2005. Evidence for

1244 subglacial water transport in the West Antarctic Ice Sheet through three-dimensional

1245 satellite radar interferometry. *Geophysics Research Letters* 32, L03501,

1246 <https://doi.org/10.1029/2004GL021387>, 2005.

1247 Hatcher, Jr., R.D., 1995. *Structural Geology: principles, concepts and problems* (second edition).

1248 Prentice Hall. Englewood Cliffs, New Jersey

1249 Hebrand, M., Amark, M., 1989. Esker formation and glacier dynamics in eastern Skane and

1250 adjacent areas, southern Sweden. *Boreas* 18, 67-81.

1251 Hodgkins, R., Tranter, M., Dowdeswell, J.A., 2004. The characteristics and formation of a High-

1252 Arctic proglacial icing. *Geografiska Annaler* A86, 265-275.

1253 Hooke, R. Le B., Fastook, J., 2007. Thermal conditions at the bed of the Laurentide Ice Sheet in

1254 Maine during deglaciation: implications for esker formation. *Journal of Glaciology* 53, 646-

1255 658.

1256 Hopkins, O.B., 1923. Some structural features of the plains area of Alberta caused by Pleistocene

1257 glaciation. *Bulletin of the Geological Society of America* 34, 419-430.

1258 Hoppe, G., 1952. Hummocky moraine regions, with special reference to the interior of Norrbotten.

1259 *Geografiska Annaler* A34, 1-72.

1260 Howarth, P.J., 1971. Investigations of two eskers at eastern Breidamerkurjokull, Iceland. *Arctic and*

1261 *Alpine Research* 3, 305-318.

1262 Jennings, C.E., 2006. Terrestrial ice streams – a view from the lobe. *Geomorphology* 75, 100-124.

1263 Johnson, M.D., Clayton, L., 2003. Supraglacial landsystems in lowland terrain. In: Evans, D.J.A. (Ed.),

1264 *Glacial Landsystems*. Arnold, London, pp. 228-251.

1265 Johnston, W.A., Wickenden, R.T.D., 1931. Moraines and glacial lakes in southern Saskatchewan and

1266 southern Alberta, Canada. *Royal Society of Canada Transactions* 31, 81-95.

1267 Kehew, A.E., Lord, M.L., 1986. Origin and large scale erosional features of glacial lake spillways in the

1268 northern Great Plains. *Geological Society of America Bulletin* 97, 162-177.

1269 Kehew, A.E., Lord, M.L., 1987. Glacial lake outbursts along the midcontinent margins of the

1270 Laurentide ice sheet. In: Mayer, L., Nash, D. (Eds.), *Catastrophic Flooding*, Allen and Unwin,

1271 Boston, pp. 95-120.

1272 Kehew, A.E., Clayton, L., 1983. Late Wisconsinan floods and development of the Souris- Pembina

1273 spillway system in Saskatchewan, North Dakota and Manitoba. In: Teller, J.T., Clayton, L.

1274 (Eds.), *Glacial Lake Agassiz*, Geological Association of Canada, (Special Paper 26) pp. 187-209.

1275 Kehew, A.E., Kozlowski, A.L., 2007. Tunnel channels of the Saginaw Lobe, Michigan, USA. In:

1276 Johansson, P., Sarala, P. (eds.), *Applied Quaternary Research in the Central Part of Glaciated*

1277 *Terrain*. Geological Survey of Finland, Special Paper 46, pp. 69-78.

1278 Kjær, K.H., Larsen, E., van der Meer, J.J.M., Ingólfsson, Ó., Krüger, J., Benediktsson, Í.Ö., Knudsen,

1279 C.G., Schomacker, A., 2006. Subglacial decoupling at the sediment/bedrock interface: a new

1280 mechanism for rapid flowing ice. *Quaternary Science Reviews* 25, 2704-2712.

1281 Kjeirsgaard, A.A., 1988. Reconnaissance soil survey of the Oyen map sheet – 72M. Alberta Soil

1282 Survey Report S-76-36.

1283 Knudsen, O., 1995. Concertina eskers, Bruarjökull, Iceland: an indicator of surge-type glacier  
1284 behaviour. *Quaternary Science Reviews*, 14, 487-493.

1285 Krüger, J., 1995. Origin, chronology and climatological significance of annual moraine ridges at  
1286 Myrdalsjökull, Iceland. *The Holocene* 5, 420-427.

1287 Kupsch, W.O., 1962. Ice-thrust ridges in western Canada. *Journal of Geology* 70, 582-594.

1288 Larsen, N.K., Piotrowski, J.A., Christoffersen, P., Menzies, J., 2006. Formation and deformation of  
1289 basal till during a glacier surge; Elisebreen, Svalbard. *Geomorphology* 81, 217-234.

1290 Le Heron, D.P., Etienne, J.L., 2005. A complex subglacial clastic dyke swarm, Solheimajökull, southern  
1291 Iceland. *Sedimentary Geology* 181, 25-37.

1292 Lelandais, T., Ravier, E., Pochat, S., Bourgeois, O., Clark, C.D., Mourgues, R., Strzeczynski, P., 2018.  
1293 Modelled subglacial floods and tunnel valleys control the life cycle of transitory ice streams.  
1294 *The Cryosphere* 12, 2759-2772.

1295 Lemieux, J-M., Sudicky, E.A., Peltier, W.R., Tarasov, L., 2008. Dynamics of groundwater recharge  
1296 and seepage over the Canadian landscape during the Wisconsinian glaciation. *Journal of*  
1297 *Geophysical Research* 113, F01011, doi:10.1029/2007JF000838, 2008

1298 Livingstone, S.J., Evans, D.J.A., Ó Cofaigh, C., Hopkins, J., 2010. The Brampton Kame Belt and Pennine  
1299 Escarpment Meltwater Channel System (Cumbria, UK). *Morphology, Sedimentology and*  
1300 *Formation. Proceedings of the Geologists' Association* 121, 423-443.

1301 Livingstone, S.J., Utting, D., Ruffell, A., Clark, C.D., Pawley, S., Atkinson, N., Fowler, A.C., 2016.  
1302 Discovery of relict subglacial lakes and the mechanism and geometry of drainage. *Nature*  
1303 *Communications* 7:11767, doi: 10.1038/ncomms11767

1304 Mandl, G., Harkness, R.M., 1987. Hydrocarbon migration by hydraulic fracturing. In: Jones, M.E.,  
1305 Preston, R.M.F. (Eds.), *Deformation of Sediments and Sedimentary Rocks*. Geological Society  
1306 of London, Special Publication, vol. 29, pp. 39-53.

1307 Margold, M., Stokes, C.R., Clark, C.D., 2015. Ice streams in the Laurentide Ice Sheet: Identification,  
1308 characteristics and comparison to modern ice sheets. *Earth Science Reviews* 143, 117-146.

1309 Margold M., Stokes C.R., Clark C.D., 2018. Reconciling records of ice streaming and ice margin  
1310 retreat to produce a palaeogeographic reconstruction of the deglaciation of the Laurentide  
1311 Ice Sheet. *Quaternary Science Reviews* 189, 1-30.

1312 Mazzini, A., Svensen, H.H., Forsberg, C.F., Linge, H., Lauritzen, S-E., Haflidason, H., Hammer, Ø.,  
1313 Planke, S., 2017. A climatic trigger for the giant Troll pockmark field in the northern North  
1314 Sea. *Earth and Planetary Science Letters* 464, 24-34.

1315 Mokhtari Fard, A., 2002. Large dead-ice depressions in flat-topped eskers: evidence of a Preboreal  
1316 jökulhlaup in the Stockholm area, Sweden. *Global and Planetary Change* 35, 273-295.

1317 Mollard, J.D., 2000. Ice-shaped ring-forms in Western Canada: their airphoto expressions and  
1318 manifold polygenetic origins. *Quaternary International* 68-71, 187-198.

1319 Mooers, H.D., 1990. Ice-marginal thrusting of drift and bedrock: thermal regime, subglacial aquifers  
1320 and glacial surges. *Canadian Journal of Earth Sciences* 27, 849-862.

1321 Moran, S.R., Clayton, L., Hooke, R., Fenton, M.M., Andriashek, L.D., 1980. Glacier-bed landforms of  
1322 the prairie region of North America. *Journal of Glaciology* 25, 457-473.

1323 Mossop, G.D., Shetsen, I., 1994. *Geological Atlas of the Western Canada Sedimentary Basin*. Special  
1324 Report. Canadian Society of Petroleum Geologists and Alberta Research Council, 510 pp.

1325 Mulligan, R.P.M., Eyles, C.H., Marich, A.S., 2019. Subglacial and ice-marginal landforms in south-  
1326 central Ontario: implications for ice sheet reconfiguration during deglaciation. *Boreas* 48,  
1327 635-657.

1328 Norris, S.L., Evans, D.J.A., Ó Cofaigh, C., 2018. Geomorphology and till architecture of terrestrial  
1329 palaeo-ice streams of the southwest Laurentide Ice Sheet: A borehole stratigraphic  
1330 approach. *Quaternary Science Reviews* 186, 186-214.



- 1331 Ó Cofaigh, C., 1996. Tunnel valley genesis. *Progress in Physical Geography* 20, 1-19.
- 1332 Ó Cofaigh, C., Evans, D.J.A., Smith, I.R., 2010. Large-scale reorganization and sedimentation of  
1333 terrestrial ice streams during late Wisconsinan Laurentide ice sheet deglaciation. *Geological*  
1334 *Society of America Bulletin* 122, 743-756.
- 1335 Parizek, R.R., 1969. Glacial ice-contact ridges and rings. *Geological Society of America Special Paper*  
1336 123, 49-102.
- 1337 Patterson, C.J., 1994. Tunnel valley fans of the St Croix moraine, east-central Minnesota, USA. In:  
1338 Warren, W.P., Croot, D.G. (eds.), *Formation and Deformation of Glacial Deposits*. Balkema,  
1339 Rotterdam, pp. 69-87.
- 1340 Patterson, C.J., 1997. Southern Laurentide ice lobes were created by ice streams: Des Moines Lobe in  
1341 Minnesota, USA. *Sedimentary Geology* 111, 249-261.
- 1342 Patterson, C.J., 1998. Laurentide glacial landscapes: the role of ice streams. *Geology* 26, 643-646.
- 1343 Paulen, R.C., McClenaghan, M.B., 2015. Late Wisconsin ice-flow history in the Buffalo Head Hills  
1344 kimberlite field, north-central Alberta. *Canadian Journal of Earth Sciences* 52, 51-67.
- 1345 Perkins, A.J., Brennand, T.A., Burke, M.J., 2016. Towards a morphogenetic classification of eskers:  
1346 implications for modelling ice sheet hydrology. *Quaternary Science Reviews* 134, 19-38.
- 1347 Peters, L. E., Anandakrishnan, S., Alley, R. B., Smith, A.M., 2007. Extensive storage of basal  
1348 meltwater in the onset region of a major West Antarctic ice stream. *Geology* 35, 251-254.
- 1349 Pettapiece, W.W., 1986. *Physiographic Subdivision of Alberta*. Agriculture and Agri-  
1350 Food Canada, Ottawa.
- 1351 Phillips, E., Evans, D.J.A., Atkinson, N., Kendall, A., 2017. Structural architecture and glacetectonic  
1352 evolution of the Mud Buttes cupola hill complex, southern Alberta, Canada. *Quaternary*  
1353 *Science Reviews* 164, 110-139.
- 1354 Phillips, E., Everest, J., Reeves, H., 2013. Micromorphological evidence for subglacial multiphase  
1355 sedimentation and deformation during overpressurized fluid flow associated with  
1356 hydrofracturing. *Boreas* 42, 395-427.
- 1357 Price, N.J., Cosgrove, J.W. 1990. *Analysis of Geological Structures*. Cambridge University Press,  
1358 Cambridge.
- 1359 Price, R. J., 1969. Moraines, sandar, kames and eskers near Breiðamerkurjökull, Iceland. *Transactions*  
1360 *of the Institute of British Geographers* 46, 17-43.
- 1361 Price, R.J., 1982. Changes in the proglacial area of Breiðamerkurjökull, southeastern Iceland: 1890-  
1362 1980. *Jökull* 32, 29-35.
- 1363 Raymond, C. F., Johannesson, T., Pfeffer, T., Sharp, M., 1987. Propagation of a glacier surge into  
1364 stagnant ice. *Journal of Geophysical Research*, 92, 9037-9049.
- 1365 Roberts, D.H., Yde, J., Long, A.J., Knudsen, N.T., Lloyd, J.M., 2009. Ice marginal dynamics during surge  
1366 activity, Kuannersuit Glacier, Disko Island, West Greenland. *Quaternary Science Reviews* 28,  
1367 209-222.
- 1368 Rose, J., 1989. Glacier stress patterns and sediment transfer associated with the formation of  
1369 superimposed flutes. *Sedimentary Geology* 62, 151-176.
- 1370 Ross, M., Campbell, J.E., Parent, M., Adams, R.S., 2009. Palaeo-ice streams and the subglacial  
1371 landscape mosaic of the North American mid-continental prairies. *Boreas* 38, 421-439.
- 1372 Russell A.J., Gregory A.G., Large A.R.G., Fleisher P.J., Harris T., 2007. Tunnel channel formation during  
1373 the November 1996 jökulhlaup, Skeiðarárjökull, Iceland. *Annals of Glaciology* 45, 95-103.
- 1374 Russell, A.J., Knight, P.G., van Dijk, T.A.G.P., 2001b. Glacier surging as a control on the development  
1375 of proglacial, fluvial landforms and deposits, Skeiðarársandur, Iceland. *Global and Planetary*  
1376 *Change* 28, 163-174.
- 1377 Russell, A. J., Knudsen, Ó., Fay, H., Marren, P. M., Heinz, J., Tronicke, J., 2001a. Morphology and



1378 sedimentology of a giant supraglacial, ice-walled, jökulhlaup channel, Skeiðarársandur,  
 1379 Iceland. *Global and Planetary Change* 28, 203-226.  
 1380 Sauer, E.K., 1978. The engineering significance of glacier ice thrusting. *Canadian Geotechnical Journal*  
 1381 15, 457–472.  
 1382 Schomacker, A., Krüger, J., Kurth, K., 2006. Ice-cored drumlins at the surge-type glacier Bruarjökull,  
 1383 Iceland: a transitional-state landform. *Journal of Quaternary Science* 21, 85–93.  
 1384 Sharp, M.J., 1985a. “Crevasse-fill” ridges—A landform type characteristic of surging? *Geografiska*  
 1385 *Annaler* A67, 213-220.  
 1386 Sharp, M.J., 1985b. Sedimentation and stratigraphy at Eyjabakkajökull - an Icelandic surging glacier.  
 1387 *Quaternary Research* 24, 268-284.  
 1388 Shetsen, I., 1987. Quaternary geology, southern Alberta. Alberta Research Council, Alberta  
 1389 Geological Survey, Map 207, scale 1:500 000.  
 1390 Shetsen, I., 1990. Quaternary geology, central Alberta. Alberta Research Council, Alberta Geological  
 1391 Survey, Map 213.  
 1392 Siegfried, M. R., Fricker, H. A., Carter, S. P., Tulaczyk, S., 2016. Episodic ice velocity fluctuations  
 1393 triggered by a subglacial flood in West Antarctica. *Geophysics Research Letters* 43, 2640–  
 1394 2648.  
 1395 Sjogren, D.B., Rains, R.B., 1995. Glaciofluvial erosional morphology and sediments of the Coronation-  
 1396 Spondin scabland, east-central Alberta. *Canadian Journal of Earth Sciences* 32, 565–578.  
 1397 Slater, G., 1927. Structure of the Mud Buttes and Tit Hills in Alberta. *Bulletin of the Geological*  
 1398 *Society of America*, p. 38.  
 1399 Sookhan, S., Eyles, N., Arbelaez-Moreno, L., 2018. Converging ice streams: a new paradigm for  
 1400 reconstructions of the Laurentide Ice Sheet in southern Ontario and deposition of the Oak  
 1401 Ridges Moraine. *Canadian Journal of Earth Sciences* 55, 373-396.  
 1402 Sproule, J. C., 1939. The Pleistocene geology of the Cree Lake region, Saskatchewan. *Transactions of*  
 1403 *the Royal Society of Canada, Series 3*, 33, 101-7.  
 1404 Stalker, A.M., 1960. Ice-pressed drift forms and associated deposits in Alberta. *Bulletin* 57.  
 1405 *Geological Survey of Canada, Ottawa*.  
 1406 Stalker, A.M., 1961. Buried valleys in central and southern Alberta. *Bulletin* 15. *Geological Survey of*  
 1407 *Canada, Ottawa*.  
 1408 Stalker, A.M., 1973. [The large interdrift bedrock blocks of the Canadian Prairies. Geological Survey](#)  
 1409 [Canada, Paper 75-1A. 421–422.](#)  
 1410 Stalker, A.M., 1976. Megablocks, or the enormous erratics of the Albertan Prairies. *Geological Survey*  
 1411 *of Canada, Paper 76-1C*, 185-188.  
 1412 St-Onge, D.A., 1972. Sequence of glacial lakes in north-central Alberta. *Bulletin* 213. *Geological*  
 1413 *Survey of Canada, Ottawa*.  
 1414 Storrar, R.D., Stokes C.R., Evans, D.J.A., 2014a. Increased channelization of subglacial drainage during  
 1415 deglaciation of the Laurentide Ice Sheet. *Geology* 42, 239–242.  
 1416 Storrar, R.D., Stokes, C.R., Evans, D.J.A., 2014b. Morphometry and pattern of a large sample  
 1417 (>20,000) of Canadian eskers and implications for subglacial drainage beneath ice sheets.  
 1418 *Quaternary Science Reviews* 105, 1–25.  
 1419 Storrar, R.D., Evans, D.J.A., Stokes, C.R., Ewertowski, M., 2015. Controls on the location, morphology  
 1420 and evolution of complex esker systems at decadal timescales, Breiðamerkurjökull,  
 1421 southeast Iceland. *Earth Surface Processes and Landforms* 40, 1421–1438.  
 1422 Storrar, R.D., Ewertowski, M., Tomczyk, A., Barr, I.D., Livingstone, S.J., Ruffell, A., Stoker, B.J., Evans,  
 1423 D.J.A., in press. Equifinality and preservation potential of complex eskers. *Earth Surface*  
 1424 *Processes and Landforms*.  
 1425 Tsui, P.C., Cruden, D.M., Thomson, S., 1989. Ice thrust terrains and glaciotectonic settings in central

- Alberta. Canadian Journal of Earth Sciences 26, 1308-1318.
- Utting, D. J., Atkinson, N., Pawley, S.M., Livingstone, S.J., 2016. Reconstructing the confluence zone between Late Wisconsinan Laurentide and Cordilleran ice along the Rocky Mountain Foothills, Alberta. Journal of Quaternary Science 31, 769-787.
- van der Meer, J.J.M., Kjær, K.H., Krüger, J., Rabassa, J., Kilfeather, A.A., 2009. Under pressure: clastic dykes in glacial settings. Quaternary Science Reviews 28, 708–720.
- Vaughan, D.G., Corr, H.F.J., Smith, A.M., Pritchard, H.D., Shepherd, A., 2008. Flowswitching and water piracy between Rutford ice stream and Carlson inlet, west Antarctica. Journal of Glaciology 54, 41-48.
- Wickenden, R.T.D., 1931. An area of little or no drift in southern Saskatchewan. Transactions of the Royal Society of Canada 25, 45-47.

## Figure captions

Fig. 1: The palaeo-ice streams of the southern Canadian Prairies and summary of their related flow sets mapped on SRTM digital elevation model (after Ó Cofaigh et al., 2010; Norris et al., 2018). CAIS = Central Alberta Ice Stream; HPIS = High Plains Ice Stream.

Fig. 2: Location map and DEM showing place names referred to in text and major geomorphological features of the study area and its regional context. Inset map of the surficial geology of the study area (from Fenton et al., 2013) shows: E - aeolian deposits; LG - glaciallacustrine deposits; FG - glacialfluvial deposits; M - undifferentiated moraine (diamict); MS - stagnation moraine; MF - fluted moraine; MT - ice thrust moraine.

Fig. 3: Glacial geomorphology map of the Neutral Hills Upland area of southeast central Alberta. Grid lines define bespoke co-ordinate system for ease of reference when using following figures. Following figure captions use this co-ordinate system to identify the mid-point of the grid square in which the landform examples occur (e.g., C7, F14, A5).

Fig. 4: Examples of major glacitectonic thrust masses: a) Nose Hill viewed from the southeast (C7); b) Google Earth (Landsat 7 at 15 m resolution) oblique view of the west Neutral Hills with Gooseberry Lake (3.4 km long) in the foreground (F7); c) exposure through the Mud Buttes cupola hill, showing deformed bedrock strata (G4). Field truck (circled) for scale; d) exposure through deformed bedrock ridge near Mushroom Lake (F14).

Fig. 5: Examples of overprinted glacitectonic thrust masses: a) the Killarney Lake area (I11-12), where three phases of deformation are apparent in the surface lineaments. Phase 1 involved the lateral displacement of a mega-raft 25 km to the south near St Lawrence Lake. Location of sections KL1 and KL2 are shown; b) stratigraphic exposures through the Killarney Lake thrust masses, showing sediments and structures and clast macrofabrics for sections KL1 (upper) and KL2 (lower); c) LiDAR extracts showing the area south of Sounding Lake (upper, F7) and the western Neutral Hills and the Nose Hill/Ribstone Creek area (lower, C7).

Fig. 6: Complex overprinting of thrust masses in the Misty Hills, Sharp Hills, Mud Buttes and Esther uplands (G4). Area highlighted in green is the western block, which is the most recently displaced part of the complex, deformed by easterly flowing ice, as documented by fluted till. The Grassy

Island Moraine, indicative of widespread stagnant ice melt out, is also demarcated by orange dashed line.

Fig. 7: Features associated with major thrust masses: a) LiDAR image of ridge-rimmed depressions or doughnuts, locally aligned to form discontinuous chains on the summit of the east Neutral Hills (chain examples are circled by black outline; I6). Also visible on the eastern end of the thrust mass is a fan-shaped assemblage of doughnut forms with a channel at its apex marked by a chain of ponds and an esker trending towards the east-northeast; b) isolated pit containing a small pond and cutting across the structural grain (ridges and furrows) of the west Neutral Hills; c) LiDAR image of large pits, some lying in chains, bounded by fault scarps and located on the distal slopes of the western Neutral Hills (F7); d) large mass movement feature resembling a retrogressive flow scar, located on the distal slope of the west end of the eastern Neutral Hills (H6).

Fig. 8: Examples of short lineaments and ridges: a) and b) LiDAR images of non-fluted MTR type 1 corrugation ridges at the west end of the western Neutral Hills (C8) and near New Brigden (G/H3) respectively; c) LiDAR image of cross-cutting lineaments directly southeast of Nose Hill, displaying ridge fragmentation and dense pitting indicative of ice melt-out after tectonic grain development (C/D7). Lineaments run north-south and east-west; d) Semi-transparent Google Earth image draped over LiDAR DEM of MTR type 2 (recessional push moraines) south of Sedalia and near Sounding Creek (F-G, 1/2).

Fig. 9: LiDAR images of examples of areas overridden moraines and cupola hills: a) arcuate series of muted moraine ridges surrounding Coronation (A6/7), which likely originated as composite thrust ridges; b) streamlined cupola hill located NE of Sounding Lake, showing faint surface fluting (white lines), localised geometric ridge networks and surface pits indicative of ice melt-out (H7/8); c) overridden thrust masses (circled) exhibiting structural lineaments parallel to the direction of overriding ice flow as defined by flutings (white lines). Located south of the Sounding Creek depression (G1). Ice flow was towards the east.

Fig. 10: LiDAR imagery of examples of rubble terrain: a) elongate assemblage located southeast of Kirriemuir (I4) and containing Quaternary sediment, best illustrated at quarry outcrop marked by the "x" label (see Fig. 10e). Broken lines trace faint surface flutings; b) isolated rafts lying within an area of ice-walled lake plains and hummocky terrain in the Altario Moraine (H5); c) incipient, partially fragmented rafts (outlined) and their tear fault-bounded depressions located north of Little Gem (E4). Tear fault traces are marked by straight broken lines; d) "rubble stripes" located south of the eastern Neutral Hills (H6), with overridden and quarried thrust mass outlined; e) sedimentary and structural details and clast macrofabric from quarry exposure through Quaternary deposits in a single raft in the Kirriemuir elongate assemblage (see "x" on Fig. 10a).

Fig. 11: LiDAR images of examples of multiple parallel lineations (flutings) and groove features with mega rafts: a) NNW-SSE aligned flutings on the bed of the Central Alberta Ice Stream, south of Coronation (A5-6), showing a grooved terrain lying between relatively higher topography containing overridden composite thrust ridges, geometric ridge networks and/or fluviially eroded residual bars of the "Coronation-Spondin scabland". Inset shows a succession of hill-hole pairs in the grooved terrain; b) rubble stripes on the footprint of the Fabyan-Amisk palaeo-ice stream (demarcated by the

black dashed lines; C-D, 11-15). Insets show that the fluting pattern is locally composed of linear mega-raft chains (outlined); c) groove and mega-raft pairs, illustrated by an example from the bed of the former easterly flowing Ice Stream 2A, north of Battle River (upper), and an example from overridden thrust moraines immediately northwest of the map area, where westerly flowing ice displaced a thin-skinned mega-raft.

Fig. 12: LiDAR images of examples of geometric ridge networks: a) the CAIS footprint around the town of Brownfield (B8), showing extensive geometric ridges as well as several zig-zag eskers; b) the footprint of the Prospect Valley lobe near Lloydminster (immediately northeast of the map area), showing the location of a sedimentary exposure through a ridge together with a section cliff image and clast macrofabric data.

Fig. 13: LiDAR images showing examples of eskers: a) large, flat-topped esker passing laterally into flat-topped hills (ice-walled lake plains) on the floor of the Sounding Lake-Eyehill Creek depression (E-H, 8-10), illustrating the torturous alignment of the main ridge and its circular deflection that forms a 180° change in direction. Note the increasingly wider flat-topped summit starting at the area of the circular deflection and then towards the northwest; b) flat-topped eskers and their tributary and distributary branches located 10 km south of Wainwright and in the area of Ribstone Lake (D-F13), illustrating a large flat-topped ridge that fans out and terminates at pitted outwash on the distal edge of the Prospect Valley composite thrust moraine belt. Dashed line delineates a chain of elongate depressions that are inferred to have resulted from collapse into a buried tunnel channel; c) tunnel channels near Kinsella (immediately northwest of the map area) within an area of hummocky terrain and flat-topped hills (ice-walled lake plains) and containing segments of flat-topped ridges that rise above the channels walls; d) hummocky terrain north of Hardisty (B13), containing flat-topped hills (ice-walled lake plains) and minor eskers and doughnut chains grading southeasterly into an area of complex and meandering esker ridges contained within channels of variable width and displaying arcuate cliff segments.

Fig. 14: LiDAR image of hummocky terrain north of Irma (A15), illustrating a range of landforms typical of this type of landscape, including eskers, contiguous doughnuts and doughnut chains and excellent examples of ridge-rimmed mounds or flat-topped hills (ice-walled lake plains). At the centre of the image is a prime example of an “unstable ice-walled lake plain” through which subglacial tunnel channels and muted hummocks can be detected.

Fig. 15: Examples of pitted and hummocky terrain interpreted as areas of formerly ice-cored glacitectonic thrust mass: a) LiDAR image of an area located directly south of the western Neutral Hills thrust complex (D/E7) and containing substantial lakes with cliffed, often rectilinear or arcuate boundaries and details of a hummock exposure located at the yellow “X” symbol that show significant deformation, thrust faulting and diapirism of bedrock and Quaternary sediments; b) LiDAR image of an area of largely chaotically pitted Quaternary materials with discontinuous lineaments located immediately north of the western Neutral Hills (E9); c) LiDAR image of the “North Altario depression” (I6), with the main landforms annotated. The veneer of glacialacustrine deposits linked to flat-topped hills is outlined by the dashed line.

Fig. 16: Examples of hummocky terrain: a) LiDAR image and ground photograph of the Veteran Moraine (D6) showing its component landforms of hummocks, flat-topped hills and eskers; b) details of an exposure through a typical hummock in the Veteran Moraine, showing clay-rich diamicton with sheared sand lenses; c) LiDAR image of the Altario Moraine (H5/6), showing contiguous doughnut mounds, short sinuous hummocky ridges, ice-walled lake plains, eskers and associated doughnut chains; d) LiDAR image showing locations of hummocky terrain exposures in the Viking Moraine around Kinsella (A15; see also Figs. 13d and 14) and annotated photographs of the stratigraphic details and clast macrofabrics. White dotted lines highlight thrust structures.

Fig. 17: LiDAR images of examples of erosional channels, large terraces and cliffs: a) prominent channels with cliffed margins in the area around Hardisty, west of the Battle River (A10-14), which occupies the large trench on the bottom right of the image. The reticulate pattern, which isolates polygonal-shaped areas of prairie surface containing overridden thrust mass lineaments (MTR Type 1); b) probable subglacial tunnel channels identifiable as sinuous chains of elongate lakes partially obscured by glacial depositional landforms and in places (i.e. Wilkins Lake) aligned with eskers (i = C11; ii = G10; iii = I9); c) spillway channel networks, illustrated by the Loyalist Creek and Monitor Creek channels (left; F-G5) incised through glacitectonic thrust masses on the west side of the Monitor Creek basin and by Sounding Creek (right; H-I, 2-5), which is incised through the Misty Hills/Esther Uplands thrust moraine complex and then through the pitted glaci-fluvial deposits of the Grassy Island Moraine.

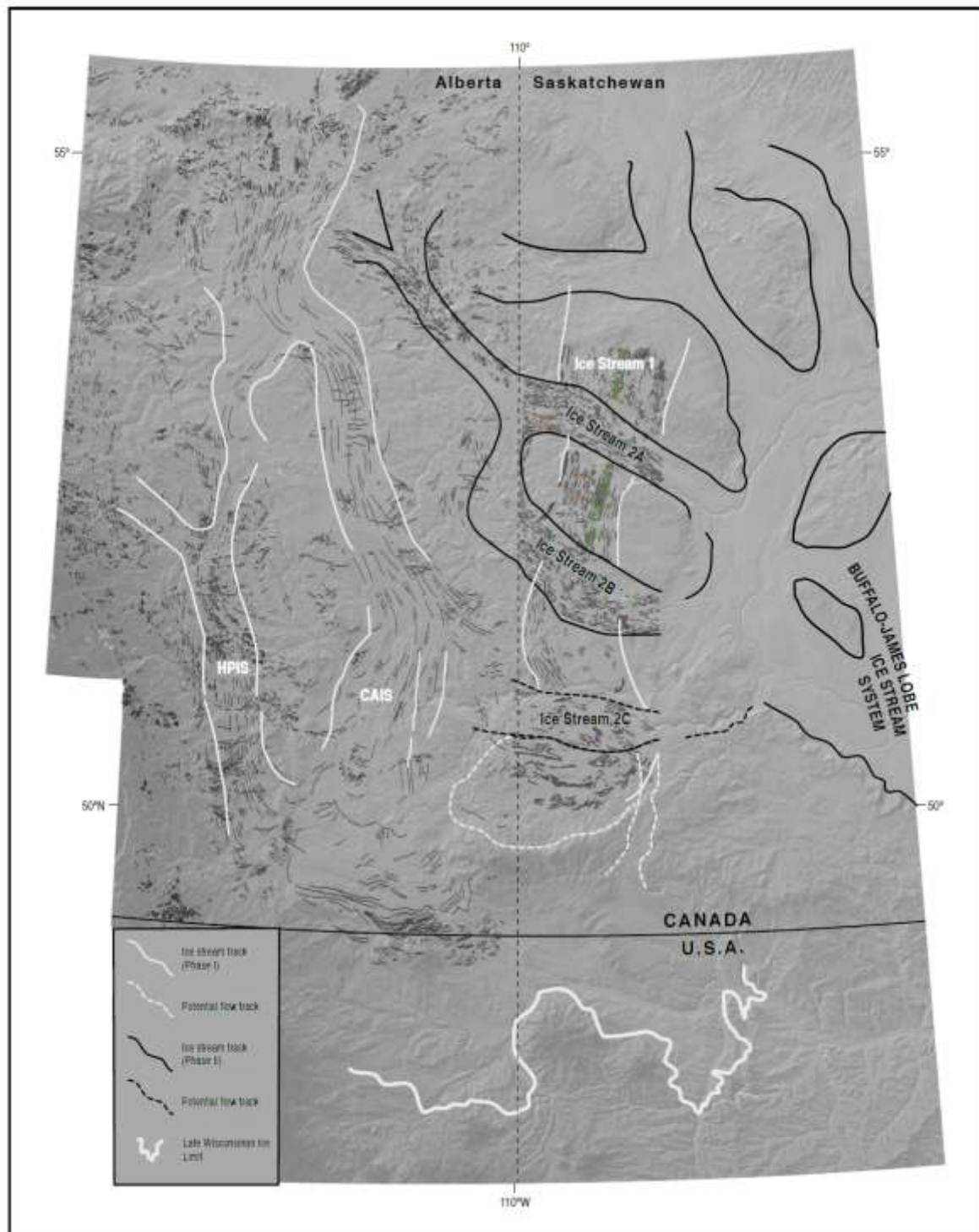
Fig. 18: Summary maps (annotated on the regional DEM) of: a) the major glacial landform components and landsystem imprints, showing the inset arcuate assemblages of moraine arcs that demarcate the repeat surging of the ice lobes of “eastern” provenance flowing south-southwesterly into the eastern margin of the CAIS and alternating with the CAIS-derived flow set 4 footprint; and b) palaeo-ice stream extents, flow sets and relative event chronology for the map area and immediate environs based on the distribution of landsystems and their cross-cutting relationships. Note that the large esker network of the Eyehill Creek-Sounding Lake depression is highlighted as an example of reversed drainage back into and through stagnating ice, in this case the ice that was responsible for the Flow set 4 footprint.

Fig. 19: Details of the Event 5 lobate ice stream surge in the Lloydminster/Prospect Valley area: i) to iii) LiDAR images of the main landsystem components identified on an extract from the geomorphology map in Fig. 3; b) oblique aerial photograph of a modern analogue for the ice-cored surge moraine, Skeiðarárjökull foreland, Iceland. Note that this moraine still contains significant buried snout ice but ongoing melt-out has initiated the fragmentation and pitting of inset linear ridges related to folds and thrust slices. Esker ridges can also be seen emerging through the downwasting landform complex.

Fig. 20: Conceptual model of the landsystem signature produced by surging into areas of stagnant ice lying over Cretaceous bedrock on the Canadian prairies, with example figures of typical landforms labelled: a) Phase A shows ice sheet marginal downwasting and recession during which large areas of ice may get buried by glaci-fluvial outwash. 1 = ice sheet margin, 2 = meltwater drainage pathways with 2a representing earlier tunnels and 2b the later stage of englacial drainage adjusting to aggrading outwash fans, 3 = aggrading glaci-fluvial outwash comprising regional

northeasterly-directed drainage along the ice margin (3a) and proglacial/supraglacial ice-contact fans (3b), and 4 = sub-marginal till wedges; b) Phase B shows the advanced stages of local ice stagnation, where buried glacier ice (1) contains an extensive karst network from which ice-walled lake plains, eskers and kame and kettle topography emerge (2). Englacial to subglacial drainage networks have by this time been developed by northeasterly draining meltwater (i.e. reversed drainage), in which eskers, doughnut chains and till eskers form. Extensive areas of doughnuts (4) also form due to subglacial squeezing of till into cavities beneath thin ice and/or blow-out or degassing through the glacial sediment cover; c) Phase C shows the surge of the ice sheet margin (1) and its construction of a composite thrust moraine due to glacial tectonic disruption of Cretaceous bedrock (2), which is then pushed into the area of stagnating glacier ice (3). The ice is dislocated into thrust masses and its englacial material is consequently deformed. The area of former outwash lying distal to the stagnant ice is also compressed in the proglacial stress field (4). Large melt-out pits and retrogressive slumps gradually evolve in the ice-cored thrust mass. Pressurised aquifers create hydrofractures and blow-out features (doughnuts) in the composite thrust moraine. Crevasse squeeze ridges are developed on the proximal slopes of the proglacial thrust complex and subglacial surface due to intensive surge-related crevassing.

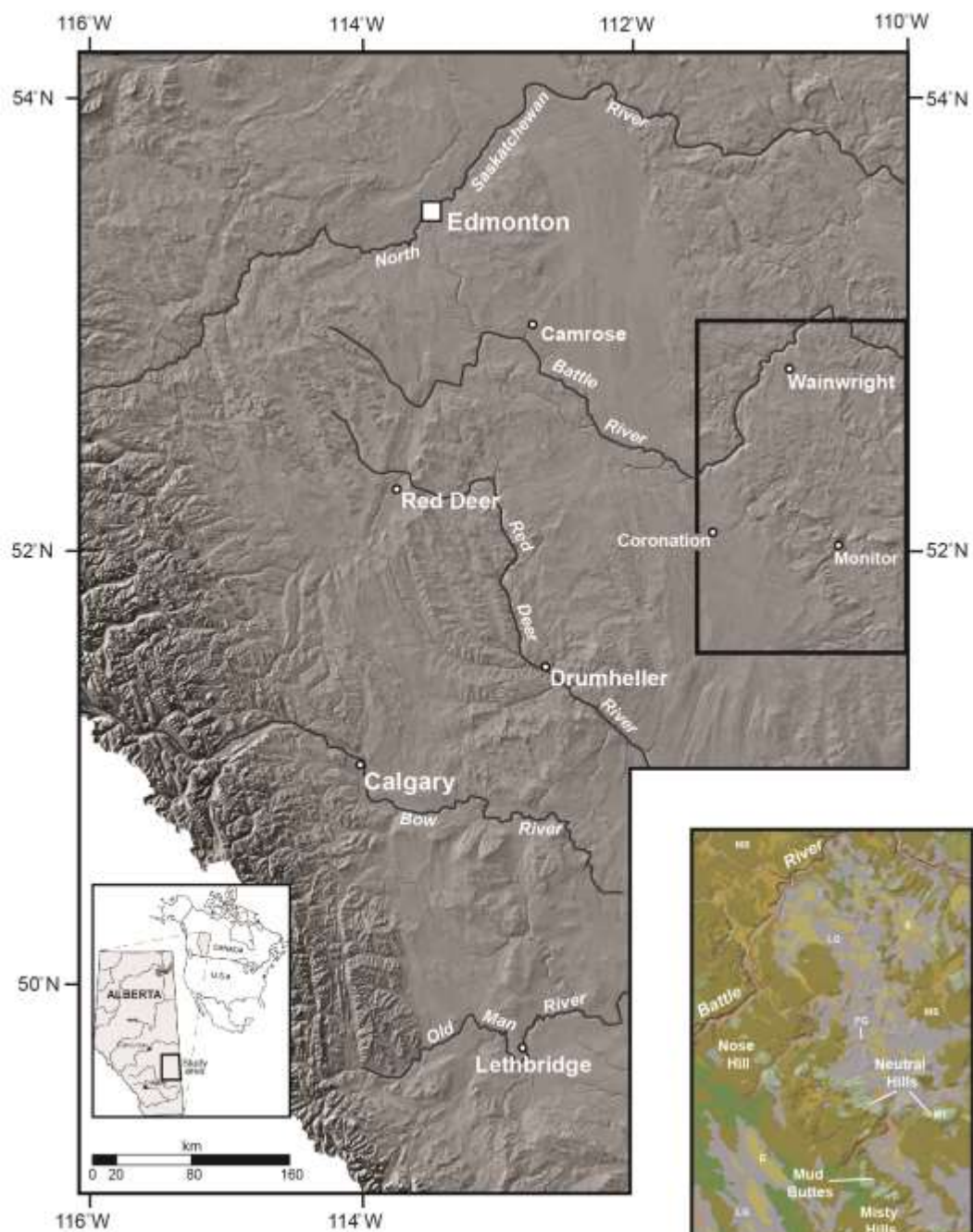
1618



1619

1620





1621

1622



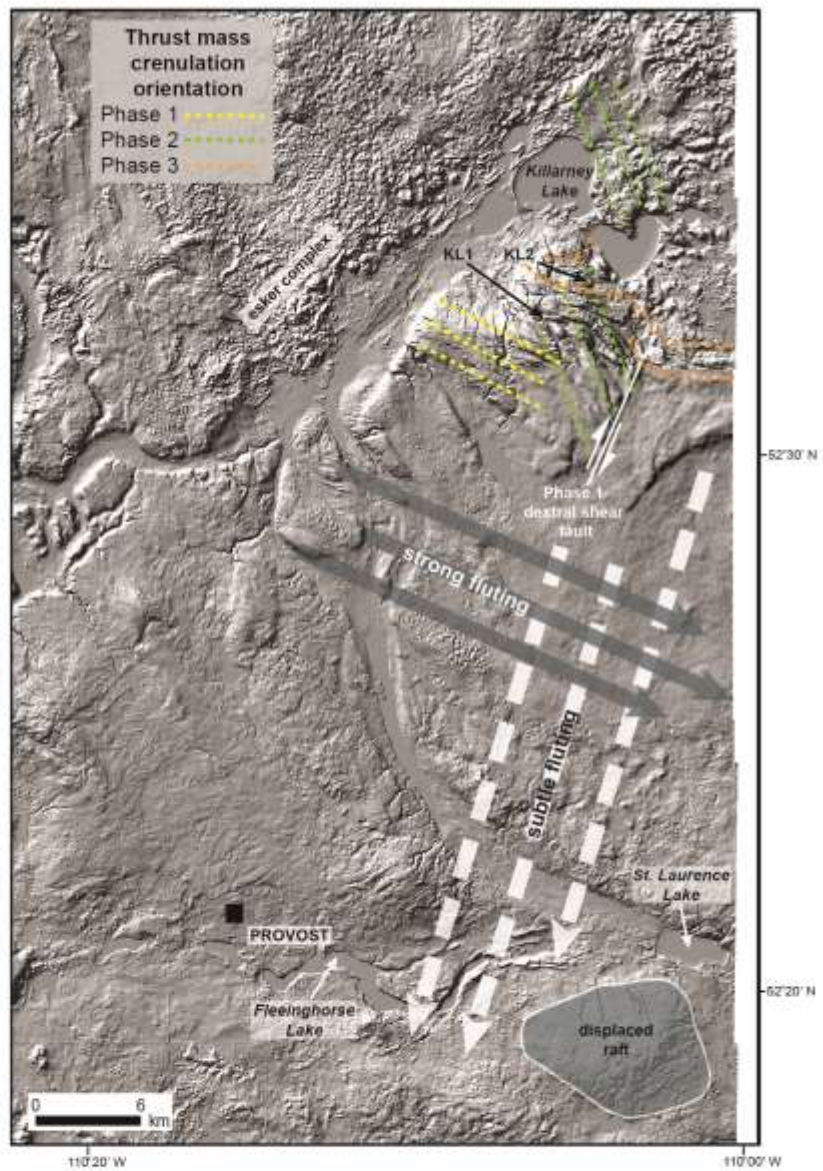




1625

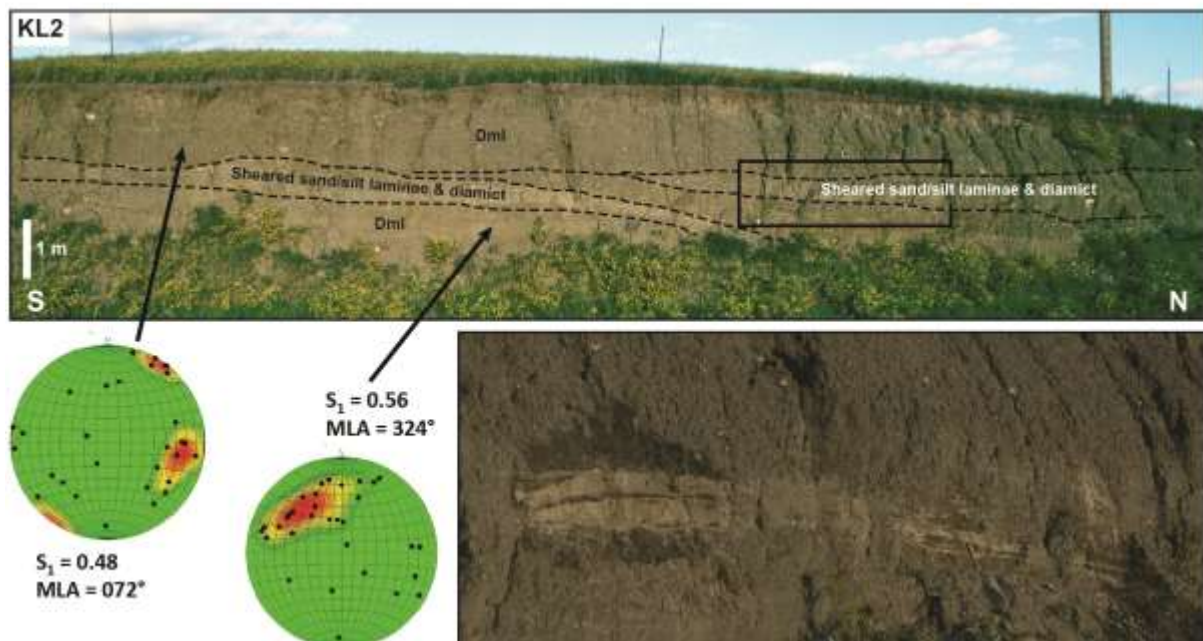
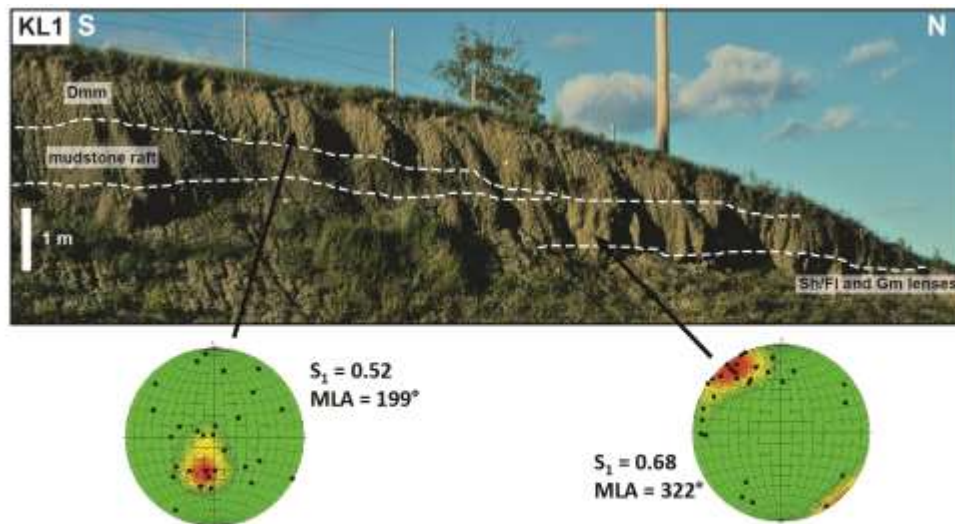
1626





1627

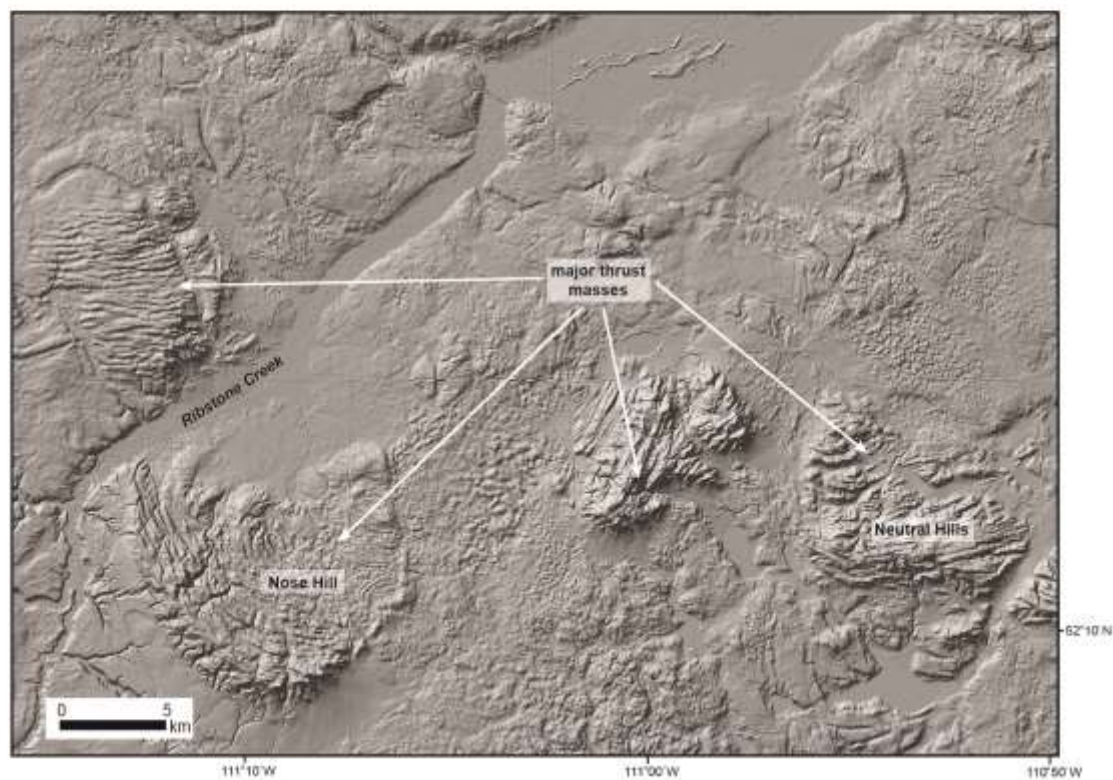
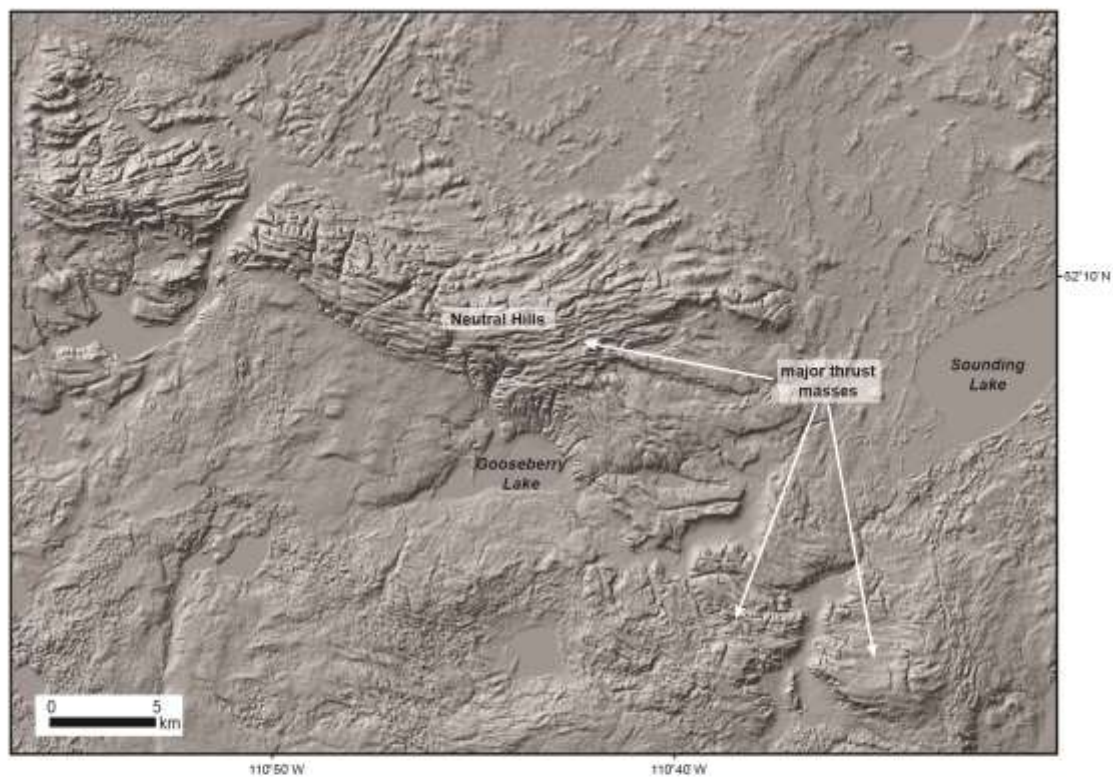
1628



1629

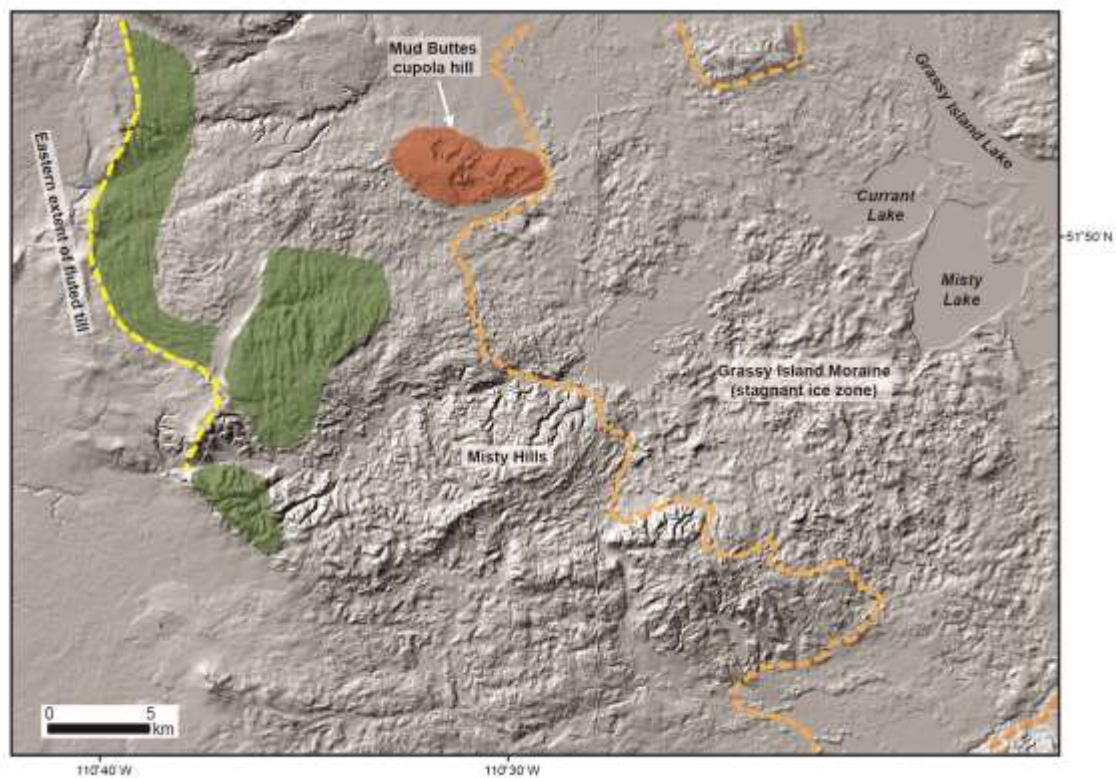
1630





1631

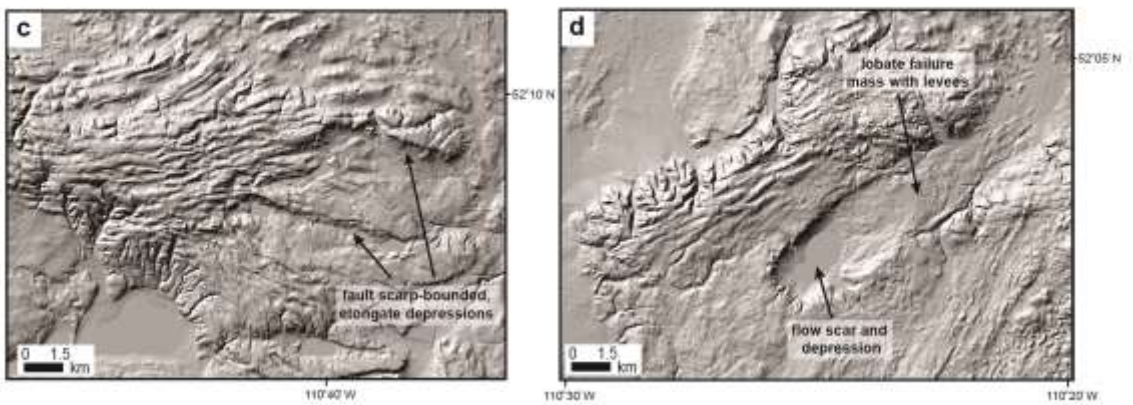
1632



1633

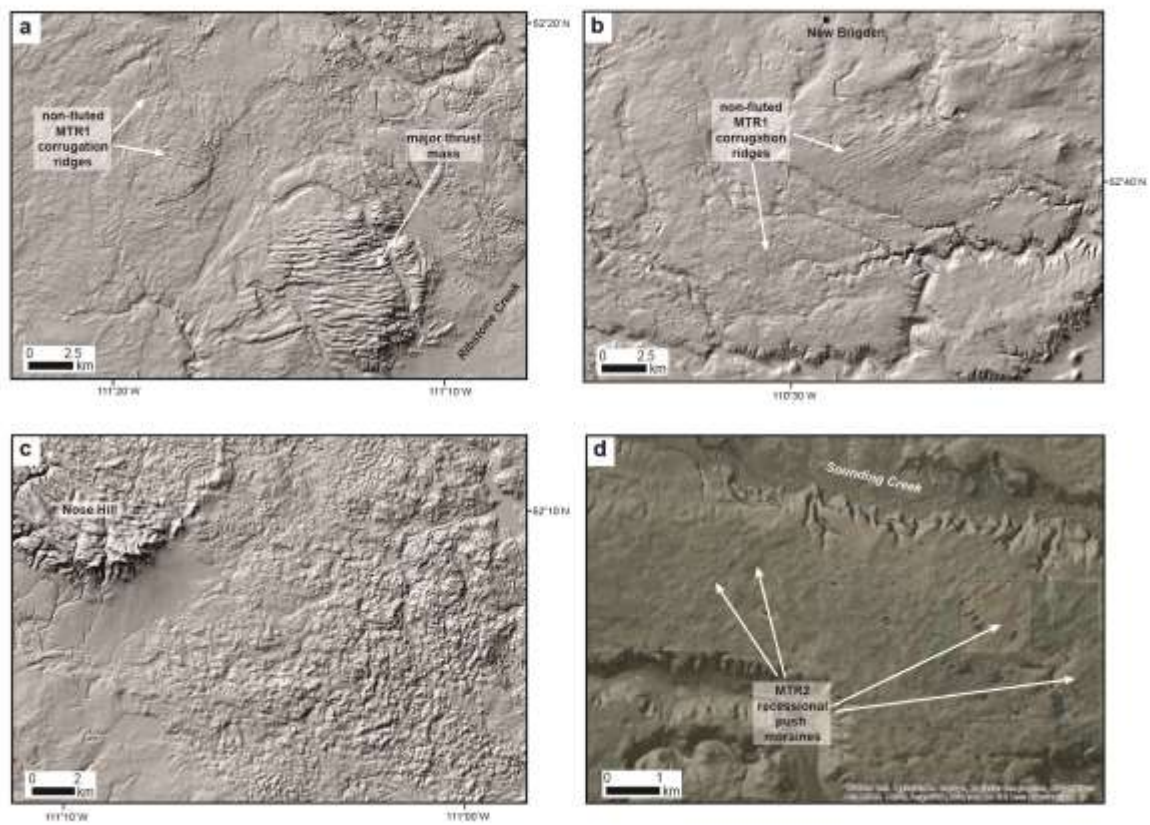
1634





1635

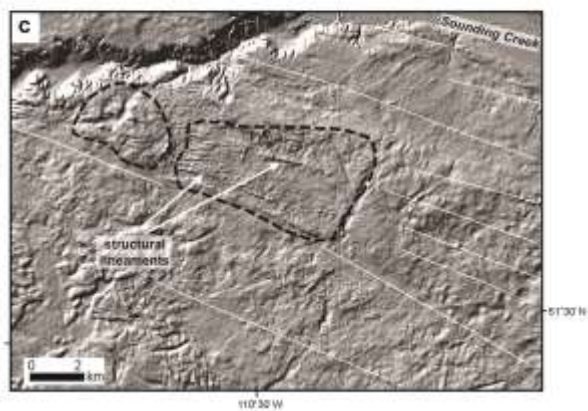
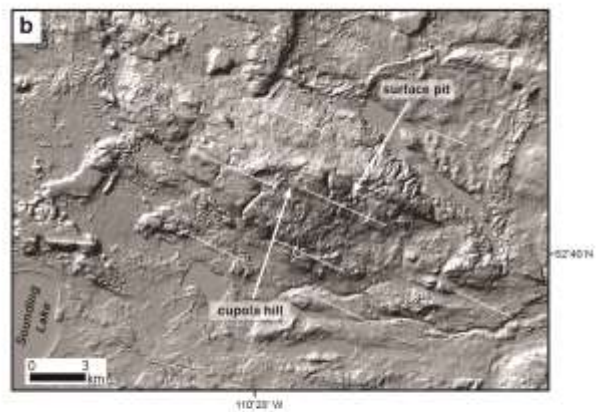
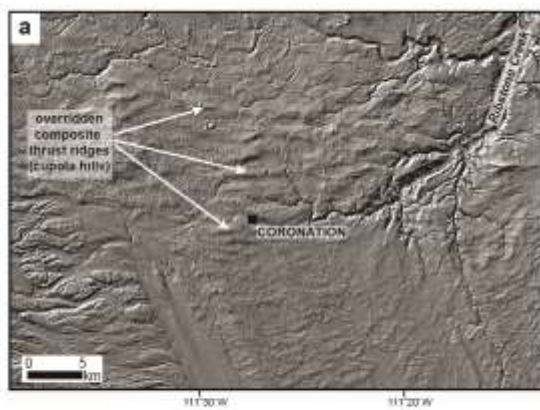
1636



1637

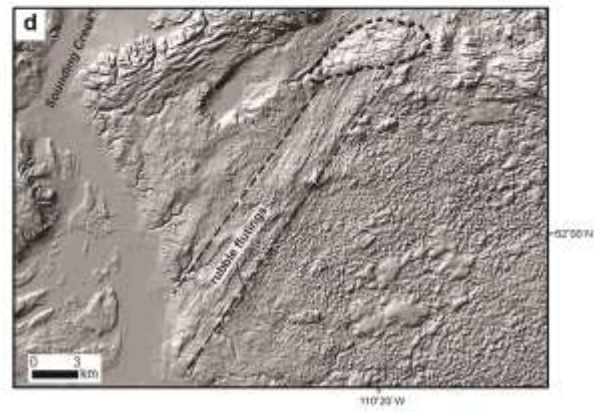
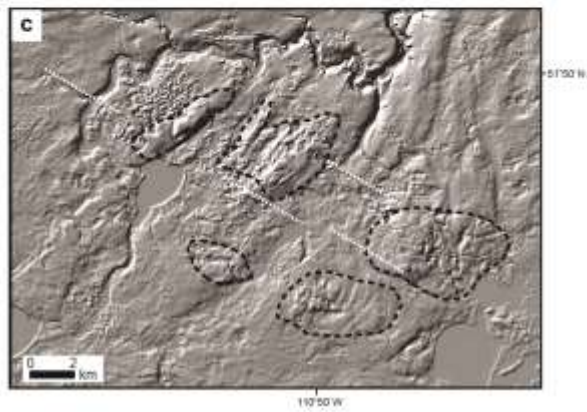
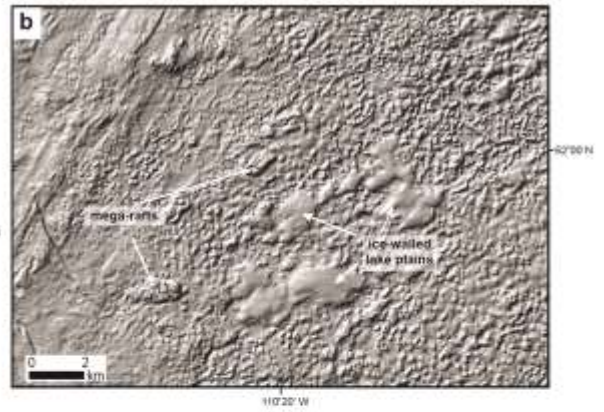
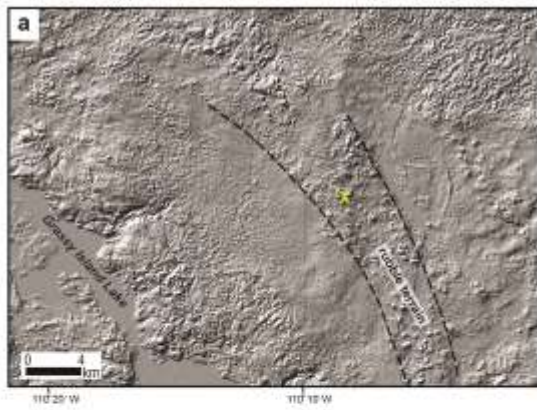
1638





1639

1640



1641

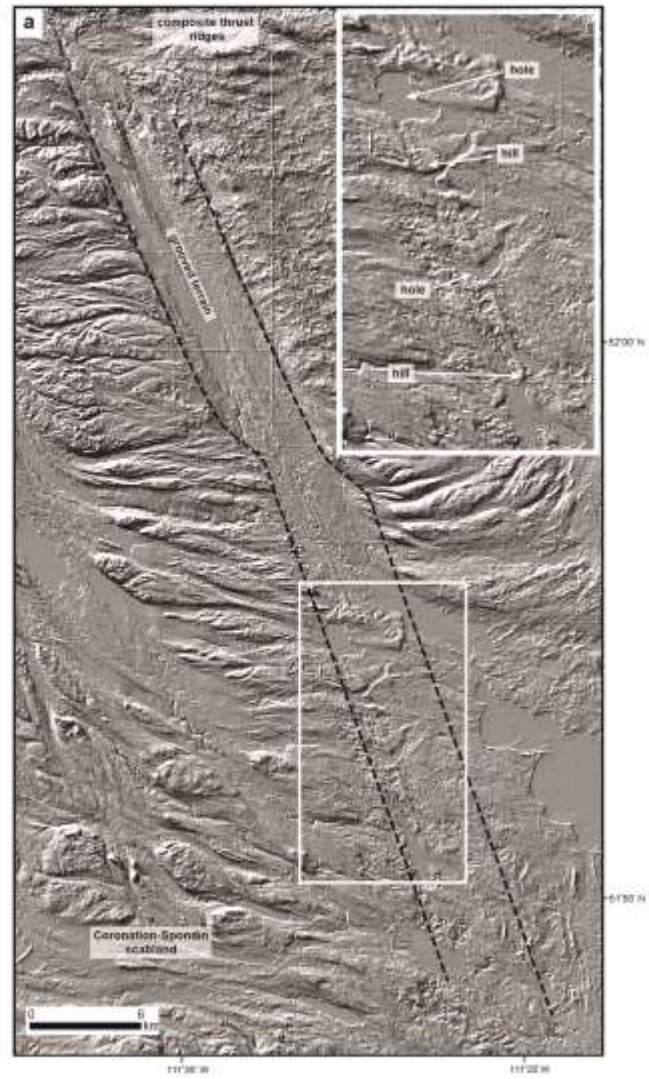
1642



1643

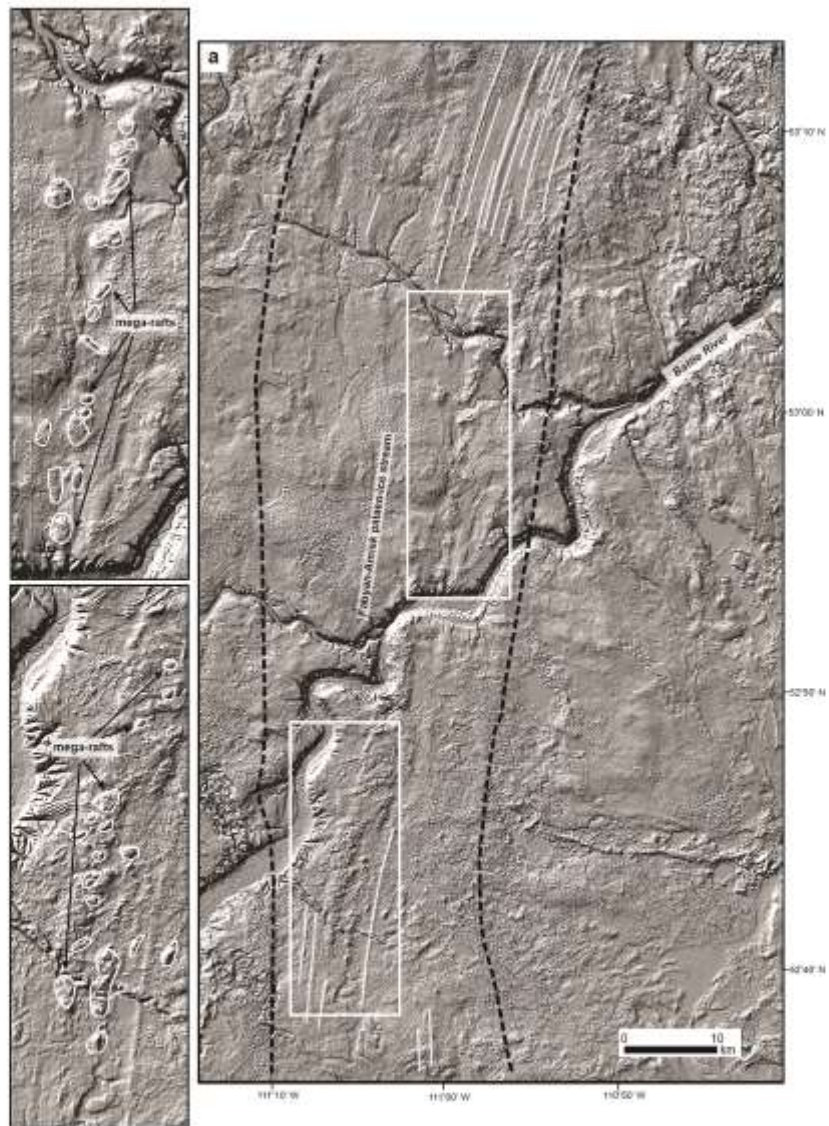
1644





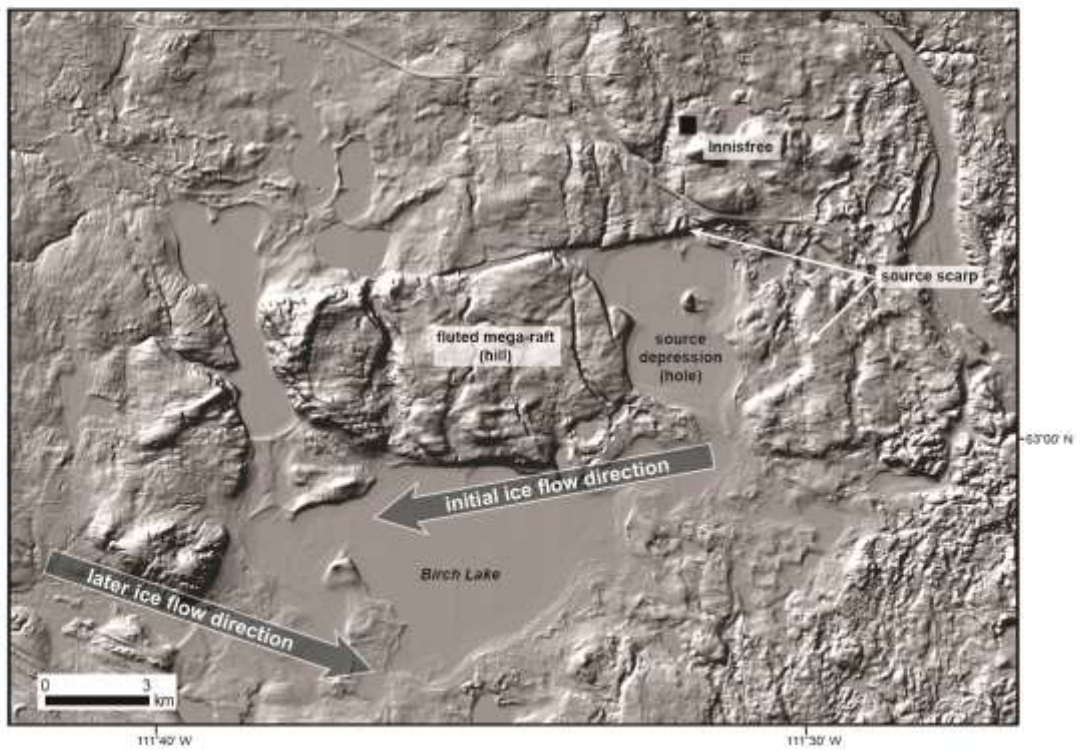
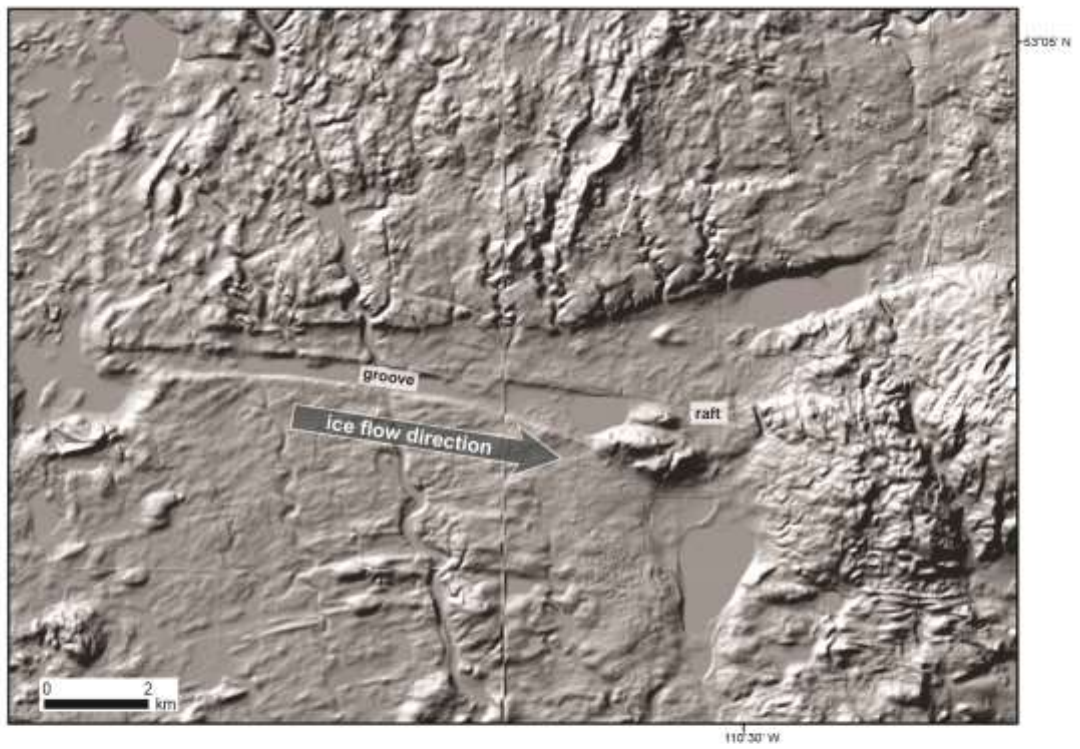
1645

1646



1647

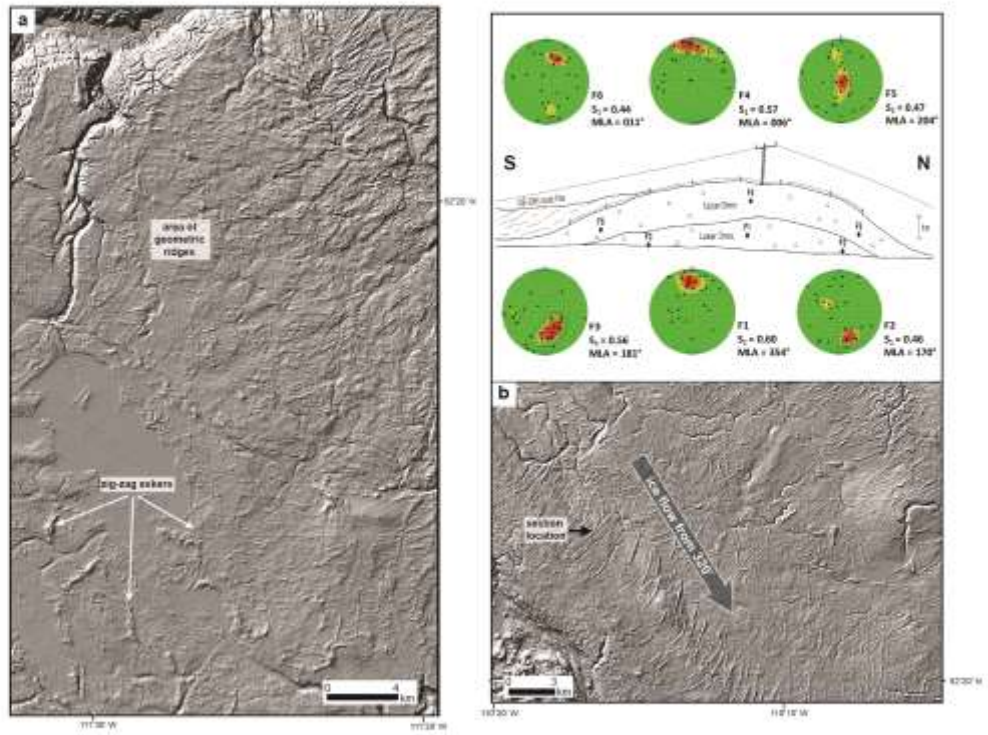
1648



1649

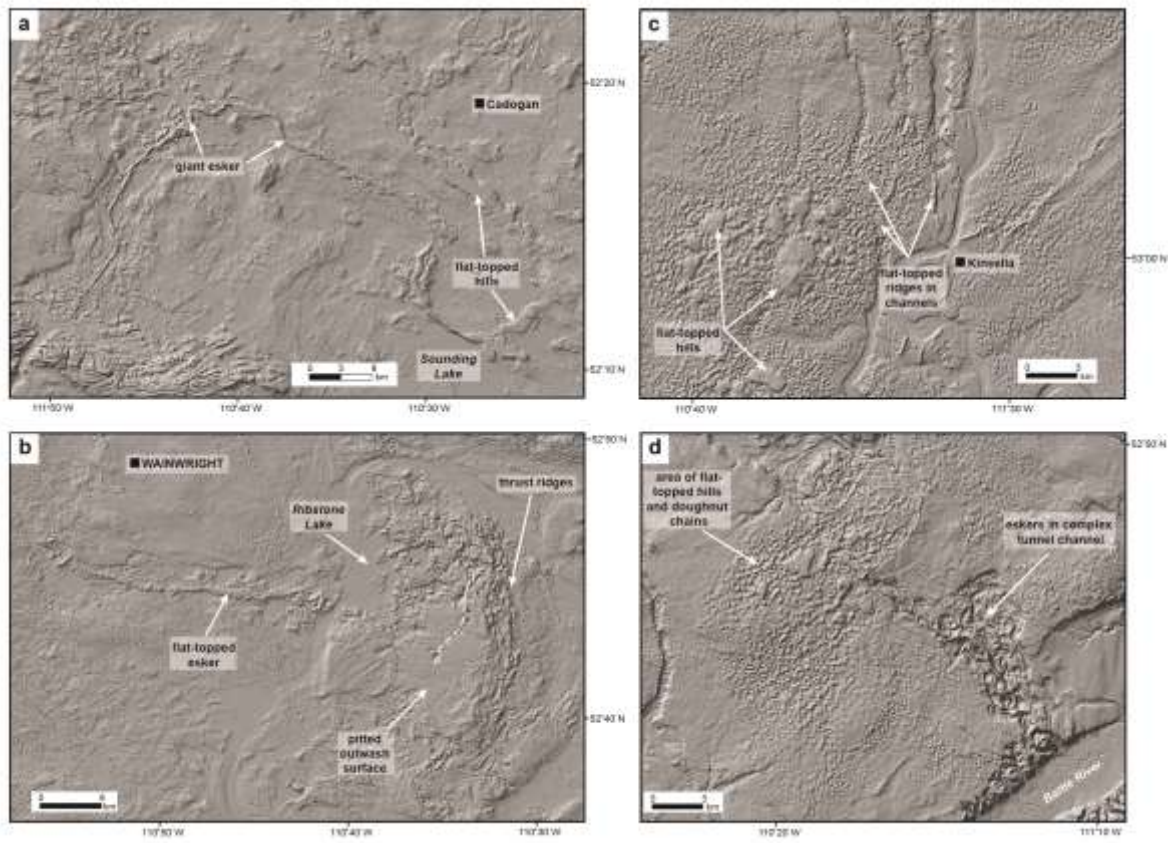
1650





1651

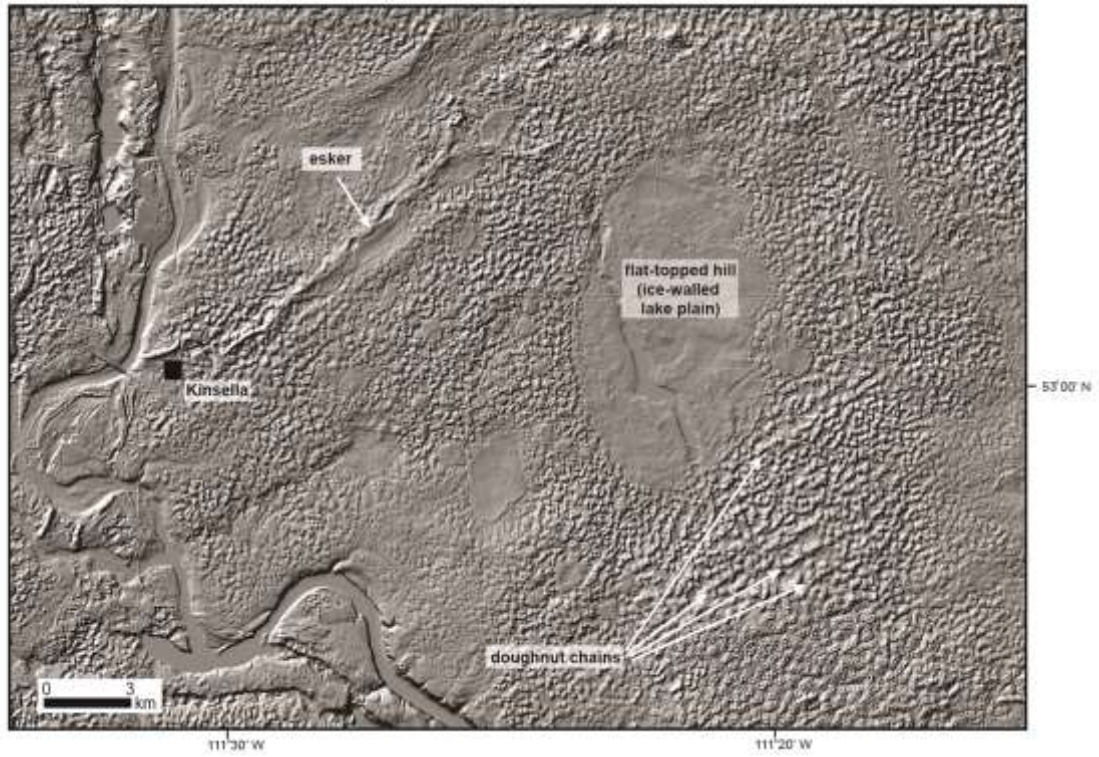
1652



1653

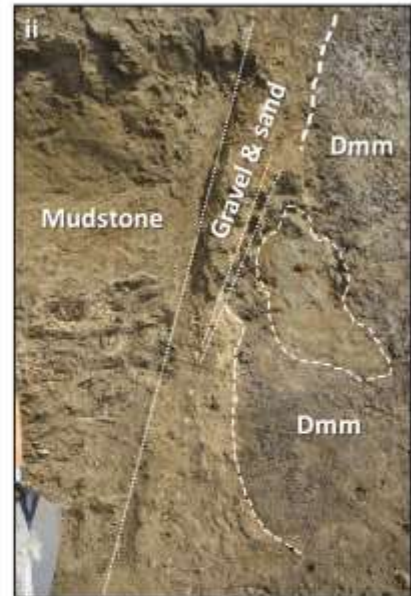
1654





1655

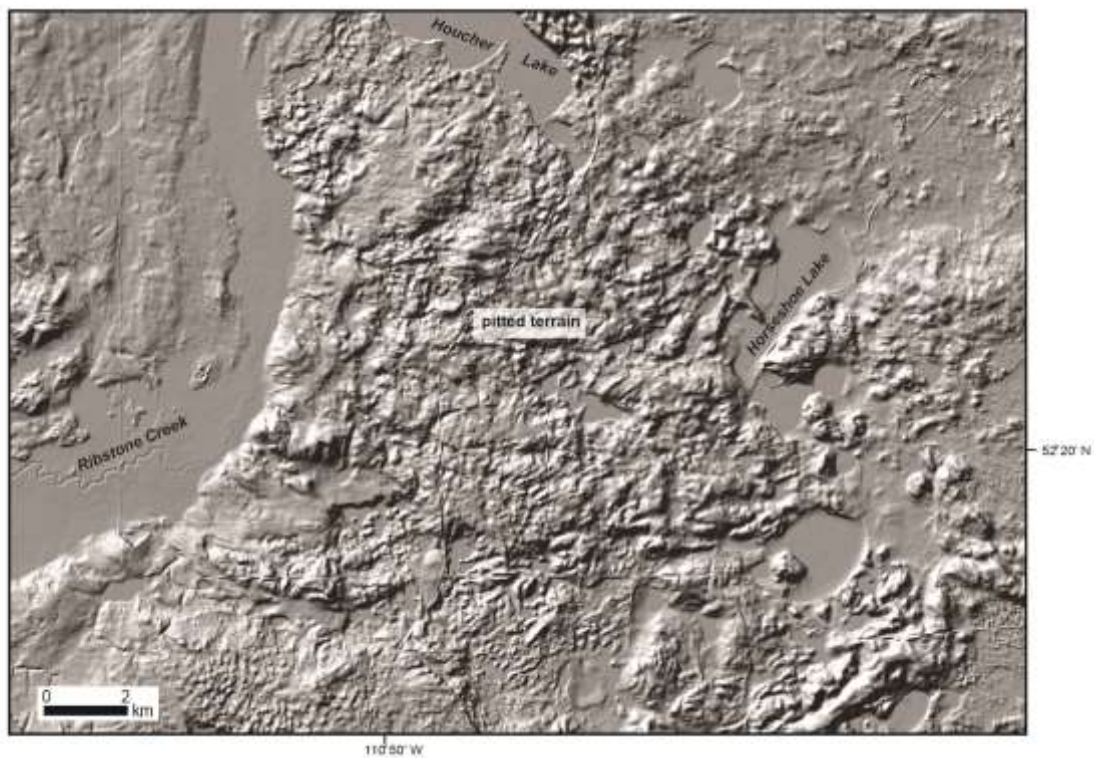
1656



1657

1658



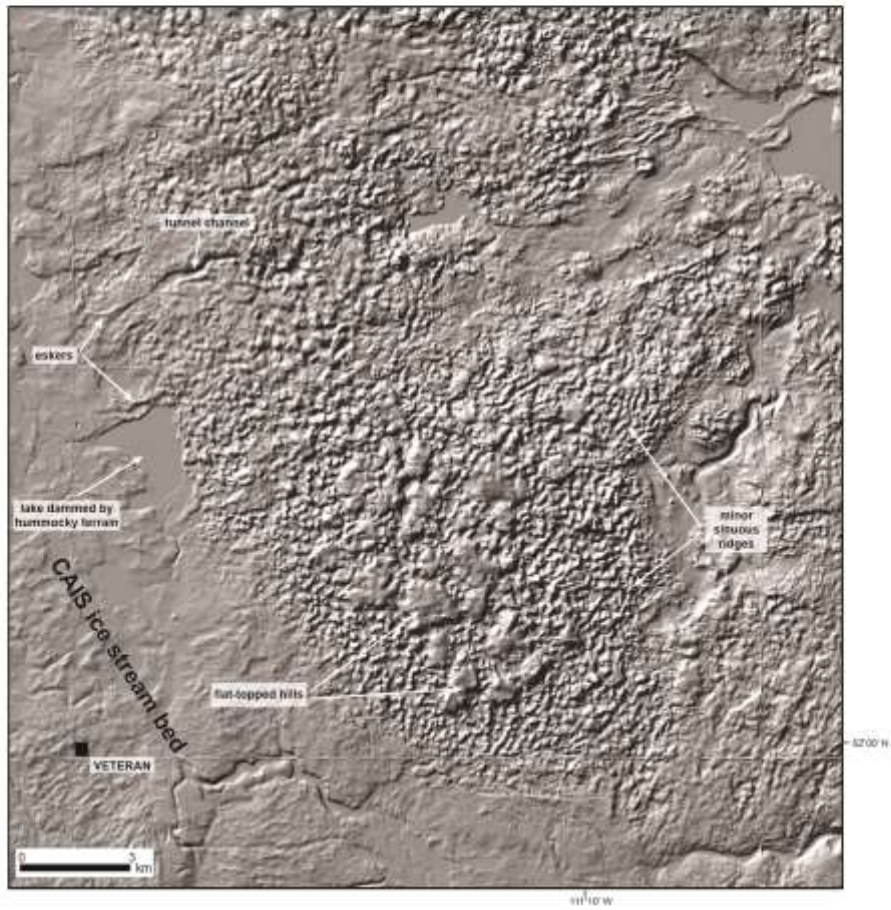


1659



1660

1661



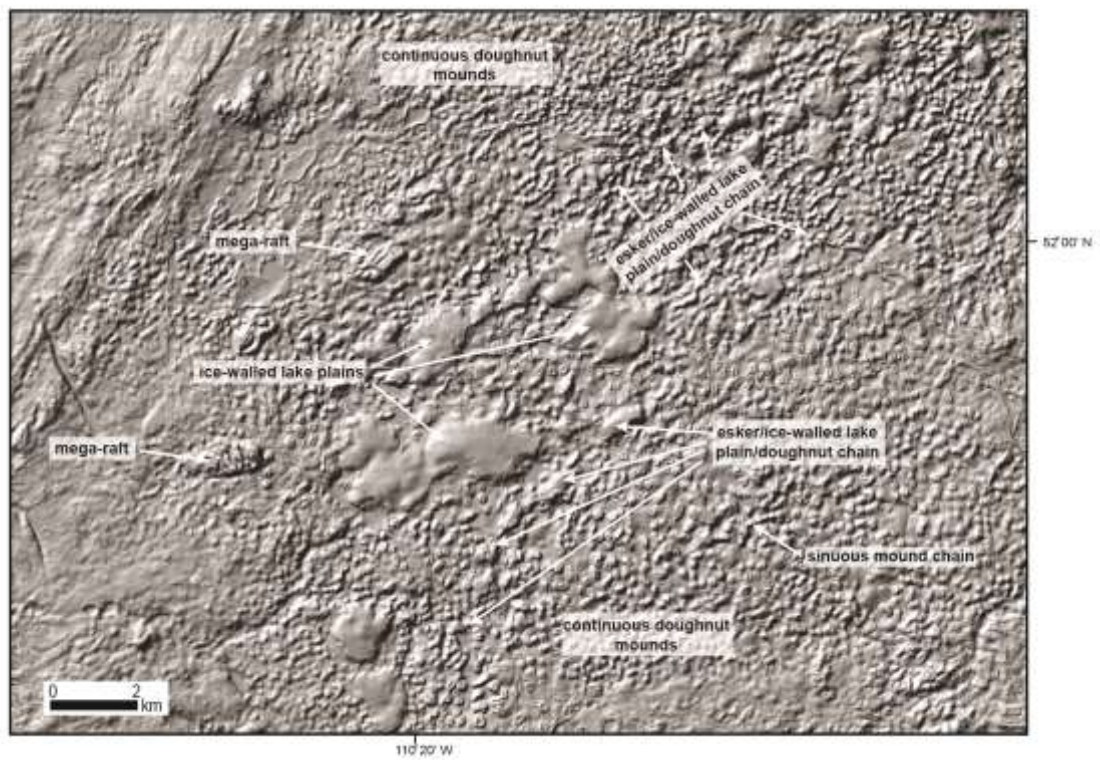
1662

1663



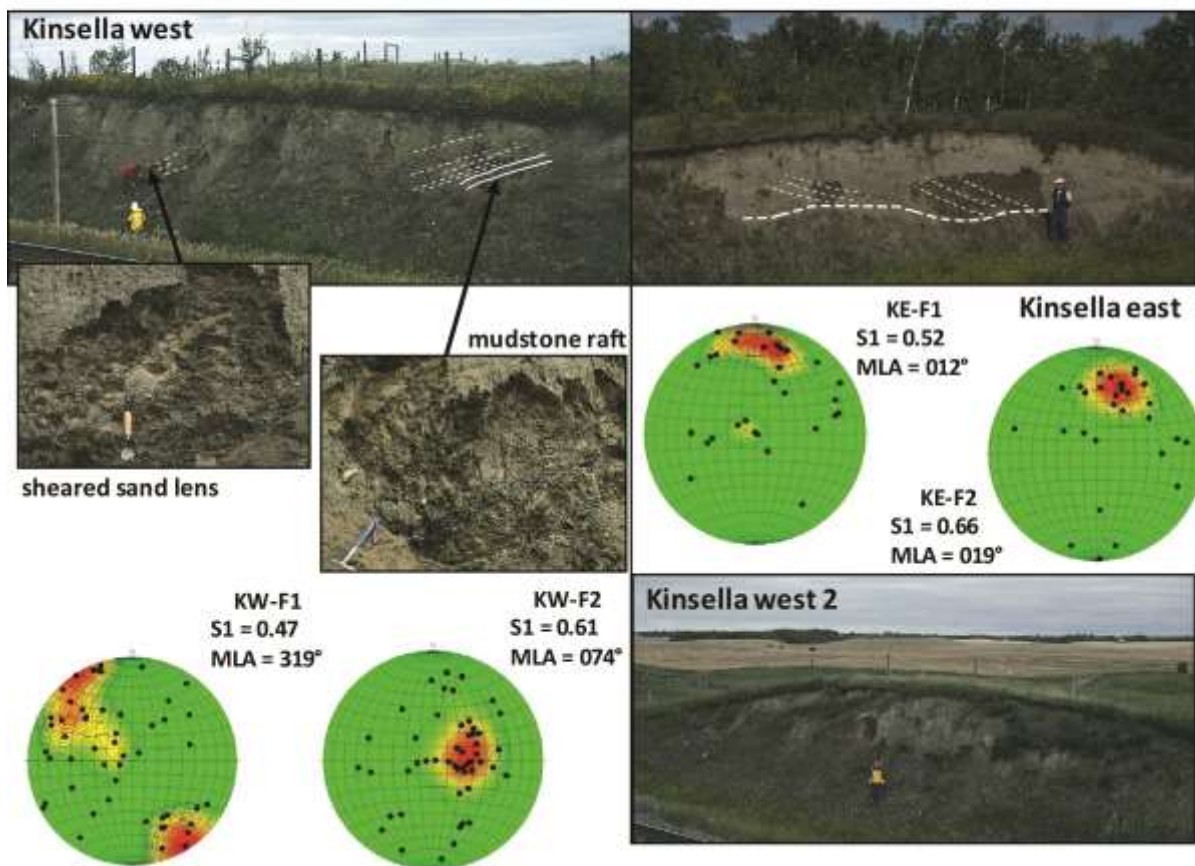
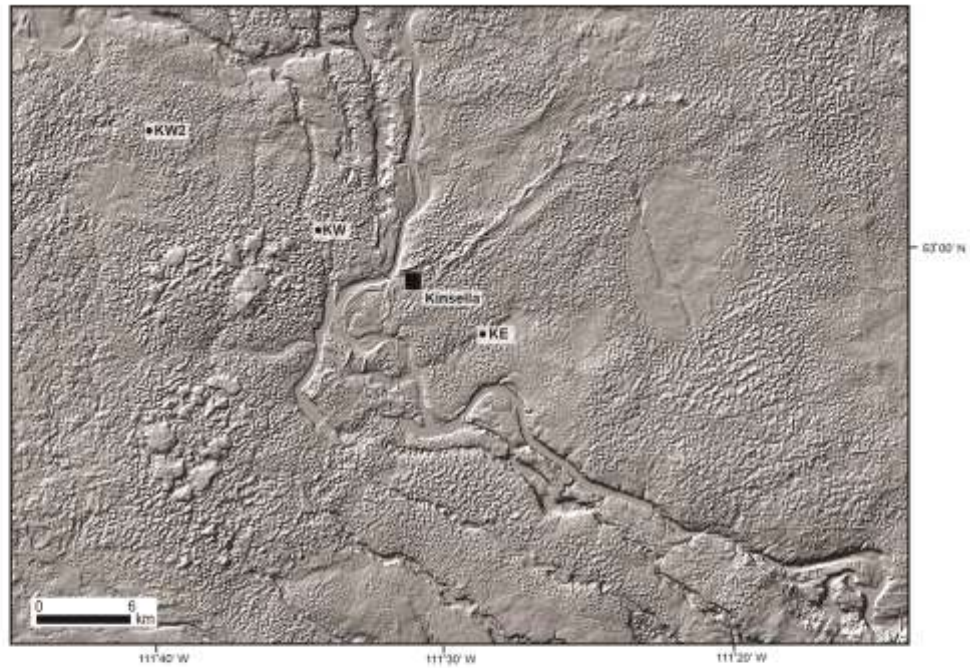


1664



1665

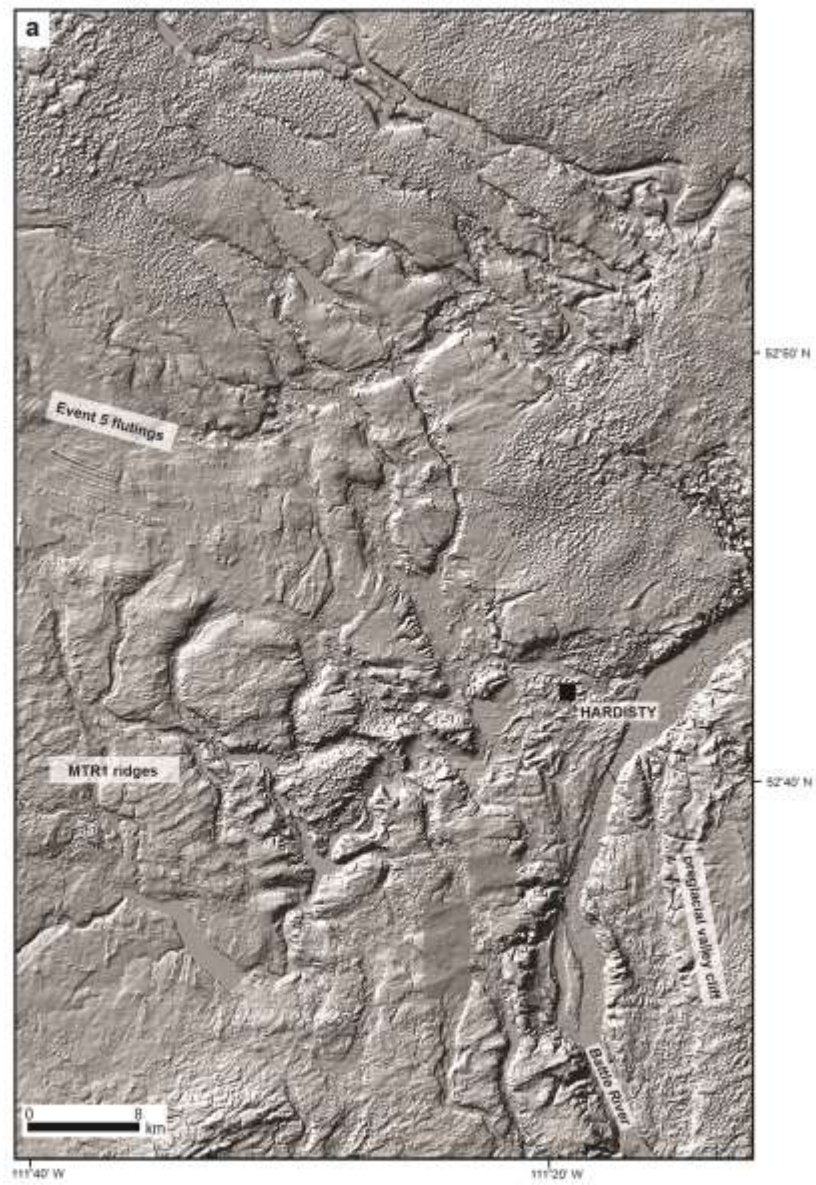
1666



1667

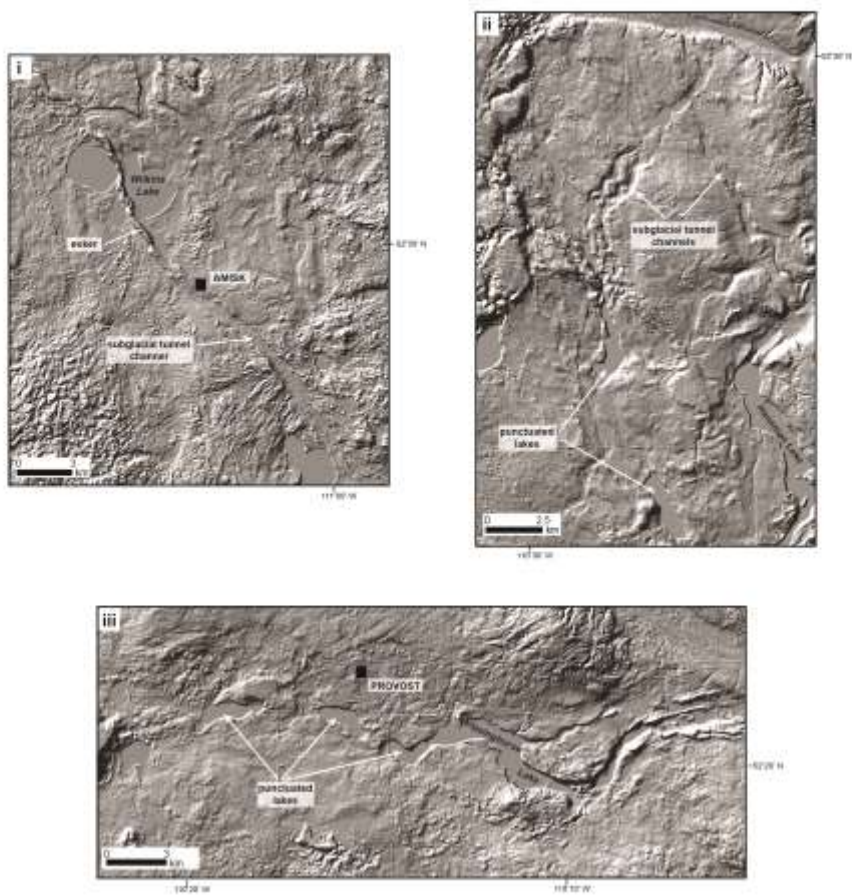
1668





1669

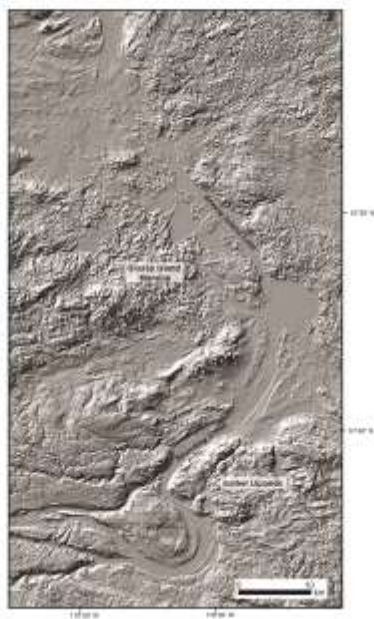
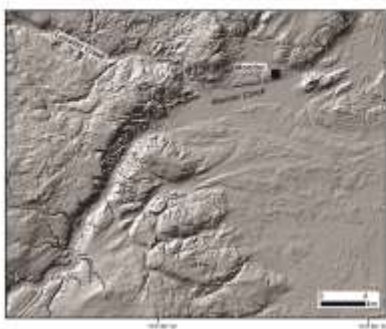
1670



1671

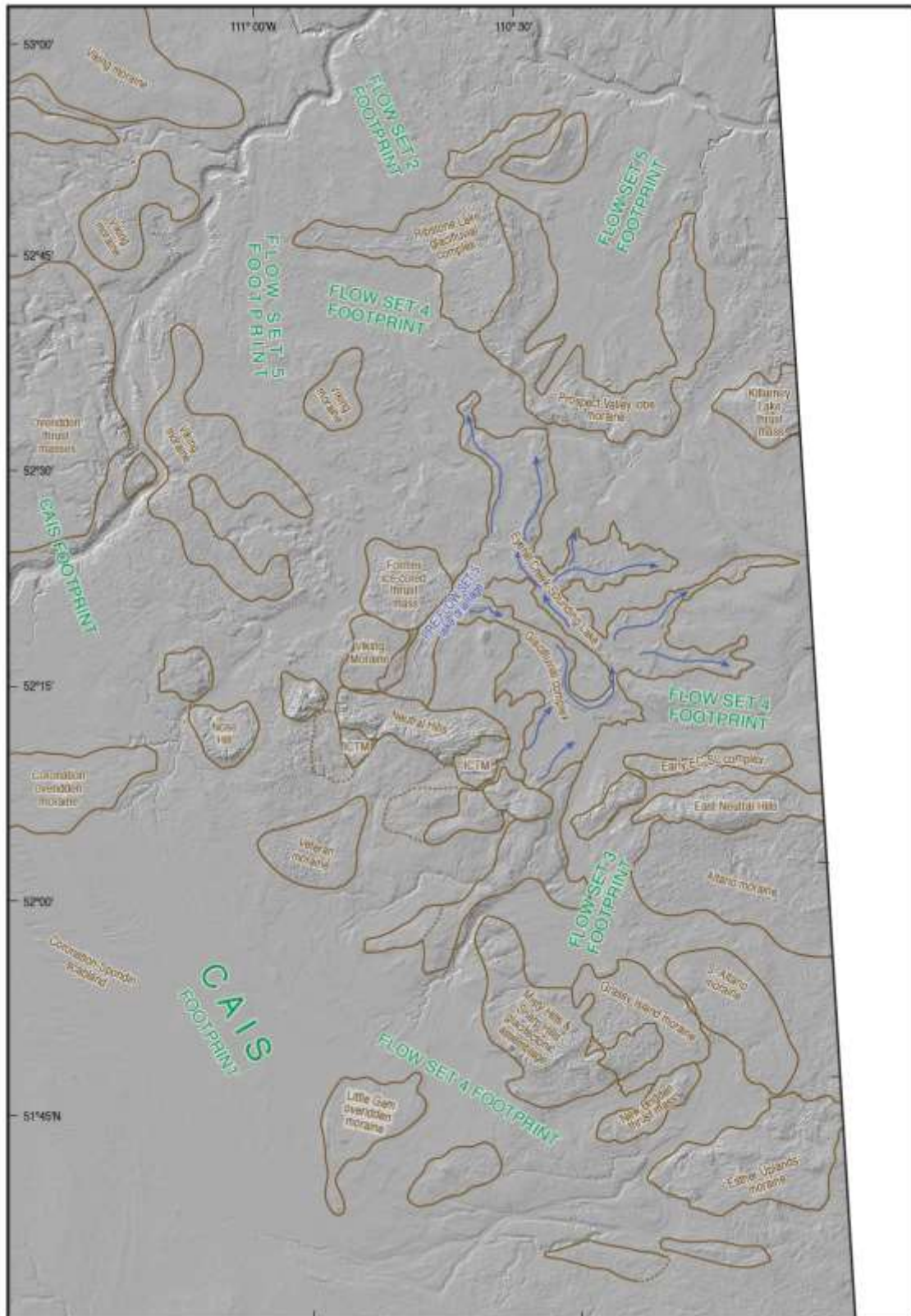
1672





1673

1674



1675

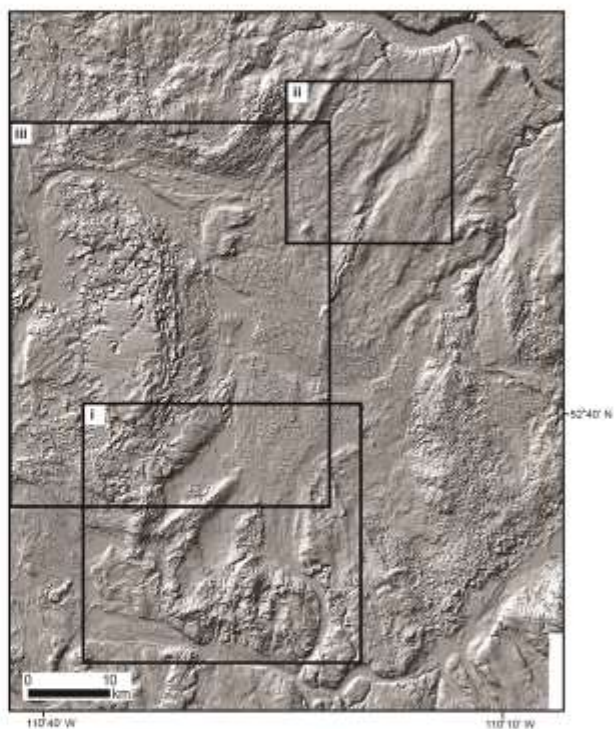
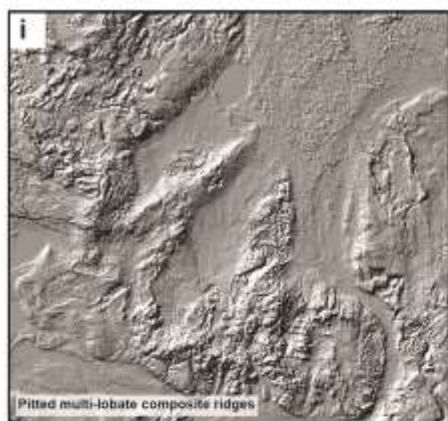
1676



1677

1678





1679

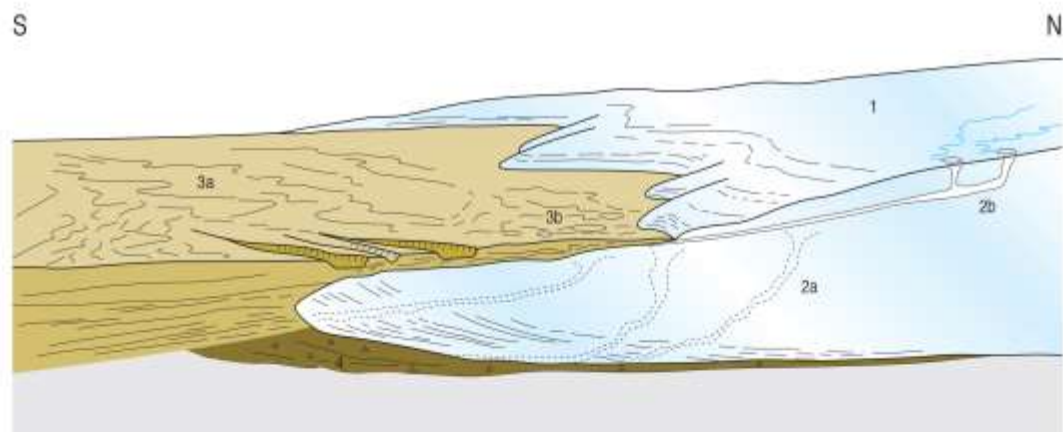
1680



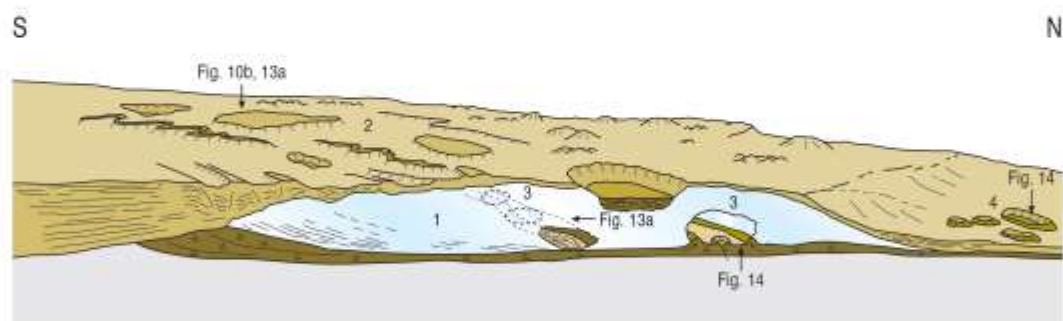
1681

1682

# **PHASE A - ice sheet marginal recession**



# **PHASE B - localised ice stagnation (Fig. 6, 13, 16c)**



# **PHASE C - ice lake surge (Fig.5 19a)**

